Doctoral Dissertation

Effect of Salt Addition on the Properties of Poly(vinyl alcohol)

Riza Asma'a Saari

Supervisor: Prof. Masayuki Yamaguchi

Graduate School of Advanced Science and Technology

Japan Advanced Institute of Science and Technology

Materials Science

September 2021

Effect of Salt Addition on the Properties of Poly(vinyl alcohol)

Riza Asma'a Saari

Poly(vinyl alcohol) (PVA) is known as one of the most important biodegradable plastics and have the potential to solve the current problem related to marine pollution from conventional plastics. The excellent mechanical properties of PVA originated from intermolecular hydrogen bonds, such as high modulus and high yield strength, are sufficient to fulfill the requirements to replace from rigid non-biodegradable plastics. However, in commercially available products, strong hydrogen bonding could lead to poor mechanical properties of the fibers and films because it prohibits a high level of molecular orientation. Incorporation of specific salts, such as lithium bromide (LiBr), lithium chloride (LiCl), and magnesium chloride ($MgCl_2$) can reduced the hydrogen bonding between polymer chains. From the previous studies, the addition of the salts could retard the PVA crystallization rate greatly. This phenomenon is caused by the interaction between hydroxyl groups and cations which attributed to the restricted segmental motion. However, there is no specific studies about the effects of ion species on the mechanical and thermal properties of PVA.

The present study focused on the effects of the addition of potassium, sodium, magnesium, and lithium salts on the rheological properties of PVA aqueous solutions, solid state of PVA films and also fibers. A plateau modulus can be detected in the low frequency region of shear storage modulus for PVA aqueous solution. This phenomenon demonstrates that hydrogen bonding of the PVA have developed a network structure. The addition of lithium salts evidently decreased the value of the plateau modulus with temperature. The anion species in the salt plays an important role in determining the rheological properties, including the magnitude of the plateau modulus as demonstrated by the experimental results. In the Hofmeister series (HS), the iodide anion was classified as a "water-structure-breaker" ion, it can decrease both plateau modulus including the oscillatory shear moduli effectively. Besides, at high temperatures, the modulus decreased with the LiI addition owing to the reduced extent of hydrogen bonding. The data obtained in this study demonstrated that the strong ion-dipole interactions between anions and PVA chains also have a significant impact on glass transition temperature and crystallinity. This study is the first to reveal that the impact of the salts addition follows the Hofmeister series. The study using different type of bromine salts revealed that Li^+ is more effective at disrupting the water structure than other salts such as Na^+, K^+, or Mg^{2+}. Furthermore, further experiments using lithium salts with various anion species verified that lithium salts are responsible in determining the hydrogen bonding within aqueous PVA and crystallinity, and therefore affect the mechanical properties of films. This phenomenon clearly follows the HS in order of $LiClO_4$ > LiI > LiBr > $LiNO_3$ > LiCl. Besides, magnesium salts also show an interesting result as the glass transition temperature T_g of the PVA films was enhanced and this result was attributed to the strong ion-dipole interactions between magnesium salts and PVA chains.

In case of PVA fiber, the addition of LiBr in spinning solution reduced the inter- and intramolecular hydrogen bonding in the PVA chains greatly and which results in the higher level of molecular orientation. It was evident from the results obtained in these studies, that the addition of metal salts gives significant impact on the properties of PVA aqueous solutions, films, and fibers, which corresponds to the HS.

Keywords: Poly(vinyl alcohol), Metal salt, Hofmeister Series, Crystallization, Hydrogen Bonding

Abstract

Poly(vinyl alcohol) has been widely studied in the field of industrial applications, where its fiber is regarded as one the most preferred reinforcements owing to its promising characteristics such as good chemical resistance, biocompatibility, good thermal stability, good cost performance and biodegradability. The present study focused on modification of PVA by salt addition and its application to material design by using the Hofmeister series concept. Their outstanding mechanical properties of PVA are coming from the strong intermolecular interactions due to hydrogen bonding. Considering such situation, modification of PVA has been tried so far. In this study, the modification of mechanical and properties of PVA have been achieved by the addition of various types of metal salts to PVA. This method can be established as a new material design. The structures and properties of the obtained PVA containing salts were characterized in detail.

Riza Asma'a Saari

Acknowlegements

It is a genuine pleasure to express my deep sense of thanks and gratitude to my supervisor, Prof. Dr. Masayuki Yamaguchi. His dedication and keen interest above all his overhelming attitude to help his students had been solely and mainly responsible for completing my research study. His timely advice, meticulous scrutiny, scholarly advice, and scientific approach have helped me to a very great extent to accomplish this study.

I gratefully acknowledge Prof. Dr. Tatsuo Kaneko, Prof. Dr. Noriyoshi Matsumi, Prof. Dr. Kazuaki Matsumura, and Prof Junichi Horinaka for their prompt inspirations, timely suggestions have enabled me to complete my thesis. I am also grateful to everyone for helpful discussion and also gave me a very good advice.

I thank profusely all the Yamaguchi laboratory members for their kind help and co-operation throughout my study. I am extremely thankful to my tutor and first Japanese friend, Riho Nishikawa for always be kind to me. I also would like to express my appreciation to our best Yamaguchi laboratory's secretary, Masami Matsumoto who always cheerful and kind to us. Not to forget, our kind assistant professor, Dr. Takumitsu Kida who helped me a lot before and after my defense.

It is my privilege to thank to my husband, Muhammad Shahrulnizam Nasri for his constant encouragement throughout my research study.

I would like to acknowledge Kuraray Co., Ltd., Japan who was kindly provided the PVA for analysis and measurements.

Finally, I would like to express my deepest gratitude to my family for all their blessed and support during my PhD journey.

Contents

Chapter 1 General introduction

1-1 History and development of PVA

Poly(vinyl alcohol) (PVA) is a polymer of vinyl alcohol. However, its production method has a limitation because the vinyl alcohol monomer cannot be isolated nor obtained at high concentration. Therefore, PVA is known as a special synthetic polymer that is not prepared from the monomer. In 1924, two researchers, H. Haehnel and W. O. Herrmann tried to mix a clear poly(vinyl acetate) (PVAc) solution with an alkali to saponify the polymeric ester. Fortunately, from that experiment, they successfully produced an ivory white-colored PVA [1]. At first, PVA was practically used as a wrap sizing material in rayon textiles. Eventually, the uses of PVA were expanded as a stabilizer in emulsion polymerization, at which it acts as an emulsifier and thickening agent for aqueous dispersions.

In 1931, they registered PVA for a patent and claimed that the fiber can be produced from the dry and wet spinning method. The high cohesive strength with physical and chemical treatments greatly improves the water resistance and makes it possible to be used for textile application [2]. After that, applications of PVA were expanded continuously for various purposes including a thread for surgical as a silk and catgut replacement [3].

1-2 Molecular structure of PVA

1-2-1 Chain configuration

It has been shown that industrial polymerization process for PVA predominantly

produce polymer chains bearing the substituents on alternate carbon atoms with successive monomer units oriented in the same direction, thus creating a head-to-tail or 1,3-glycol structure [4]. This type of structural arrangement reflects the selectivity of monomer addition to the free-radical chain polymerization. Despite the predominance of the 1,3-glycol structure, study shows that the head-to-head or tail-to-tail structure are also possible, in which a pair of substituents alternate regularly on consecutive carbon atoms. These arrangements yield a 1,2-glycol structure. Commercial PVA product usually contains about 1-2% of head-to-head or tail-to-tail configurations with 1,2-glycol units, an amount that is considered to have insignificant influence on the physical properties of PVA [5,6]. Figure 1.1 shows the head-to-head and head-to-tail configurations of PVA.

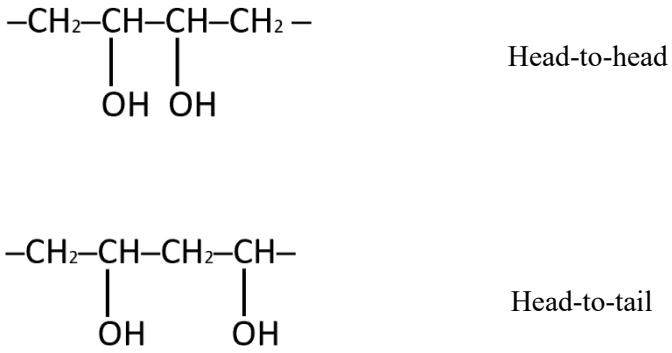

Figure 1.1 Head-to-head and head-to-tail configurations of PVA.

1-2-2 Tacticity

The three stereo regularities of isotactic, syndiotactic, and atactic can be obtained depending on the type of vinyl ester monomer used to produce the PVA. The conventional polymerization of vinyl acetate and subsequent hydrolysis of PVA results mainly in atactic configuration with substituents randomly oriented on either side of the polymer

backbone. Various vinyl monomer is used to obtain a variety of stereo regularities, including vinyl pivalate, *t*-butyl vinyl ether, benzyl vinyl ether, and vinyl formate [7-10]. In general, the ninyl ether monomers yield isotactic-rich polymers, while the vinyl esters yield syndiotactic-rich polymer [11]. High molecular weight of PVA with high syndiotacticity was successfully prepared from saponification of vinyl pivalate. The effect of the tacticity of PVA on its physical properties is known to be significant. An increase in the syndiotacticity of PVA has been reported to affect the physical properties such as solubility in the solvents, melting temperature, heat resistance, tensile strength, and the modulus [12,13]. Figure 1.1 shows the three stereo regularities of isotactic, syndiotactic, and atactic of PVA.

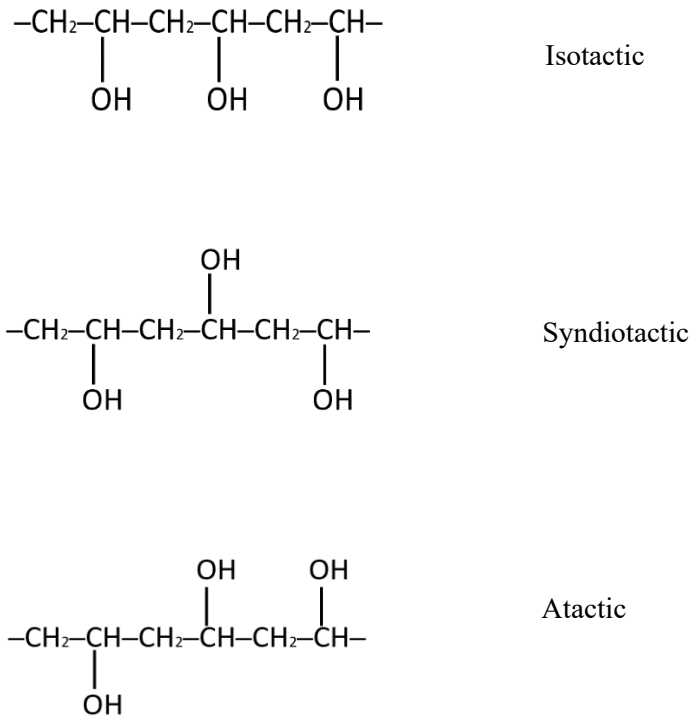

Figure 1.2 Stereo regularities of isotactic, syndiotactic, and atactic of PVA.

1-3 PVA fiber

Generally, the starting process of PVA production is the saponification either by

full or partial hydrolysis of poly(vinyl acetate) (PVAc). Basically, the production of PVA fiber is possible only via dry and wet-spinning. In contrast, a melt-spinning method is not appropriate because pure PVA itself is not melted even by heat treatment process. Therefore, a PVA aqueous solution is used for the most common methods to produce fiber. Compared to the other synthetic fibers, PVA fiber is generally soluble in water after the spinning process. Therefore, the PVA fiber needs to undergo some treatment methods before using in textile industry to enhance their water resistance by hot air treatment following acetalization [9]. Figure 1.3 shows the manufacturing process of PVA fiber.

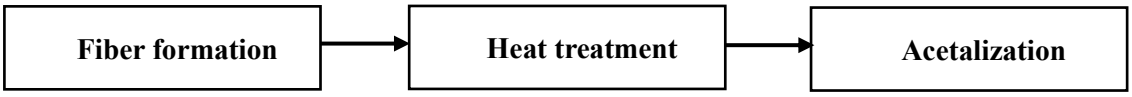

Figure 1.3 Flow for the manufacture of PVA fiber [9].

1-3-1 Wet-spinning process

The wet-spinning was named after the processing technique as the fibers are extruded directly into a coagulation bath. For the wet-spinning process, PVA was firstly dissolved in a hot water to produce a PVA spinning solution. Once PVA was totally dissolved, the filtration process will take place to remove all the residual that will cause a problem during spinning process. Later on, the spinning solution will directly be extruded through fine holes of a spinneret into the saturated aqueous solution of sodium sulphate that acts as a coagulation bath. The fiber is then dried, drawn in hot air, and undergoes for heat treatment process. The schematic illustration of wet-spinning process

is shown in Figure 1.4.

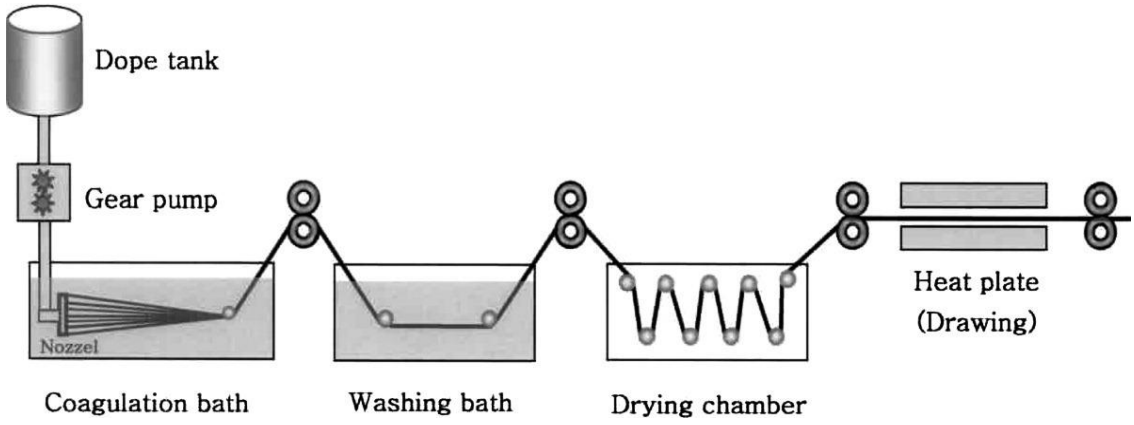

Figure 1.4 Schematic illustration of wet-spinning process [10]

1-4 Modification of polymers using additives

Poor physical properties for a certain single plastic material restrict engineering applications. Therefore, their improvements are requested. In particular, modifications by a simple addition of another material [11-17] are preferred from the viewpoints of cost-performance as compared with synthesis of new materials. Such modifications improve the glass transition temperature T_g, durability, heat resistance, molecular orientation, and crystallinity based on our specific requirement [18-21]. However, for polymer blends, the selection of the materials need to be concerned as most of different polymers are immiscible, and thus, their blends often have a coarse morphology, leading to poor mechanical properties. Therefore, in order to obtain a homogenous polymer blend, the selection of additives plays an important role.

1-4-1 Modification of polymers with nanoparticles

Among various additives, nanoparticles are well known to improve physical and

mechanical properties of a polymer, such as strength, thermal stability, rigidity, and hydrophilicity [17,22]. There have been a lot of reports on the modification of PVA properties by nanoparticles. For instance, Cheng et al. reported that the addition of graphene oxide (GO) nanoparticles greatly improved the mechanical properties such as the tensile strength and Young's modulus of PVA films. Furthermore, it was also revealed that the GO addition enhanced toughness of PVA film and increased the rigidity [17].

A similar technique is also applicable for different nanoparticles. Li et al. reported that PVA composites show a good mechanical strength and hydrophilicity surface after the modification with graphene oxide and carbon nanotubes. The properties were significantly improved with these nanoparticles [23].

1-4-2 Modification of PVA with salts

Although PVA is known to show high mechanical strength, its properties still have the limitation, especially for fiber application. In wet-spinning process, it is difficult to attain a high molecular orientation because of the strong intermolecular hydrogen bonding between hydroxyl groups. Therefore, the addition of a salt is a good method to reduce the hydrogen bonding, but still a challenging method to enhance the molecular orientation of PVA fiber. Figure 1.5 shows the illustration on the concept of the effect of the salt addition on the PVA crystal, and chain orientation after stretching.

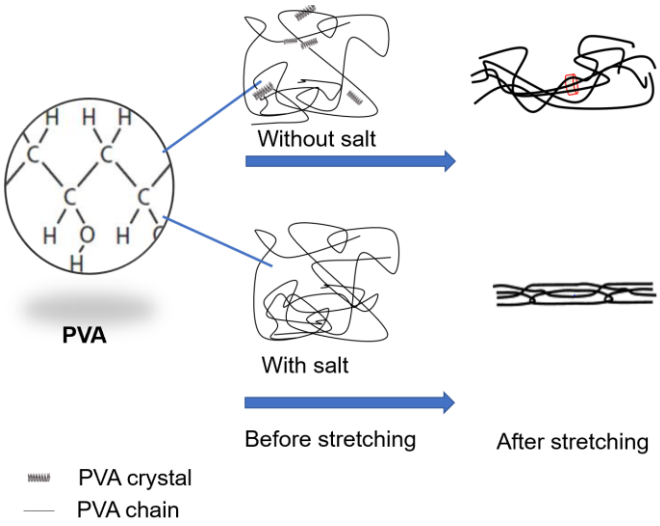

Figure 1.5 Schematic illustration of the effect of salt addition on the structure of PVA

The addition of a salt has been studied by previous researchers to improve the mechanical properties of PVA. Jiang et al. reported that PVA films with inorganic salts, such as LiCl, $MgCl_2$, $CaCl_2$, and $AlCl_3$, showed a low crystallinity and higher elongation than pure PVA [22]. Another study by Patachia et al. revealed that the addition of a salt, such as NaCl, $NaNO_3$, and Na_2SO_4, gave a different result in terms of crystallinity and mechanical properties. The data reported show that the ions present in the PVA solution influence the interaction between PVA -water and PVA-PVA chains [23].

1-5 Interaction between PVA and ions species

Since PVA has hydroxyl groups as the main substituents in the chain as shown in Figure 1.6, the properties of PVA are dependent strongly upon to its structure. The high modulus and strength of PVA fibers also come from the hydrogen bonding of PVA itself. However, this strong intermolecular interaction prohibits high level of molecular orientations. Therefore, the modulus of commercially available PVA fiber is significantly lower than the theoretical value of the perfectly oriented fiber.

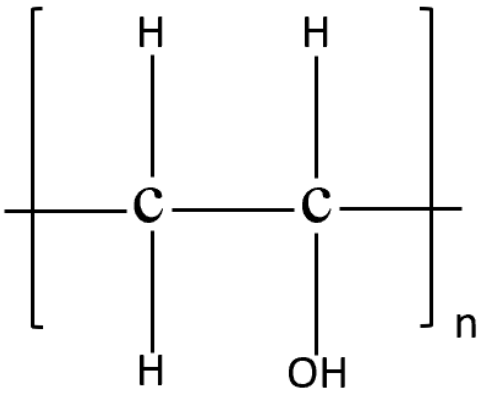

Figure 1.6 Structure of poly(vinyl alcohol) [24]

The interaction between polar polymers and cations has attracted many researchers' interests to study more details. Tomie et al. reported the effect of the lithium trifluorometahnesulfonate ($LiCF_3SO_3$) addition on the thermal and mechanical properties of poly(lactic acid) (PLA). They found that T_g was enhanced without any loss of transparency of the PLA film. This was attributed to the ion-dipole interaction between the lithium cation and oxygen atoms in the carbonyl group of PLA [25]. Another study by Sato et al. using polyamide 6 (PA6) with LiBr also revealed that a strong ion-dipole interactions can be found between the dissociated LiBr, i.e., the amide groups in PA6 and the lithium cations. The ion-dipole interactions restricted segmental motion, which is much stronger than the hydrogen bonds in PA6 chains [26]. To specify the capability of an interaction with a polar polymer, Mohan et al. employed an ion with a larger radius and found that it has a weaker interaction force with PVA chains [27].

1-6 Hofmeister series (HS)

The Hofmeister series (HS), which was found in 1888, originally described the order of the ability for ion to be dissolved in aqueous solution [28]. It explains the solubility tendency of macromolecules (originally, protein), which strongly depends on

the species and concentration of the ions [29-32]. The order of the anion and cation series according to the HS was relevant as it was not only found in protein precipitations, but also in a variety of macroscopic phenomenon such as electrolyte solution and hydrogel [33,34].

As shown in Figure 1.7, the ions in the left side of the HS have a low solubility of macromolecules in a solvent, known as a kosmotopes or water-structure-maker, and has a salting out (aggregate) effect. In contrast, the ions in the right side have a high solubility of macromolecules, known as a chaotropes or water-structure-breaker, and has a salting in (solubilize) effect [35]. The HS originally explained in terms of the ability of various ions to "make" or "break" bulk water structure [33-36].

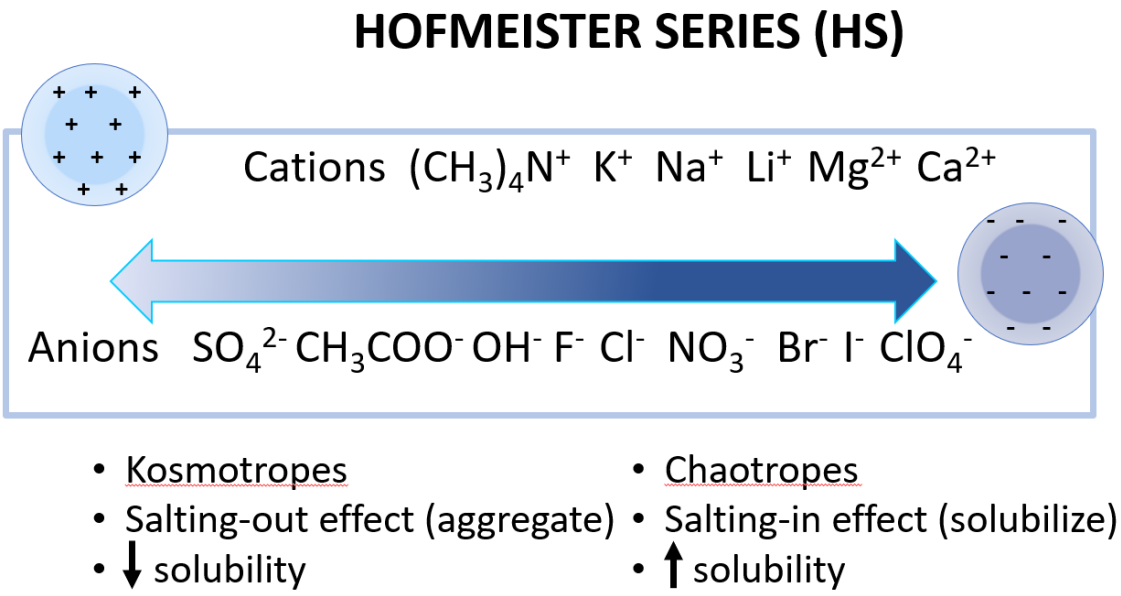

Figure 1.7 Hofmeister series

The concept of Hofmeister series is firstly used to explain the interaction between PVA and different ions in this research study.

1-7 Objectives of the study

This research is performed to modify mechanical properties of PVA by the salt addition, in order to reduce and enhance the hydrogen bonding within the PVA chains in accordance to HS concept. The rheological properties, physical and mechanical properties of PVA aqueous solution, films, and fibers were studied in detail.

Chapter 1 General introduction

The obtained results were systematically summarized for material design for films and fibers, in which the concept of the HS was originally introduced to understand the structure and properties. This thesis is composed of the followings:

Chapter 2 Rheological properties for aqueous solution of PVA with lithium salts

The viscoelastic properties of aqueous PVA solutions incorporating various salts were measured by using specific techniques to avoid vaporization of water during measurements. In particular, the rheological properties were investigated in term of the effect of the anion species of lithium salts and the results were summarized in relation to the HS. Since Li^+ is classified as a water-structure breaker, which have the capability to decrease the hydrogen bonds in the PVA chains, lithium salts should have a significant impact on rheological properties. However, to the best of my knowledge, there has not yet been a systematic study using lithium salts having different anion species.

Chapter 3 Application of Hofmeister series to structure and properties of PVA films containing metal salt

According to the HS, salts containing I^- or ClO_4^- are classified as water-structure breakers which can enhance their solubility in an aqueous solution. Thus, they reduce the intermolecular hydrogen bonds between PVA chains. Of course, their rheological properties in the aqueous solution are dependent upon the salt species. The difference in the rheological properties must affect the structure and properties of a solution-cast film obtained by drying. Therefore, various salts were employed to prepare PVA films to evaluate their structures and dynamic mechanical properties. The obtained results were discussed further on the basis of the HS. This study will lead to exploitation of new and highly efficient salts (i.e., appropriate cation and anion species) in future.

Chapter 4 Modification of PVA fibers with lithium bromide

Many researchers have tried to develop PVA fiber with a high strength. They found that a high level of molecular orientation was nearly impossible for PVA in general owing to its strong intermolecular hydrogen bonding. However, the research in this thesis proved that the addition of LiBr to an aqueous solution of PVA has the capability to reduce the hydrogen bonding between the PVA chains, since it was classified as water-structure breaker. This suggests the possibility of attaining a high level of molecular orientation. Therefore, LiBr, which was selected by the results in Chapter 3, was added to an aqueous solution of PVA to prepare fibers using a wet-spinning method. The properties and structures of the obtained fibers were characterized in detail.

Chapter 5 Impact of magnesium salt addition to structure and properties of PVA films

Not only lithium salts, but various magnesium salts were also employed to investigate the effect on the structure and properties of PVA. The rheological properties of aqueous solution, crystallization behavior, and mechanical properties of PVA films were investigated. It was found that the phenomenon occurred was in the opposite way to that reported by previous researchers, who added $Mg(NO_3)_2$ and $MgCl_2$ into PVA. These opposite results were attributed to the salt concentration. Furthermore, the phenomenon can be explained by the HS. According to the HS, salts containing CH_3COO^- or SO_4^{2-} can act as water-structure-breakers and decrease the solubility of the PVA aqueous solution, which are different from Br^- and ClO_4^- that increase the solubility of PVA. Subsequently, they enhance the intermolecular hydrogen bonds between PVA chains.

Chapter 6 Conclusion

Whole chapters are summarized using the concept of the HS. The highlights are clarified with a future aspect.

References

1. W. Haehnel, W.O Hermann, German Pat. 450, 1924, 286.
2. W.O Hermann, W. Haehnel, German Pat. 685, 1931, 048.
3. M.P.R. Guambo, L. Spencer, N.S. Vispo, K. Vizuete, A. Debut, D.C. Whitehead, F. Alexis, Natural Cellulose Fibers for Surgical Suture Applications, Polymers 12 (2020) 3042.
4. I. Sakurada, T. Okaya, Handbook of Fiber Chemistry, 2nd ed. New York, Marcel Dekker, 1998.
5. S. Murahashi, Poly(vinyl Alcohol)—Selected Topics on Its Synthesis, Pure Appl. Chem. 15 (1967) 435–452.
6. S. Matsuzawa, Handbook of Thermoplastics, New York, Marcel Dekker, 1997.
7. F.L. Marten, Encyclopedia of Polymer Science and Technology, Hoboken, New Jersey, John Wiley & Sons, 1986.
8. R.T. Fukae, O. Yamamoto, T. Sangen, T. Saso, T. Kako, M. Kamachi, Dynamic Mechanical Behaviors of Poly(vinyl Alcohol) Film with High Syndiotacticity, Polym. J. 22 (1990) 636–637.
9. C. Forder, C, S.P. Armes, N.C. Billingham, Synthesis of Polyvinyl Alcohols with Narrow Molecular Weight Distribution from Poly(benzyl Vinyl Ether) Precursors, Polym. Bull. 35 (1995) 291–297.
10. J.H. Choi, S.W. Ko, B.C. Kim, J. Blackwell, W.S. Lyoo, Phase Behavior and Physical Gelation of High Molecular Weight Syndiotactic Poly(vinyl Alcohol) Solution, Macromol. 34 (2001) 2964–2972.
11. W.S. Lyoo, S.S. Han, J.H. Choi, H.D. Ghim, S.W. Yoo, J. Lee, S.I. Hong, W.S. Ha, Preparation of High Molecular Weight Poly(vinyl Alcohol) with High Yield Using

Low-Temperature Solution Polymerization of Vinyl Acetate, J. Appl. Polym. Sci. 80 (2001) 1003–1012.

12. P.J. Flory, F.S. Leutner, Occurrence of head-to-head arrangements of structural units in polyvinyl alcohol, J. Polym. Sci. A Polym. Chem. 3 (1948) 880–890.
13. T. Yamamoto, R. Fukae, T. Saso, O. Sangen, M. Kamachi, T. Sato, Y. Fukunishi, Synthesis of High Molecular Weight Polyvinyl Alcohol of Various Tactic Contents through Photo-Emulsion Copolymerization of Vinyl Acetate and Vinyl Pivalate, Polym. J. 24 (1992) 115–119.
14. I. Sakurada, Polyvinyl Alcohol Fibers, Marcel Dekker: New York, CRC Press, 1985, Vol 6.
15. Y.S. Chung, S.I. Kang, O.W. Kwon, D.S. Shin, S.G. Lee, E.J. Shin, W.S. Lyoo, Preparation of hydroxyapatite/poly (vinyl alcohol) composite fibers by wet spinning and their characterization, J. Appl. Polym. Sci. 106 (2007) 3423-3429.
16. Y. Li, H. Shimizu, Improvement in toughness of poly (l-lactide)(PLLA) through reactive blending with acrylonitrile–butadiene–styrene copolymer (ABS): Morphology and properties, Eur. Polym. J. 45 (2009) 738-746.
17. J. Wu, Y.W. Mai, B. Cotterell, Fracture toughness and fracture mechanisms of PBT/PC/IM blend, J. Mater. Sci. 28 (1993) 3373-3384.
18. S. Patachia, C. Florea, C.H.R. Friedrich, Y. Thomann, Tailoring of poly (vinyl alcohol) cryogels properties by salts addition, Express Polym. Lett. 3 (2009) 320-331.
19. O.N. Tretinnikov, S.A. Zagorskaya, Effect of inorganic salts on the crystallinity of polyvinyl alcohol, J. Appl. Spectrosc. 78 (2012) 904-908.
20. H.K.F. Cheng, N.G. Sahoo, Y.P. Tan, Y. Pan, H. Bao, L. Li, J. Zhao, Poly (vinyl

alcohol) nanocomposites filled with poly (vinyl alcohol)-grafted graphene oxide, ACS Appl. Mater. Inter. (2012) 2387-2394.

21. X. Jiang, H. Li, Y. Luo, Y. Zhao, L. Hou, Studies of the plasticizing effect of different hydrophilic inorganic salts on starch/poly (vinyl alcohol) films, Int. J. Biol. Macromol. 82 (2016) 223-230.
22. S. Kashyap, S.K. Pratihar, S.K. Behera, Strong and ductile graphene oxide reinforced PVA nanocomposites, J. Alloys Compd. 684 (2016) 254-260.
23. H.G. Karian, Handbook of Polypropylene and Polypropylene Composites, New York, Wiley Interscience, 1999.
24. J. Karger-Kocsis, Polypropylene-Structure, Blends and Composite, London, Springer, 1995.
25. W.C.J. Zuiderduin, C. Westzaan, J. Huetink, R.J. Gaymans, Toughening of polypropylene with calcium carbonate particles, Polymer, 44 (2003) 261-275.
26. Y. Li, T. Yang, T. Yu, L. Zheng, K. Liao, Synergistic effect of hybrid carbon nantube–graphene oxide as a nanofiller in enhancing the mechanical properties of PVA composites, J. Mater. Chem. 21 (2011) 10844-10851.
27. X. Jiang, H. Li, Y. Luo, Y. Zhao, L. Hou, Studies of the plasticizing effect of different hydrophilic inorganic salts on starch/poly (vinyl alcohol) films, Int. J. Biol. Macromol. 82 (2016) 223-230.
28. S. Patachia, C. Florea, C.H.R. Friedrich, Y. Thomann, Tailoring of poly (vinyl alcohol) cryogels properties by salts addition, Express Polym. Lett. 3 (2009) 320-331.
29. R. Jayasekara, I. Harding, I. Bowater, G. Lonergan, Biodegradability of a selected range of polymers and polymer blends and standard methods for assessment of

biodegradation, J. Polym. Environ. 13 (2005) 231-251.

30. S. Tomie, N. Tsugawa, M. Yamaguchi, Modifying the thermal and mechanical properties of poly (lactic acid) by adding lithium trifluoromethanesulfonate, J.Polym. Res. 25 (2018) 1-6.
31. Y. Sato, A. Ito, S. Maeda, M. Yamaguchi, Structure and optical properties of transparent polyamide 6 containing lithium bromide. J. Polym. Sci. B Polym. Phys. 56 (2018) 1513-1520.
32. V.M. Mohan, W. Qiu, J. Shen, W. Chen, Electrical properties of poly (vinyl alcohol)(PVA) based on LiFePO 4 complex polymer electrolyte films, J. Polym. Res. 17 (2010) 143-150.
33. J. Wang, M. Satoh, Novel PVA-based polymers showing an anti-Hofmeister series property, Polymer 50 (2009) 3680-3685.
34. P. Jungwirth, B. Winter, Ions at aqueous interfaces: From water surface to hydrated proteins, Annu. Rev. Phys. Chem. 59 (2008) 343-366.
35. W.F. McDevit, F.A. Long, The Self-Interaction of Mandelic Acid as Determined from Solubilities in Salt Solutions, J. Am. Chem. Soc. 74 (1952) 1090-1091.
36. E. Thorman, RSC Advances, 2012, 2, 8297-8305.
37. W.J. Xie, Y.Q. Gao, A simple theory for the Hofmeister series, J. Phys. Chem. Lett. 4(2013) 4247-4252.
38. T. Nakano, H. Yuasa, Y. Kanaya, Suppression of agglomeration in fluidized bed coating. III. Hofmeister series in suppression of particle agglomeration, Pharm. Res. 16 (1999) 1616-1620.
39. S. Nihonyanagi, S. Yamaguchi, T. Tahara, Counterion effect on interfacial water at charged interfaces and its relevance to the Hofmeister series, J. Am. Chem.

Soc. 136 (2014) 6155-6158.

40. Y. Zhang, P.S. Cremer, Interactions between macromolecules and ions: the Hofmeister series, Curr. Opin Chem. Biol. 10 (2006) 658-663.

41. J. Wang, M. Satoh, Novel PVA-based polymers showing an anti-Hofmeister series property, Polymer, 50 (2009) 3680-3685.

Chapter 2 Rheological properties for aqueous solution of poly (vinyl alcohol) with lithium salts

2-1 Introduction

2-1-1 PVA aqueous solution

As mentioned in Chapter 1, PVA is one of the most useful polymers for various engineering applications. It is necessary to study rheological properties of PVA aqueous solution to understand more details about their interaction and phenomenon that occurs in the PVA aqueous solution. For PVA aqueous solutions, the rheological properties directly affect the solid-state properties of the end product attributed by the inter- and intramolecular hydrogen bonds between hydroxyl groups [1,2]. The previous study by Gao et al. on the rheological properties of PVA aqueous solutions with various concentrations (10 wt% to 25 wt%) found that as the concentration increased, the storage modulus increased. Therefore, it was very clear that the intermolecular hydrogen bonds and shear-induced orientation in the solution, affect the rheological properties of such solutions [3].

2-1-2 Interaction between PVA and metal salts in an aqueous solution

The mechanical properties of a polar polymer were changed by the addition of metal salts. Patachia et al. found that the shear storage modulus G' was much higher than the loss modulus G'' for an aqueous solution containing 12 wt% PVA at room temperature [4]. This phenomenon occurs because the solution behaved like a solid attributed by its network structure. Besides, they proved that the interamolecular hydrogen bonds were well-developed by the addition of cations such as Na^+ and K^+. The effects of the addition of sodium chloride (NaCl) on the physical properties of PVA hydrogel systems was studies by Yamaura and Natoh [5]. They found that the crystallinity increased with the NaCl content.

2-1-3 Viscosity of PVA solution

The relationship between the viscosity and the concentration of dilute aqueous solution of PVA is important for estimating the limiting viscosity number [η]. The viscosity of the concentrated aqueous solution, especially the spinning solution, is technically important for the spinning process. When aqueous solution of PVA is allowed to stand for a long time at room temperature or at low temperatures, the viscosity of these solutions increases progressively with time and the fluidity ultimately disappears. The viscosity change in the initial stage is expressed by the following equation:

$$\eta_{0t} = \eta_{00}\,(1+\alpha t) \tag{2.1}$$

where η_{00} is the initial zero-shear viscosity of the solution, η_{0t} is the zero-shear viscosity at a time t, and α is a constant. The constant α is independent of the mean degree of polymerization and of its distribution, but is dependent on the concentration as shown:

$$\alpha = KC^2 \tag{2.2}$$

The increase in the viscosity of a PVA solution becomes remarkably smaller for PVA containing several amounts of acetyl groups [6], for a copolymer composed of vinyl alcohol with allyl alcohol [7], and for a copolymer of vinyl alcohol and a small amount of isopropenyl alcohol [8].

2-2 Experimental

2-2-1 Materials

A commercially available PVA with a degree of polymerization of 1700 and a saponification of 99.8 mol% was kindly provided by Kuraray Co., Ltd., Japan. The other PVA with saponification of 99.5 mol% was kindly provided by Japan Vam & Poval (grade code VH). The lithium salts, such as lithium chloride (LiCl), lithium bromide (LiBr), and lithium iodide (LiI), were bought from Sigma Aldrich in bead or powder form. Potassium bromide (KBr) and sodium bromide (NaBr) were purchased from Kanto Chemical Co., Ltd., Japan. All these salts were used without further purification. The deionized water was used throughout the study.

2-2-2 Preparation of aqueous solution

The lithium salts such as LiI and LiBr were added to the solutions at various molar ratios; 0, 0.025, 0.050 and 0.100 relative to the quantity of PVA hydroxyl groups, while the other salts were always added at a 0.100 molar ratio. The concentration of PVA was fixed at 15 wt%. Each PVA aqueous solution was prepared by dissolving 7.5 g of PVA in 42.5 mL of deionized water at 90 °C using a magnetic stirrer operating at 400 rpm. Then, the salt was subsequently added with continued stirring at 400 rpm for approximately 3 h until complete dissolution.

2-2-3 Measurements

The rheological properties of each solution were evaluated using a parallel-plate rheometer with a 40 mm diameter (TA instruments, AR2000ex, New Castle, USA). The frequency sweep tests were carried out from 0.05 to 500 rad/s at various temperatures. All measurements were carried out within the linear viscoelastic region because the strain level was determined by the strain sweep test. A schematic illustration of the rheology measurement apparatus is shown in Figure 2.1. The gap between plates was 1 mm and the plates were covered with a wet filter paper (Advantec, Toyo Roshi Kaisha, Japan) inside a solvent trap system, in order to increase the humidify in the system. Besides, water was also added to the top of the upper plate to increase the humidity in the system and a coating of di-2-ethylhexyl phthalate (DOP) was applied to the sample edges to inhibit water vaporization. This coating did not affect the experimental measurements because the viscosity of DOP (approximately 56 mPa·s at 25 °C) which is much lower than that of a PVA solution. The temperature was precisely controlled by the Peltier system with a fluid circulator. Each measurement was repeated at least three times without changing the sample to confirm that water vaporization was minimized.

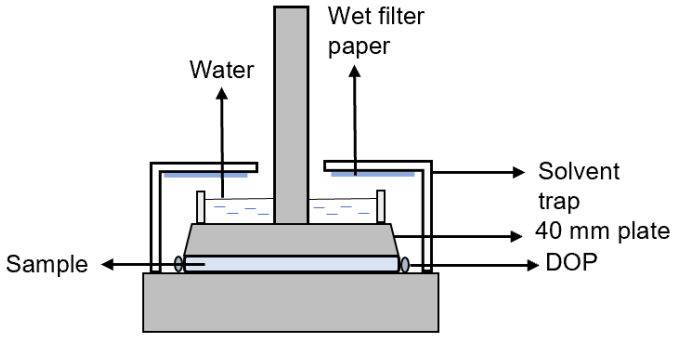

Figure 2.1 Parallel-plate geometry and solvent trap system employed in this study.

The shear viscosity of each solution was determined also using an electro-magnetically spinning sphere (EMS) viscometer (EMS-1000, Kyoto Electronics Manufacturing Co., Japan) at Tosoh Analysis Center Co., Ltd., Japan. In these trials, a metal sphere with a 2 mm diameter was immersed in the sample solution, and a rotating 100 mT magnetic field was generated by two permanent magnets attached to the rotor [9]. A capped glass tube with a 6 mm diameter that restricted water vaporization was used as the sample cell, and measurements were performed at various temperatures. Two trials were carried out at each temperature and the mean values were reported.

2-3 Results and Discussion

2-3-1 Reproducibility of the rheological measurements

Figure 2.2 shows the angular frequency ω dependence of the oscillatory shear moduli, storage modulus G' and loss modulus G'', for an aqueous solution of PVA at room temperature. In order to confirm that water vaporization was negligible, each measurement was repeated three times without changing the sample. Since the frequency sweep test need 20 minutes, it takes 60 minutes for whole measurements. As shown in Figure 2.2, rheological data at 60 °C can be obtained by using the parallel-plate geometry with the solvent trap system.

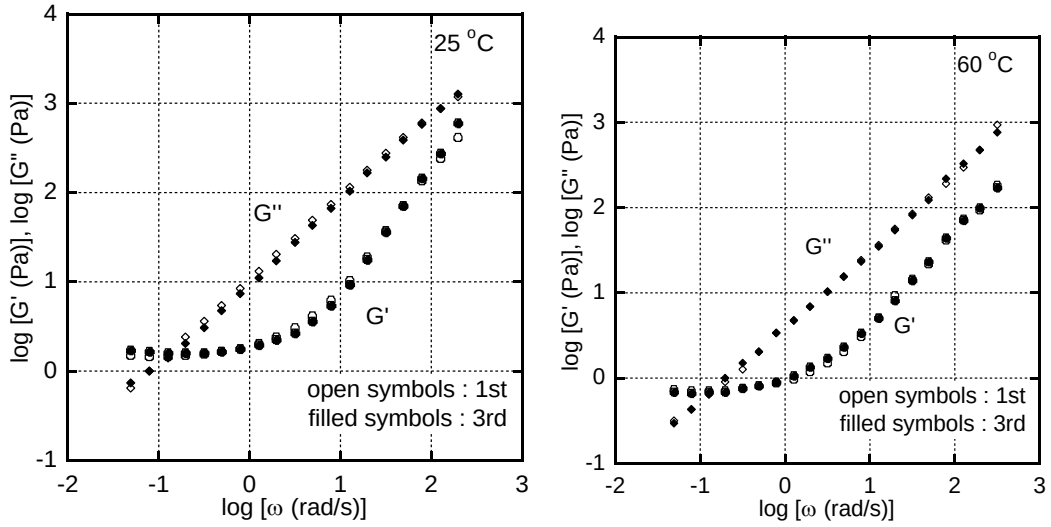

Figure 2.2 Angular frequency dependence of the shear storage modulus *G'* and loss modulus *G"* of an aqueous PVA solution at 25 °C and 60 °C.

The dynamic viscosity is not greatly affected by the angular frequency (Newtonian) as the the slope of the G'' data is almost proportional to the angular frequency. Since G' exhibits a plateau at low frequencies, the viscoelastic properties are not in the Newtonian region. This phenomenon was also reported by Li et al. [10], and will be discussed in detail later. It should also be noted that the frequencies at which the plateau appears are much lower than the inverse of the average relaxation time ascribed to entanglement couplings.

2-3-2 Effect of degree of saponification

The viscoelastic properties of solution (15 wt%) at 25°C was presented in Figure 2.3. It was apparent that $PVA_{99.8}$ and $PVA_{99.5}$ showed almost similar G' values at high frequencies. However, $PVA_{99.8}$ showed a lower plateau modulus in the low frequency. This will be attributed to strong hydrogen bonding [11]. G'' of the $PVA_{99.5}$ solution was

lower than that of the $PVA_{99.8}$ solution, demonstrating that the $PVA_{99.5}$ solution had lower shear viscosity.

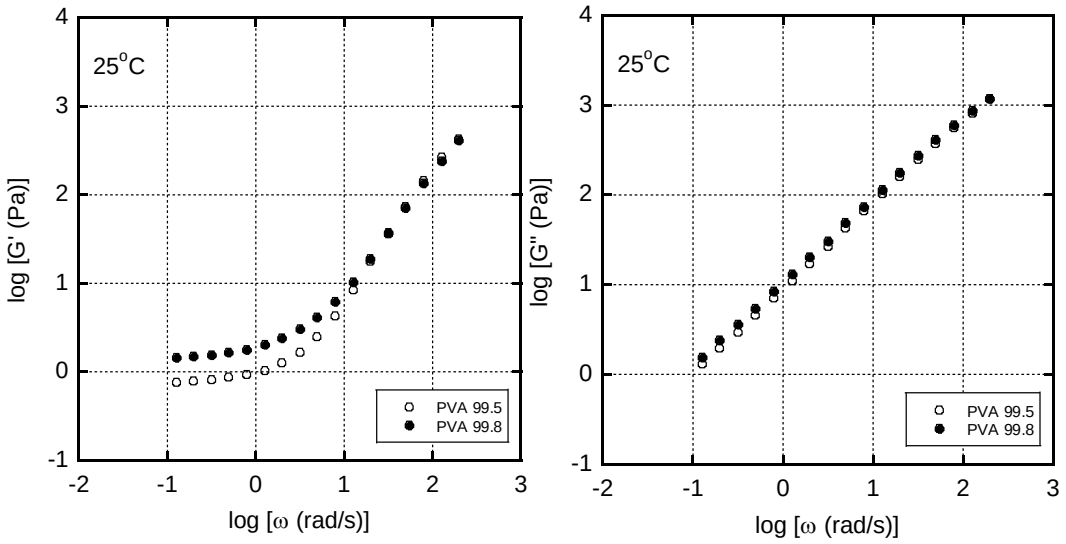

Figure 2.3 Angular frequency dependence of the shear storage modulus *G'* and loss modulus *G''* of aqueous solutions with $PVA_{99.8}$ and $PVA_{99.5}$ at 25 °C

Similar viscoelastic properties were detected at 40 °C and 60 °C as shown in Figure 2.4 and Figure 2.5. The plateau value of G' in the low frequency was sensitive to the temperature for $PVA_{99.5}$. Both moduli, i.e., G' and G'', decreased as the temperature increased because the interaction between PVA chains became weak. It was found that higher degree of saponification, $PVA_{99.8}$, provided stronger hydrogen bonds.

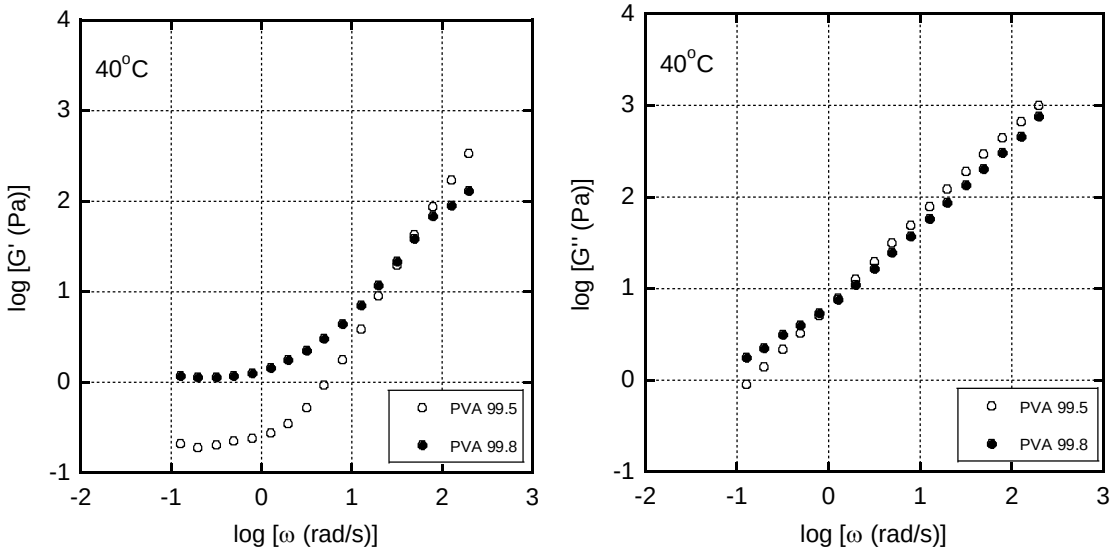

Figure 2.4 Angular frequency dependence of shear storage modulus G' and loss modulus G'' of an aqueous PVA solution with $PVA_{99.8}$ and $PVA_{99.5}$ at 40 °C

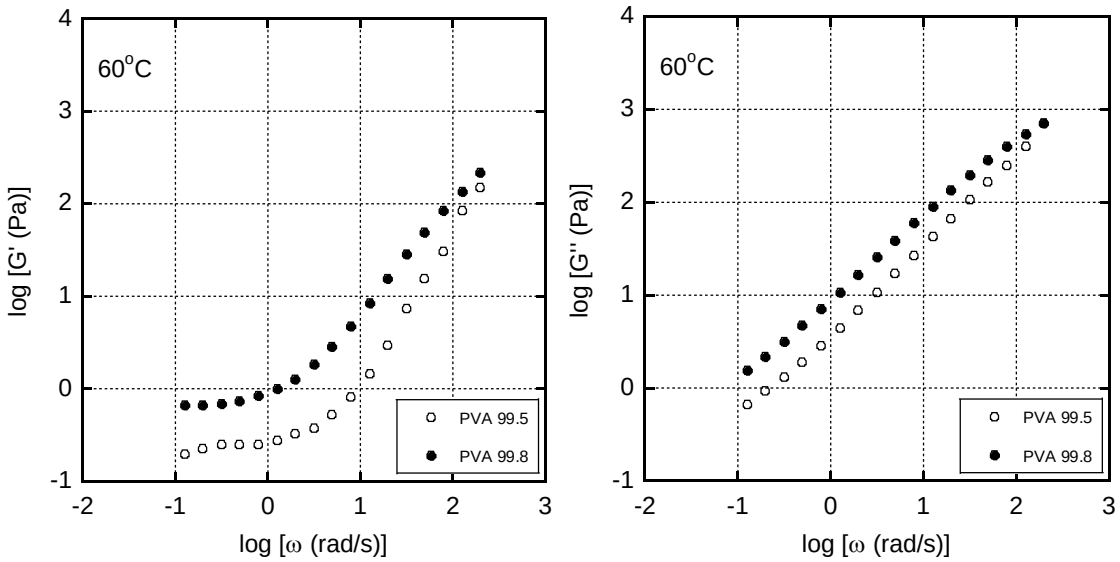

Figure 2.5 Angular frequency dependence of shear storage modulus G' and loss modulus G'' of aqueous solutions with $PVA_{99.8}$ and $PVA_{99.5}$ at 60 °C

2-3-3 Effect of temperature

The rheological measurements were performed at various temperatures because the viscoelastic properties were greatly affected by the hydrogen bonding, and very sensitive to ambient temperature [12]. Therefore, the flow activation energy and temperature dependence of the plateau modulus were measured. The angular frequency dependence of G' and G'' at 25, 40 and 60 °C was shown in Figure 2.6. It can be seen from the data that the plateau modulus in the low frequency region decreased with temperature, indicating that the time-temperature superposition principle is not applicable for the system. This finding is expected as the hydrogen bonding is weakened at high temperatures.

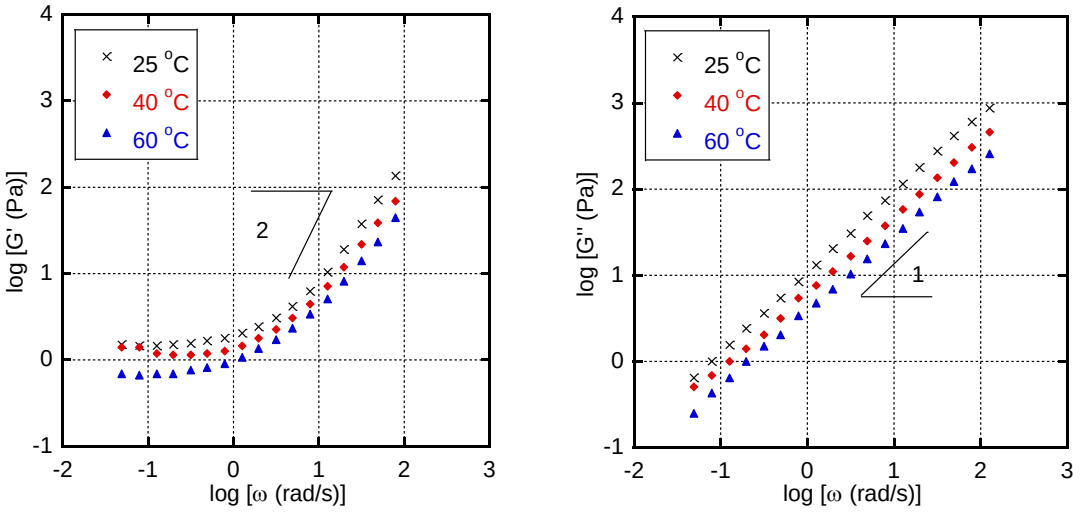

Fig. 2.6 Angular frequency dependence of shear storage modulus *G'* and loss modulus *G"* of an aqueous PVA solution at various temperatures.

As reported by many researchers, the formation of a network structure based on hydrogen bonding provides a plateau in the G' curve [12-15]. According to the classical theory of rubber elasticity [16], the average molecular weight between neighboring

crosslink points M_x can be calculated using the plateau modulus G_{pl} as:

$$M_x = \frac{\rho RT}{G_{pl}} , \tag{2.3}$$

where ρ is the density and R is the gas constant.

M_x is calculated to be 1.7 x 10^7, as the density at room temperature is approximately 1000 kg/m^3 and G_{pl} is 1.48 Pa. The critical molecular weight, which equals approximately twice the entanglement molecular weight M_e, is known to be in the range of 5300-7500 for PVA [17]. Because M_e in a solution is inversely proportional to the volume fraction of the polymer [18], the M_e value for the present 15 wt% solution is estimated to be in the range of 18,000-25,000. Therefore, M_x is much larger than M_e. Considering that the average molecular weight M is calculated to be approximately 78,000, there are three to four entanglement couplings in a PVA chain on average.

The angular frequency dependence of G'' at various temperatures was shown in Figure 2.6. As the temperature increases, the G'' decreases monotonically. Because the slope of G'' plot is close to 1, the zero-shear viscosity η_0, given by G''/ω, can be estimated to be approximately 1.11, 0.88, and 0.68 Pa·s at 25, 40, and 60 °C, respectively. Moreover, the apparent flow activation energy is calculated to be 28.2 kJ/mol.

2-3-4 Interaction between PVA and metal salts in an aqueous solution

Figure 2.7 summarizes the angular frequency dependence of the oscillatory shear moduli at 25 °C for PVA solutions with various lithium salts. The salt was added at a 0.1 molar ratio relative to the quantity of hydroxyl groups in an aqueous solution of PVA. Obviously, the plateau modulus in the low frequency region decreased and gave a lower G'' value by the addition of a salt. These results are due to the reduction of hydrogen bondings between PVA chains; i.e., the intermolecular interactions are reduced by the

addition of the salt. A similar phenomenon was found by Briscoe et al. in the study using NaCl [19]. These data proved that the anion species affects the rheological properties of the solution, even though it was known that Li^+ breaks the hydrogen bonds [20-23]. The figure also shows that the lowest plateau modulus was obtained in the PVA solution with LiI, while a similar plateau modulus is seen for the solutions containing LiBr and LiCl. This phenomenon can be explained by the HS theory [24-26]. Weakly hydrated anions such as I^- and SCN^-, known as chaotropes or water-structure-breakers. In accordance to HS, they exhibit the salting-in effect. Besides, strongly hydrated anions such as SO_4^{2-} is known as kosmotropes or water-structure-makers, where it shows a salting-out effect that causes deswelling of aqueous hydrogels. Thus, LiI will reduce hydrogen bonds between PVA chains because it act as a water-structure-breaker in an aqueous PVA solution. These results indicated that LiI has a significant effect on the rheological properties of the aqueous solutions, further trials were performed by varying the LiI concentration.

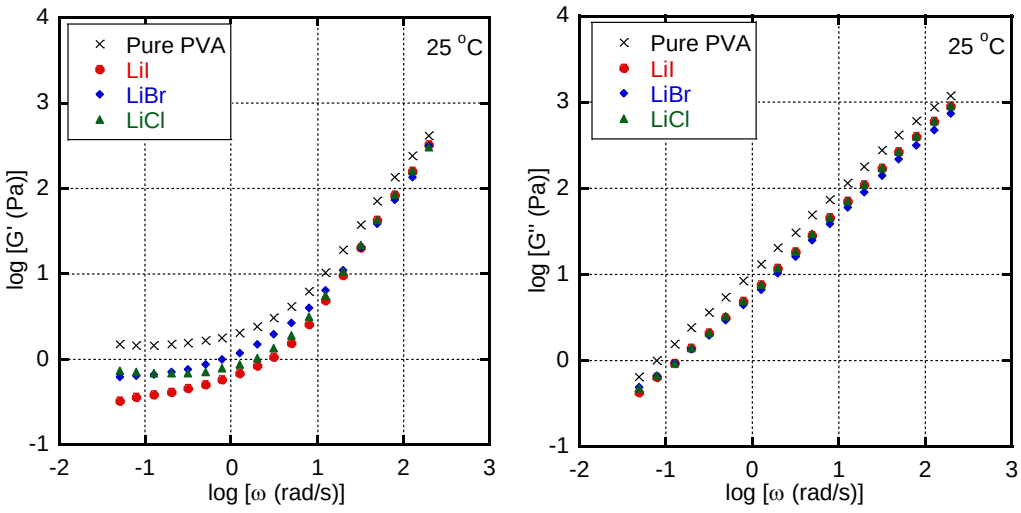

Figure 2.7 Angular frequency dependence of the oscillatory shear moduli at 25 °C for aqueous PVA solutions with various lithium salts added at a 0.1 molar ratio.

2-3-5 Effect of salt concentration

Figure 2.8 shows the angular frequency dependence of the oscillatory shear moduli of aqueous PVA solutions with various concentrations of LiI at 25 °C. As the LiI concentration increased, G_{pl} in the low frequency region decreased while G'' also decreased. However, the G_{pl} value for the solution containing a 0.1 LiI molar ratio was almost equivalent to that with a 0.2 molar ratio. This result indicates that the effect of LiI addition is saturated at a molar ratio of approximately 0.1. Although I^- is known to act as a "water-structure-breaker", the ability to decrease the order in water is saturated at a 0.1 molar ratio. As a result, the G_{pl} does not decrease by a large amount of LiI. In other words, the hydrogen bondings between PVA chains are affected by the structure of water rather than the I^- content [27].

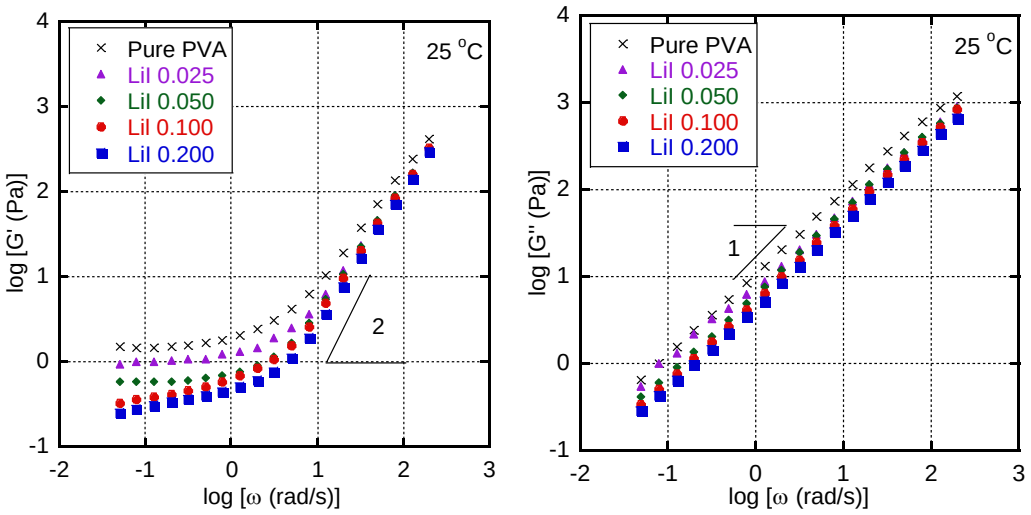

Fig. 2.8 Angular frequency dependence of the oscillatory shear moduli at 25 °C of aqueous PVA solutions containing various concentrations of LiI.

Figure 2.9 summarizes the values of η_0 obtained at different temperatures, which were calculated from G''/ω. It is obviously that η_0 decreases as the temperature. Moreover,

η_0 decreases as the LiI concentration was raised, suggesting that both salt content and the temperature affect the viscosity of the PVA solutions. The viscosity decrease by the addition of the salts was most probably due to the decrease in the inter- and intra-chain hydrogen bondings between PVA chains. The G_{pl} data presented in Figure 2.10 exhibit similar trends, implying that the network structure was not well-developed at high temperatures due to weak hydrogen bonding [35-38]. The LiI addition also reduced the G_{pl} values, although the effect was again saturated at a molar ratio of approximately 0.1 at all temperatures.

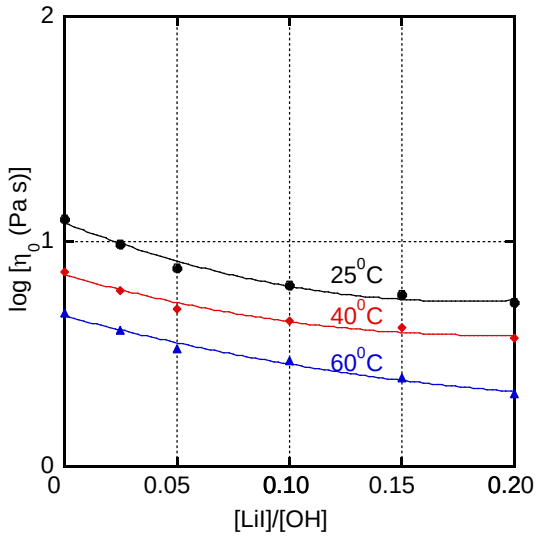

Figure 2.9 Zero-shear viscosity η_0 of aqueous PVA solutions with various LiI concentrations at different temperatures.

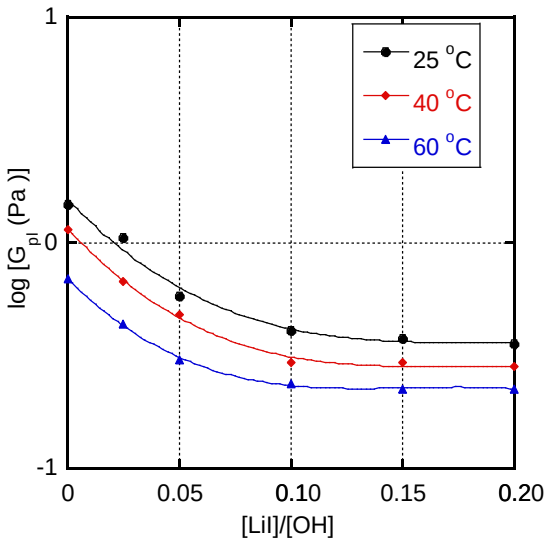

Figure 2.10 Plateau modulus G_{pl} for aqueous PVA solutions with various LiI concentrations at different temperatures.

Figure 2.11 presents the shear viscosity data obtained using the EMS viscometer at various temperatures for samples without LiI and with a LiI molar ratio of 0.1. This measurement method was applicable even at high temperatures because the sample solution was held in a closed system. It should be noted that the viscosity of each solution was measured in the steady-state, and therefore, the network structure would be destroyed during the acquisition of data [20,28]. However, the values obtained using this technique are almost the same as those generated in the oscillatory mode associated with the linear viscoelastic range, suggesting that the viscosity is not dependent upon the shear rate, i.e., Newtonian region. These data also confirmed that the addition of LiI decreases the viscosity to some degree. The steady-state shear viscosity of both specimens gradually decreases with increasing temperature although the difference between the two decreases at high temperatures, indicating that the effect of LiI addition on viscosity is more significant at low temperatures.

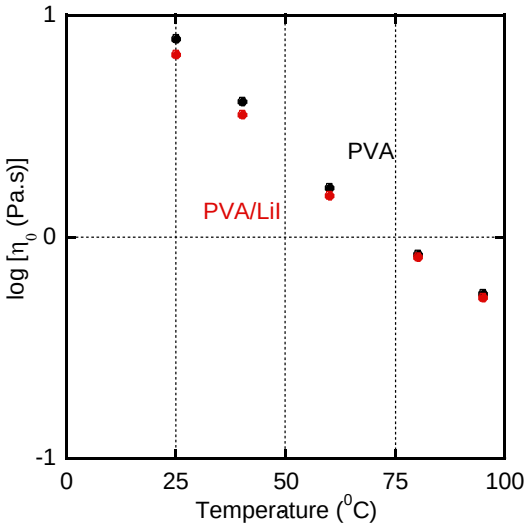

Fig. 2.11 Temperature dependence of zero-shear viscosity η_0 evaluated by an EMS viscometer for aqueous PVA solutions with/without LiI at a molar ratio of 0.1.

2-3-6 Effect of cation species

The effect of cation species in the salts was studied using LiBr, NaBr, and KBr. Figure 2.12 shows the oscillatory shear moduli at 25 °C of PVA solutions with various salts comprising bromide anion Br^-. In each sample, the salt was added at a 0.1 molar ratio relative to the quantity of hydroxyl groups in the PVA. As seen in the figure, the moduli of the solutions with NaBr and KBr are slightly higher than those of the solution without salts. In contrast, the solution containing LiBr shows a lower modulus than those with the other salts. These differences are pronounced in the low frequency region, e.g., G_{pl}. The phenomena also follow the HS, at which the strength of the capability to break the structure of water is in the order of $Li^+ > Na^+ > K^+$ [20, 29-31].

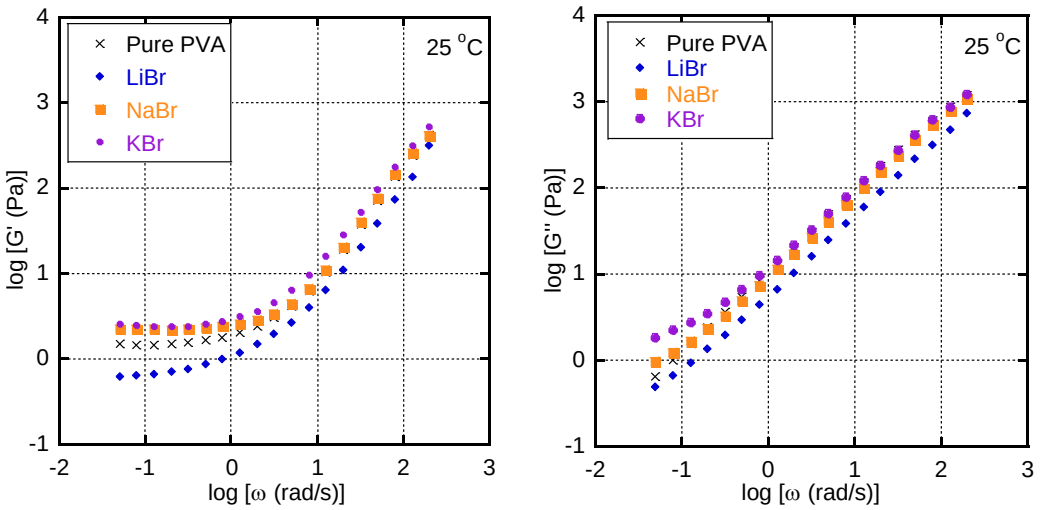

Figure 2.12 Angular frequency dependence of the oscillatory shear moduli at 25 °C of aqueous PVA solutions with various cation species added at a 0.1 molar ratio.

2-4 Conclusion

The rheological properties of aqueous PVA solutions containing lithium salts were studied. At first, reproducibility was examined without changing the sample to confirm that water vaporization was not occurring. The results obtained demonstrate that valid rheological data can be obtained using the parallel-plate geometry with the solvent trap system. Although the hydrogen bonding between PVA chains was greatly affected by the presence of cations, the results demonstrated that the anion also has a significant impact on the rheological properties. Among the lithium salts used, LiI showed the most significant effect, suggesting that iodide ions act as a water-structure-breaker in aqueous PVA solutions. This behavior was well summarized by the HS. As a result of this effect, the shear viscosity was reduced, and the plateau modulus was decreased because the network structure produced by hydrogen bonding was disrupted with the salt addition. However, at high temperatures, the effect of salt addition on the rheological properties becomes insignificant due to the reduced hydrogen bonding at such elevated temperatures.

References

1. K. Yamaura, M. Naitoh, Preparation of high-performance films from poly (vinyl alcohol)/NaCl/H_2O systems, J. Mater. Sci. 37 (2002) 705-708.
2. A. Bhattacharya, P. Ray, Studies on surface tension of poly (vinyl alcohol): effect of concentration, temperature, and addition of chaotropic agents, J. Appl. Polym. Sci. 93 (2004) 122-130.
3. H.W. Gao, R.J. Yang, J.Y. He, L. Yang, Rheological behaviors of PVA/H2O solutions of high-polymer concentration, J. App. Polym. Sci. 116 (2010) 1459-1466.
4. S. Patachia, C. Florea, C.H.R. Friedrich, Y. Thomann, Tailoring of poly (vinyl alcohol) cryogels properties by salts addition, Exp. Polym. Lett. 3 (2009) 320-331.
5. K. Yamaura, M. Naitoh, Preparation of high-performance films from poly (vinyl alcohol)/NaCl/H_2O systems, J. Mater. Sci. 37 (2002) 705-708.
6. S. Matsuzawa, I. Historical Development, Handbook of Thermoplastics, 1997, 41, 269.
7. G. Takahashi, I. Sakaruda, Handbook of Fiber Chemistry, Kobunshi Kagaku, 1956, 13, 502.
8. K. Imai, U. Maeda, M. Matsumoto, Handbook of Fiber Chemistry, Kobunshi Ronbunshyu, 1978, 35, 747.
9. M. Hosoda, T. Hirano, K. Sakai, Low-viscosity measurement by capillary electromagnetically spinning technique, Japanese J. Appl. Phys. (2011) 50 (7S):07HB03.
10. H. Li, W. Zhang, W. Xu, X. Zhang, Hydrogen bonding governs the elastic properties of poly (vinyl alcohol) in water: single-molecule force spectroscopic studies of PVA by AFM, Macromolecules 33 (2000) 33465-469.
11. W.S. Lyoo, J.H. Kim, J.H. Choi, B.C. Kim, J. Blackwell, Role of degree of

saponification in the shear-induced molecular orientation of syndiotacticity-rich ultrahigh molecular weight poly (vinyl alcohol), Macromolecules, 34 (2001) 3982-3987.

12. T. Takigawa, M. Takahashi, K. Urayama, T. Masuda, Comparison of model prediction with experiment for concentration-dependent modulus of poly (vinyl alcohol) (PVA) gels near the gelation point, Chem. Phys. Lett. 195 (1992) 509-512.
13. Chen N, Li L, Wang Q (2007) New technology for thermal processing of poly (vinyl alcohol). Plast, Rubber Compos 36(7-8):283-290.
14. M. Liu. R. Cheng, C. Wu, R. Qian, Viscometric investigation of intramolecular hydrogen bonding cohesional entanglement in extremely dilute aqueous solution of poly vinyl alcohol, J. Polym. Sci. B: Polym. Phys. 35 (1997) 2421-2427.
15. J.S. Park, J.W. Park, E. Ruckenstein, On the viscoelastic properties of poly (vinyl alcohol) and chemically crosslinked poly (vinyl alcohol), J. Appl. Polym. Sci. 82 (2001) 1816-1823.
16. L.R.G. Treloar, The physics of rubber elasticity, Oxford University Press, USA, 1975.
17. S. Arayachukiat, M. Siriprumpoonthum, S. Nobukawa, M. Yamaguchi, Viscoelastic properties and extrusion processability of poly (vinyl butyral), J. Appl. Polym. Sci. 131 (2014) 40337.
18. J.D. Ferry, Viscoelastic properties of polymers, 3rd edn. Wiley, New York, 1980.
19. T. Nakano, H. Yuasa, Y. Kanaya, Suppression of agglomeration in fluidized bed coating. III. Hofmeister series in suppression of particle agglomeration, Pharm. Res. 16 (1999) 1616-1620.

20. H. Nakao, T. Nagaoka, K. Ogura, Ion-exchange ability of polyaniline-polyvinyl alcohol colloids with various anions, Anal. Sci. 13 (1997) 327-331.

21. H. Muta, S. Kawauchi, M. Satoh, Ion-specific swelling behavior of uncharged poly (acrylic acid) gel, Colloid Polym. Sci. 282 (2003) 149-155.

22. S.I. Song, B.C. Kim, Characteristic rheological features of PVA solutions in water-containing solvents with different hydration states, Polymer 45 (2004) 2381-2386.

23. M. Mori, J. Wang, M. Satoh, Anti-Hofmeister series properties found for a polymer having a π electron system and acidic protons, Colloid Polym. Sci. 287 (2009) 123-127.

24. J. Wang, M. Satoh, Novel PVA-based polymers showing an anti-Hofmeister series property, Polymer 50 (2009) 3680-3685.

25. Y. Okazaki, K. Ishizuki, S. Kawauchi, M. Satoh, J. Komiyama, Ion-specific swelling and deswelling behaviors of ampholytic polymer gels, Macromolecules 29 (1996) 8391-8397.

26. M. Takano, K. Ogata, S. Kawauchi, M. Satoh, J. Komiyama, Ion-specific swelling behavior of poly (N-vinyl-2-pyrrolidone) gel: Correlations with water hydrogen bond and non-freezable water Polym. Gels Net. 6 (1998) 217-232.

27. A. Miyagawa, V. Ayerdurai, S. Nobukawa, M. Yamaguchi, Viscoelastic properties of poly(methyl methacrylate) with high glass transition temperature by lithium salt addition, J. Polym. Sci. B: Polym. Phys. 54 (2016) 2388-2394.

28. A. Ito, P. Phulkerd, V. Ayerdurai, M. Soga, A. Courtoux, A. Miyagawa, M. Yamaguchi, Enhancement of the glass transition temperature of poly (methyl methacrylate) by salt, Polym. J. 50 (2018) 857-863.

29. H. Muta, M. Miwa, M. Satoh, Ion-specific swelling of hydrophilic polymer gels, Polymer 42 (2001) 6313-6316.

30. J.H. Choi, S.W. Ko, B.C. Kim, J. Blackwell, W.S. Lyoo, Phase behavior and physical gelation of high molecular weight syndiotactic poly (vinyl alcohol) solution, Macromolecules 34 (2001) 2964-2972.

31. B. Briscoe, P. Luckham, S. Zhu, The effects of hydrogen bonding upon the viscosity of aqueous poly (vinyl alcohol) solutions, Polymer 41 (2000) 3851-3860.

Chapter 3 Application of Hofmeister series to structure and properties of poly(vinyl alcohol) films containing metal salt

3-1 Introduction

3-1-1 Polymer with salt addition

According to previous studies, the PVA crystallization rate is greatly retarded by salts [1-6]. This phenomenon is attributed to restricted segmental motion caused by the interaction between hydroxyl groups and cations. However, the effects of anion species on the thermal and mechanical properties of PVA have not been studied in detail.

Recently, several studies have reported on the addition of metal salts to various polar polymers, including poly(methyl methacrylate) (PMMA) [7-9], polycarbonate [10], poly(lactic acid) [11], polyamide 6 (PA6) [3], and poly(vinyl butyral) [12]. Miyagawa et al. [13] studied the effect of lithium trifluoromethanesulfonate ($LiCF_3SO_3$) on PMMA structures and properties. They found that $LiCF_3SO_3$ is dissociated into free ions in PMMA, and the cations provide ion-dipole interactions with the oxygen atoms in the PMMA chain carbonyl groups. The glass transition temperature (T_g) is greatly enhanced owing to the reduced segmental mobility [13,14]. Sato et al. revealed that LiBr retards the PA6 crystallization rate, and there is a significant increase in T_g owing to strong ion-dipole interactions between the lithium cations and the amide groups [3]. However, the effects of anion species were not investigated in these studies.

3-1-2 Viscoelastic properties of polymers

In general, the properties of solid and liquid are discussed separately, and this separation is useful for various materials. However, polymers are much more complicated

as they exhibit both elastic and viscous behaviors depending on time and temperature, i.e., viscoelastic responses [14]. Therefore, the temperature and frequency dependence of mechanical properties are often measured to investigate the behavior of polymers. One of the most useful methods to determine the viscoelastic behavior is the measurement for dynamic mechanical properties. In this measurement, an oscillatory stress or strain is applied to the film sample. The oscillatory strain is written as the following equation:

$$\gamma(t) = \gamma_o e^{i\omega t} = \gamma_o(\cos \omega t + i \sin\ \omega t) \quad , \tag{3.1}$$

where $\gamma(\mathrm{t})$ is the applied oscillatory strain as a function of time *t*, γ_o is the strain amplitude and ω is the angular frequency in radian/s (equal to $2\pi f$ where *f* is the frequency in cycle/s).

Then, the relationship between stress and strain is written as the following equation:

$$\sigma(t) = [G^{'}(\omega)\ +\ G^{''}(\omega)]\gamma_o e^{i\omega t} = [G^{'}(\omega)\ +\ G^{''}(\omega)]\,\gamma(t) \tag{3.2}$$

where $\sigma(t)$ is stress, $G'(\omega)$ and $G''(\omega)$ are the storage modulus and loss modulus, respectively. In addition, loss tangent, so called tan δ, is obtained as below:

$$\tan \delta = \frac{G^{''}(\omega)}{G^{'}(\omega)} \tag{3.3}$$

The relaxation mechanism of the entanglement chains of a polymer can be estimated by the frequency dependence of storage and loss moduli. The temperature region where the relaxation mechanism is observed reflects the molecular motion of the polymer chain.

3-1-3 Relaxation modes of polymers

Generally, there are two types of polymer structure, i.e., primary structure and higher order structure. Primary structure includes the chemical structure, molecular weight, and its distribution.

The dispersions of the dynamical relaxation modes, related to the local molecular motion in the primary structure, are usually observed in the low temperature region. For example, β dispersion derived from local molecular motion of side chains of a polymer chain can be generally observed in the temperature region below T_g [15,16]. Besides, the effects of the whole structure become dominant in the high temperature region.

3-1-4 Purpose of the study

The rheological properties of aqueous PVA containing various salts evaluated in Chapter 2 revealed that the Hofmeister series (HS), which is often used to determine the role of ion species in polymer solutions (i.e., water-structure breakers or water-structure markers), explained their behavior. According to the HS, salts containing I^- or ClO_4^- can act as water-structure breakers and increase the solubility in PVA aqueous solution. Subsequently, they reduce the intermolecular hydrogen bonds between PVA chains [17-21].

In this chapter, therefore, various salts were used to prepare PVA films and evaluated their structures and dynamic mechanical properties. The obtained results were discussed further on the basis of the HS. The exploitation of new and highly efficient salts (i.e., appropriate cation and anion species) is important and could lead to improvements in PVA film and fiber mechanical properties [22].

3-2 Experimental

3-2-1 Materials

The polymeric material used in this study was commercially available PVA, which was kindly provided by Kuraray Co., Ltd. The degree of polymerization was 1700, and the degree of saponification was 99.8 mol%. Lithium iodide (LiI) and lithium sulfate (Li_2SO_4) were purchased from Fujifilm Wako Pure Chemical Co., Ltd., Japan. Lithium nitrate ($LiNO_3$), lithium chloride (LiCl), potassium bromide (KBr), and sodium bromide (NaBr) were purchased from Kanto Chemical Co., Ltd., Japan. Potassium sulfate (K_2SO_4), lithium bromide (LiBr), and sodium sulfate (Na_2SO_4) were obtained from Tokyo Chemical Industry Co., Ltd., Japan. Lithium perchlorate ($LiClO_4$) was purchased from Nacalai Tesque, Inc., Kyoto, Japan. All salts were used without further purification.

3-2-2 Preparation of aqueous solution

PVA and the salt of interest were dissolved in deionized water at 90°C. The PVA content of the water was fixed at 15 wt%. The molar ratio of the salt to the hydroxyl groups in the PVA was 0.1, which were 3.9 wt% for $LiClO_4$, 3.4 wt% for LiI, 2.4 wt% for LiBr, 2.0 wt% for $LiNO_3$, 1.3 wt% for LiCl, 2.7 wt% for NaBr, 3.1 wt% for KBr, 3.3 wt% for Li_2SO_4, 4.1 wt% for K_2SO_4, and 3.6 wt% for Na_2SO_4. The solution was magnetically stirred until dissolution was complete. The solution was then cast onto a polytetrafluoroethylene-coated tray which was then preheated at 70°C for 6 h. The obtained films were dried at 100°C under vacuum for an additional 5 h. Finally, the sample was dried again at 80°C under vacuum for 4 h to avoid moisture effects before taking measurements. The schematic illustration of this procedure is shown in Figure 3.1.

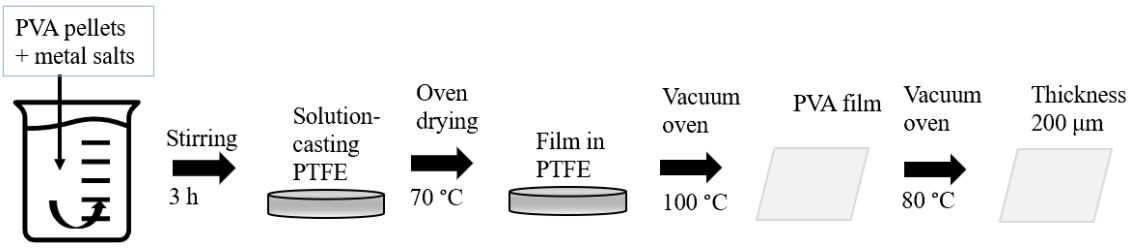

Figure 3.1 Schematic illustration of sample preparation for PVA/ metal salt blend.

3-2-3 Measurements

A dynamic mechanical analyzer (Rheogel-E4000; UBM Co., Ltd., Mukō, Japan) was used to measure the temperature dependence of tensile storage modulus E' and loss modulus E'' from 20°C to 160°C. The applied frequency was 10 Hz, and the heating rate was 2°C/min. Sample films with 200 μm thickness were cut to 5 mm wide and 10 mm long. The film was used immediately after the final drying process to avoid moisture effects which would have greatly influenced the glass transition temperature T_g [23].

The thermal properties were determined by differential scanning calorimetry (DSC) (DSC8500; PerkinElmer, Inc., Waltham, MA, USA). Each sample (~10 mg) was encapsulated in a hermetically sealed aluminum pan and heated from 25°C to 270°C at a rate of 10°C/min in a nitrogen atmosphere.

Wide-angle X-ray diffraction (WAXD) analyses were performed using an X-ray diffraction machine (SmartLab; Rigaku Corp., Akishima, Japan) in reflection mode at a scanning speed of 10°/min by a graphite-monochromatized CuKα beam generated at 40 kV and 30 mA.

The water content in the films with 200 μm thickness (5 mm in width and 10 mm in length) was measured using a coulometric Karl Fischer titrator 899 Coulometer,

(Metrohm AG, Herisau, Switzerland). The measurements were repeated three times for each film sample to confirm the reproducibility.

Fourier transformed infrared (FTIR) spectra (Spectrum 100; PerkinElmer) were collected in attenuated mode using KRS-5 as an attenuated total reflection crystal. The measurements were obtained at a resolution of 4.0 cm^{-1} by averaging 16 scans.

3-3 Results and Discussion

3-3-1 Appearance of PVA film with metal salts

Figure 3.2 exemplifies the transparent and opaque PVA films. The films that contained bromide salts, namely LiBr, NaBr, and KBr, were transparent. In contrast, the addition of sulfate salts, specifically Li_2SO_4, Na_2SO_4, and K_2SO_4, gave the films an opaque appearance due to the salt segregation. Segregation (i.e., phase separation) had to occur during water evaporation process because all the aqueous solutions used to form the samples were transparent. The difference in the appearance of the films could be explained by the HS. According to the HS, Br^- is categorized as a water-structure-breaker and is highly soluble in aqueous PVA. Therefore, the films containing Br^- anions were transparent. In contrast, the films with sulfate salts were found to be opaque, owing to salt segregation. This is reasonable because SO_4^{2-} in solution acts as a water-structure-maker and has low solubility [24-26]. The dynamic mechanical properties were evaluated using transparent films.

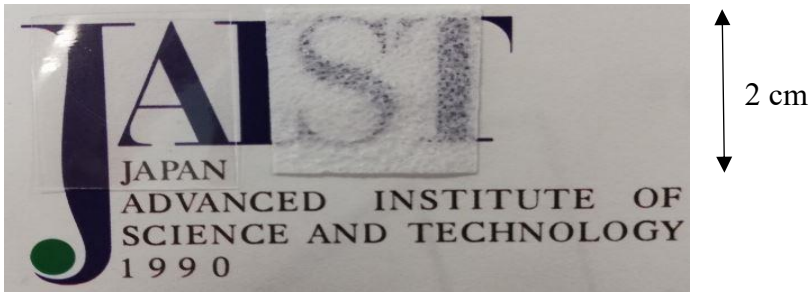

Figure 3.2 Photograph of the films with 200 μm thickness (left) PVA/LiBr and (right) PVA/Li_2SO_4

3-3-2 Effect of cation species

3-3-2-1 Temperature dependence of dynamic tensile moduli

Figure 3.3 illustrates the temperature dependence of the dynamic tensile moduli of various films. The films containing NaBr and KBr had similar E' values in the glassy region, which were almost independent of temperature. Therefore, they had higher E' values than the film comprising pure PVA, especially near the glass-to-rubber transition. Correspondingly, these films exhibited a sharp peak in E'' at approximately 80°C. Therefore, the glass-to-rubber transition of films containing NaBr and KBr occurred in a narrow temperature range leading to a clear stepwise decrease in E', even though they were prepared in the same way as the pure PVA film. Although the exact reason for the narrow transition with high E' in the glassy region was unclear, a slight decrease in crystallinity and enhanced hydrogen bonding may be responsible for this phenomenon.

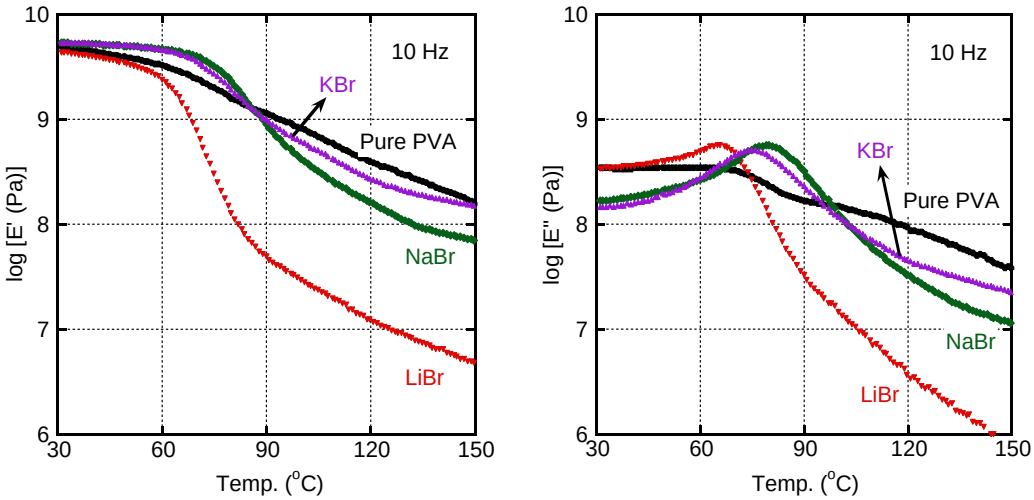

Figure 3.3 Temperature dependence of dynamic tensile moduli such as storage modulus *E'* and loss modulus *E''* at 10 Hz for the films of pure PVA and PVA with various bromide salts

Above T_g, the moduli were lower than those of pure PVA, suggesting a low degree of crystallinity. Furthermore, the *E'* values of the KBr- and NaBr-containing films were much higher than those of the LiBr-containing film. This suggested that the LiBr-containing film had little or no crystallinity. Correspondingly, the *E''* peak was very sharp at low temperatures, implying that the motion of amorphous chains was barely affected by the crystalline phase of the LiBr-containing film. Above T_g, the modulus decreased in accordance with HS, that is $Li^+ > Na^+ > K^+$ [17-19].

Another broad and weak peak could be seen in *E'* of the pure PVA film between 90°C and 140°C, which was not present in the salt-containing films. This peak was attributed to the crystalline phase relaxation. It has been reported that the α-dispersion of crystalline polymers such as polypropylene and polyethylene decreases with the decrease in crystallinity. Furthermore, the peak temperature increased with the increase in

crystalline aggregate size. This result implied that the crystalline phase structure, including the crystallinity, was modified by the salt addition. Furthermore, it was concluded that the cation species also affected the phenomenon.

3-3-2-2 Thermal properties

The thermal properties correspond to the dynamic mechanical properties was demonstrated by the DSC curves (Figure 3.4). In the case of pure PVA, there was a melting point (T_m), defined as the peak temperature, at 234.0°C with an endothermic peak of 74 J/g. This is a typical value for PVA films [29-31]. The T_m values of the NaBr- and KBr-containing films were 234.2°C and 226.5°C, respectively, and were not very different from that of pure PVA. However, they were slightly less crystalline. In contrast, the LiBr-containing film had a T_m of approximately 118°C, represented by a very weak peak which is further explained by its WAXD profile.

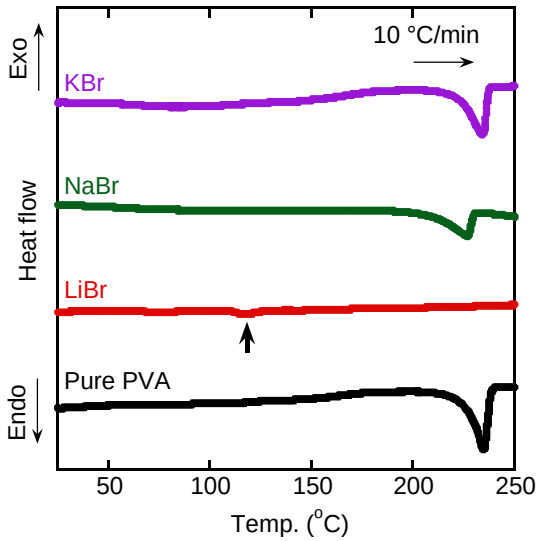

Figure 3.4 DSC heating curves at 10 ˚C/min for the films of pure PVA and PVA with bromide salts

The heat of fusion (ΔH_f) values determined from the DSC curves are provided in Table 3.1; the degree of crystallization (X_c) values were calculated using the following equation:

$$X_c = \frac{\Delta H_f}{\Delta H_f{}^0} \times 100\ (\%) \qquad (3.4),$$

where $\Delta H_f{}^0$ is the heat of fusion for a perfect crystal of pure PVA (152 J/g) [31]. The degree of crystallinity of the LiBr-containing PVA film was 3%, which is much lower than that of the pure PVA film (48%). The crystallinity of the NaBr- and KBr-containing films were 35% and 44%, respectively.

Table 3.1 Thermal properties of the films with/without salt

Metal Salt	Melting point, T_m (°C)	Heat of fusion, ΔH_f (J/g)	Crystallinity, X_c (%)
Pure PVA	234	74	48
LiBr	118	5	3
NaBr	226	42	35
KBr	234	67	44

3-3-2-3 WAXD profiles

The crystallinity was also evaluated by WAXD, as shown in Figure 3.5. A strong diffraction peak appeared at approximately 20° [10, 33], which is attributed to the $(10\bar{1})$ and (101) planes of the orthorhombic form (the numbers in parentheses represent the Miller indices) [22, 34]. The pure PVA film produced another weak diffraction peak at approximately 11°, which is presumably attributed to the (100) plane [34].

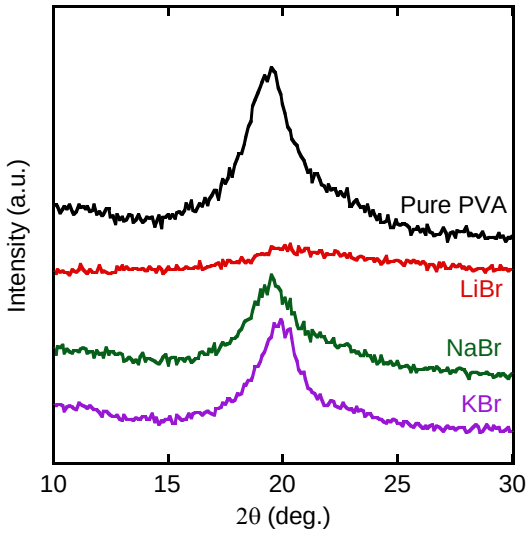

Figure 3.5 WAXD profiles for the films of pure PVA and PVA with bromide salts

It is confirmed from Figure 3.5 that the crystallinity is reduced by the addition of a salt. Furthermore, the 2θ position of the strongest peak shifted to a larger angle for films with low crystallinity. Because this peak comprises not only crystalline peaks but also a broad overlapping amorphous background, the peak position is affected by the crystallinity of the film. A similar phenomenon has been reported for a PVA film containing LiCl [9]. According to the study, the hydrogen bonding in the PVA chains was greatly affected by the presence of ions, because they form strong interactions with PVA molecules and interrupt the intermolecular hydrogen bonding within the PVA chains [21, 32].

Because the crystallinity was greatly reduced by LiBr, the effect of the anion species in the salt was evaluated using various lithium salts—i.e., LiI, LiBr, $LiNO_3$, LiCl, and $LiClO_4$.

3-3-3 Effect of anion species

3-3-3-1 Temperature dependence of dynamic tensile moduli

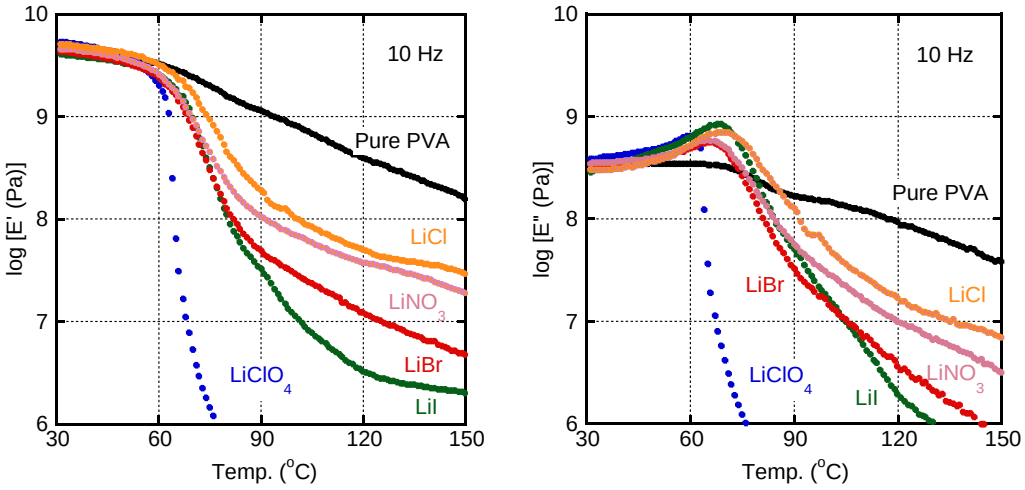

Figure 3.6 Temperature dependence of dynamic tensile moduli such as storage modulus *E'* and loss modulus *E''* at 10 Hz for the films of pure PVA and PVA with various lithium salts

Figure 3.6 shows the temperature dependence of the dynamic tensile moduli at 10 Hz. The result demonstrated that lithium salts play an important role in determining the crystallinity and hydrogen bonding, and therefore, affect the dynamic mechanical properties of films. As the figure shows, there was a significant drop in the E' curve at approximately 60°C for the films containing lithium salts, although the E' values in the glassy region were almost the same as those of pure PVA. The E'' peak attributable to the T_g shifted to a lower temperature owing to the reduced crystallinity. Above the T_g, the E' values of the lithium salt-containing films were lower than those of the pure PVA film owing to low crystallinity; this phenomenon followed the order $LiClO_4$, LiI, LiBr, $LiNO_3$, and LiCl. This observation can be further explained by the HS [34,35]. According to the

HS, the ability of an anion to disrupt the structure of water follows the order ClO_4^- > I^- > Br^- > NO_3^- > Cl^- [18]. For example, weakly hydrated anions such as I^- and ClO_4^-—which are known as chaotropes or water-structure-breakers—are responsible for the salting-in effect [9,12,32]. Therefore, the addition of LiI or $LiClO_4$ leads to reduced hydrogen bonding between the PVA chains and decreased the crystallinity. As a result, the T_g shifts to low temperatures. Moreover, the LiI- and $LiClO_4$-containing films have lower E' values than the LiBr-, $LiNO_3$-, and LiCl-containing films above T_g.

3-3-3-2 Thermal properties

The effect of lithium salts on the crystallinity of the PVA films was verified by the DSC curves, as shown in Figure 3.7. None of the films containing a lithium salt produced an obvious T_m peak. Moreover, the melting peaks were located at lower temperatures, as summarized in Table 3.2.

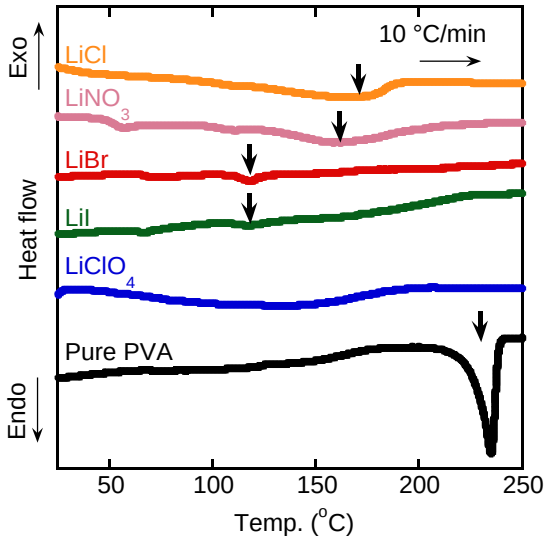

Figure 3.7 DSC heating curves at 10 ^{0}C/min for the films of pure PVA and PVA with various lithium salts

Table 3.2 Thermal properties of the films with/without salts

Lithium salt	Melting point, T_m (^{0}C)	Heat of fusion, ΔH_f (J/g)	Crystallinity, X_c (%)
Pure PVA	234	74.2	48
$LiClO_4$	-	-	-
LiI	117	2.5	2
LiBr	118	4.5	3
$LiNO_3$	156	9.2	6
LiCl	176	11.6	8

3-3-3-3 WAXD profiles

The decrease in crystallinity was also confirmed by the WAXD patterns, as shown in Figure 3.8. The $LiClO_4$-, LiI-, and LiBr-containing films produced very weak peaks. In contrast, the LiCl- and $LiNO_3$-containing films produced peaks at 20°, although they were much weaker than that produced by the pure PVA film. Together with the DSC results, these data demonstrate that anions greatly affect the crystallinity of the PVA via ion-dipole interactions, and therefore, also affect its dynamic mechanical properties.

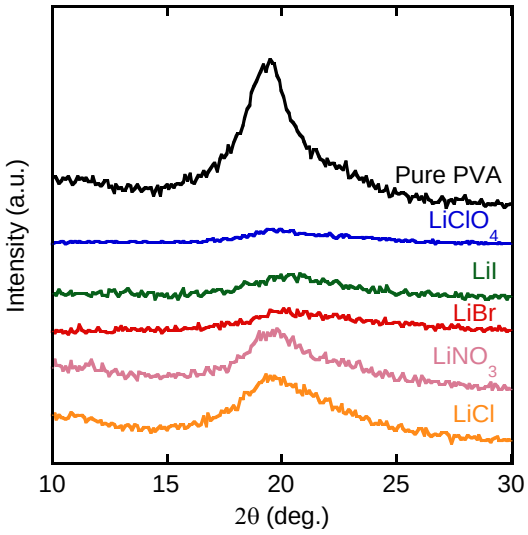

Figure 3.8 WAXD profiles for the films of pure PVA and PVA with lithium salts

3-3-3-4 Water content

Generally, water content has a great influence on the mechanical and thermal properties for PVA films [20]. Thus, the effect of the salt addition on the water content in the films was studied using the lithium salts. The measurements were performed after vacuum drying at 80 °C for 4 hours. Therefore, the content of water trapped by hydroxyl groups was evaluated. From the result obtained in Figure 3.9, the water content of films was barely affected by the salt addition at least immediately after vacuum drying.

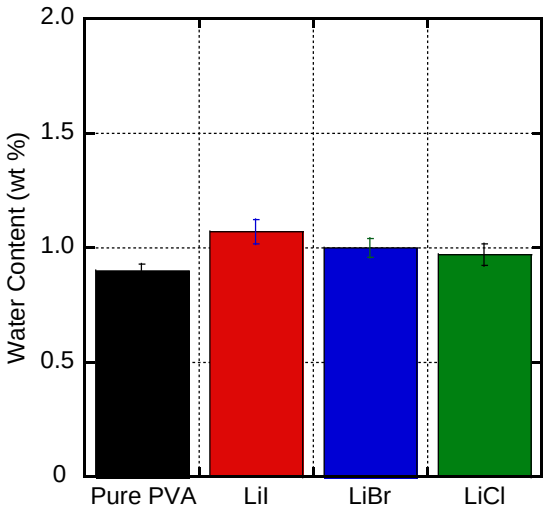

Figure 3.9 Water contents in the films of pure PVA and PVA with a lithium salt

3-3-3-5 Fourier-transform infrared spectra

Figure 3.10 shows the Fourier-transform infrared (FTIR) spectra of the films at room temperature. As shown in Figure 3.10(a), the absorbance band at 3274 cm^{-1}—which is attributable to the stretching vibration of the O-H groups in the PVA—shifted to a higher wavenumber following the addition of lithium salts. This indicates that the hydrogen bonds between the PVA chains were weakened by the salt [5,25], as demonstrated by the $LiClO_4$-, LiI-, and LiBr-containing films. The degree of the peak shift corresponds to the HS [16]. Furthermore, the magnitude of the crystalline band at approximately 1141 cm^{-1} decreased following the addition of lithium salts in the order $LiClO_4$ > LiI > LiBr > $LiNO_3$ > LiCl. These results corroborate those obtained by DSC and WAXD. The absorption band at approximately 1090 cm^{-1} is assigned to υ(C-O) stretching vibration, and its presence suggests that PVA is a semi-crystalline polymer [26,27]. The relative intensity of the band at 1090 cm^{-1} can be used to measure the degree of crystallinity of PVA. Interactions between PVA and metal salt could further

be confirmed by the broadening of the peak at 1090 cm^{-1} in the spectra PVA films.

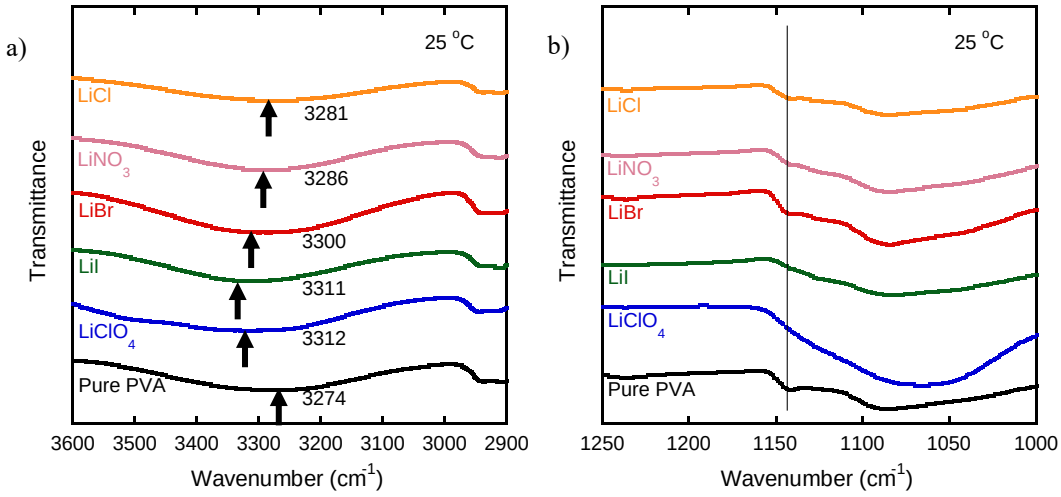

Figure 3.10 IR spectra for the films of pure PVA and PVA with lithium salts in the wavenumber of (a) 2900-3600 cm^{-1} and (b) 1000-1250 cm^{-1}

3-4 Conclusion

The addition of a salt reduced the hydrogen bonding in PVA chains and decreased the crystallinity in the film. Consequently, the T_g shifted to low temperatures, and above the T_g, the modulus decreased markedly. This study was the first to confirm that this phenomenon could be predicted by the HS. For example, the impact of the addition of bromine salts on PVA structure and properties followed the order $Li^+ > Na^+ > K^+$, i.e., the HS. Furthermore, the anions had a more significant impact on the structure and mechanical properties of the PVA films. Among the lithium salts studied, $LiClO_4$ and LiI had the most significant effect, suggesting that ClO_4^- and I^- acted as water-structure-breakers in aqueous PVA solutions, which also corresponded with the HS, i.e., $ClO_4^- > I^- > Br^- > NO_3^- > Cl^-$.

References

1. Y.Z. Xu, W.X. Sun, W.H. Li, X.B. Hu, H.B. Zhou, S.F. Weng, Investigation on the interaction between polyamide and lithium salts, J. Appl. Polym. Sci. 77 (2000) 2685-2690.
2. Y. Wu, Y. Xu, D. Wang, Y. Zhao, S. Weng, D. Xu, FT-IR spectroscopic investigation on the interaction between nylon 66 and lithium salts, J. Appl. Polym. Sci. 91 (2004) 2869-2875.
3. Y. Sato, A. Ito, S. Maeda, M. Yamaguchi, Structure and optical properties of transparent polyamide 6 containing lithium bromide, J. Polym. Sci. B: Polym. Phys. 56 (2018) 1513-1520.
4. O.N. Tretinnikov, S.A. Zagorskaya, Determination of the degree of crystallinity of poly (vinyl alcohol) by FTIR spectroscopy, J. Appl. Spectrosc. 79 (2012) 521-526.
5. L.Z. Zhang, Y.Y. Wang, C.L. Wang, H. Xiang, Synthesis and characterization of a PVA/LiCl blend membrane for air dehumidification, J. Membrane Sci. 308 (2008) 198-206.
6. B. Wang, C. Lu, J. Hu, W. Lu, Property improvements of EVOH by enhancing the hydrogen bonding, Plast. Rubber Compos. 49 (2020) 18-24.
7. A. Miyagawa, V. Ayerdurai, S. Nobukawa, M. Yamaguchi, Viscoelastic properties of poly(methyl methacrylate) with high glass transition temperature by lithium salt addition, J. Polym. Sci. B: Polym. Phys. 54 (2016) 2388-2394.
8. A. Ito, R. Maeno, M. Yamaguchi, Control of optical and mechanical properties of poly(methyl methacrylate) by introducing lithium salt, Opt. Mater. 83 (2018) 152-

156.

9. A. Ito, P. Phulkerd, V. Ayerdurai, M. Soga, A. Courtoux, A. Miyagawa, Enhancement of the glass transition temperature of poly (methyl methacrylate) by salt, Polym. J. 50 (2018) 857-863.
10. T. Sako, A. Miyagawa, M. Yamaguchi, Modulus enhancement of polycarbonate by addition of lithium perchlorate, J. Appl. Polym. Sci. 134 (2017) 44882-44887.
11. S. Tomie, N. Tsugawa, M. Yamaguchi, Modifying the thermal and mechanical properties of poly (lactic acid) by adding lithium trifluoromethanesulfonate, J. Polym. Res. 25 (2018) 206-212.
12. N. Tsugawa, A. Ito, M. Yamaguchi, Effect of lithium salt addition on the structure and optical properties of PMMA/PVB blends, Polymer 146 (2018) 242-248.
13. J.S. Kim, R.J. Jackman, A. Eisenberg, Filler and percolation behavior of ionic aggregates in styrene-sodium methacrylate ionomers, Macromolecules 27 (1994) 2789-2803.
14. M.M. Coleman, P.C. Painter, J.F. Graf, Specific interactions and the miscibility of polymer blend, Second Edition, New York: CRC Press, 1995.
15. H. Hirao, S. Koseki, H. Takano, Molecular dynamics study of relaxation modes of a single polymer chain, J. Phys. Soc. Japan 66 (1997) 3399-3405.
16. T. Pakula, S. Geyler, T. Edling, D. Boese, Relaxation and viscoelastic properties of complex polymer systems, Rheologica acta 35 (1996) 631-644.
17. H. Muta, S. Kawauchi, M. Satoh, Ion-specific swelling behavior of uncharged poly (acrylic acid) gel, Colloid Polym. Sci. 282 (2003) 149-155.
18. M. Mori, J. Wang, M. Satoh, Anti-Hofmeister series properties found for a

polymer having a π electron system and acidic protons, Colloid Polym. Sci. 287 (2009) 123-127.

19. J. Wang, M. Satoh, Novel PVA-based polymers showing an anti-Hofmeister series property, Polymer 50 (2009) 3680-3685.

20. N. Ahad, E. Saion, E. Gharibshahi, Structural, thermal, and electrical properties of PVA-sodium salicylate solid composite polymer electrolyte, J. Nanomater. 2012 (2012) 94.

21. T. Nakano, H. Yuasa, Y. Kanaya, Suppression of agglomeration in fluidized bed coating. III. Hofmeister series in suppression of particle agglomeration, Pharm. Res. 16 (1999) 1616-1620.

22. R.F. Bhajantri, V. Ravindrachary, A. Harisha, V. Crasta, S.P. Nayak, B. Poojary, Microstructural studies on BaCl2 doped poly (vinyl alcohol), Polymer 47 (2006) 3591-3598.

23. M. Mohsin, A. Hossin, Y. Haik, Thermal and mechanical properties of poly (vinyl alcohol) plasticized with glycerol, J. Appl. Polym. Sci. 122 (2011) 3102-3109.

24. T. Akahane, T. Mochizuki, Planar orientation of molecular chains in crystalline polymer films, J. Polym. Sci. Pol. Lett. 8 (1970) 487-491.

25. A. Mráček, J. Varhaníková, M. Lehocký, L. Gřundělová, A. Pokopcová, V. Velebný, V, The influence of Hofmeister series ions on Hyaluronan swelling and viscosity, Molecules 13 (2008) 1025-1034.

26. D.K. Buslov, N.I. Sushko, O.N. Tretinnikov, IR investigation of hydrogen bonds in weakly hydrated films of poly (vinyl alcohol), Polym. Sci. Ser. A. 53 (2011) 1121-1127.

27. H. Wang, P. Fang, Z. Chen, S. Wang, Synthesis and characterization of CdS/PVA nanocomposite films, Appl. Surf. Sci. 253 (2007) 8495-8499.

Chapter 4 Modification of poly(vinyl alcohol) fibers with lithium bromide

4-1 Introduction

4-1-1 Outline of the PVA fiber production

As mentioned, poly(vinyl alcohol) is soluble in water. Therefore, its fiber is usually spun with a wet process in a concentrated aqueous solution of sodium sulfate as the coagulation bath. As PVA is soluble in water, the fiber cannot be washed with water. However, when PVA filament is stretched, it is not soluble in water at room temperature, and X-ray analysis clearly shows that the fiber is then partly crystalline, similar to highly stretched, natural rubber. When the stretched PVA is relaxed, it again can be dissolved in water. Therefore, it is hard to proceed the chemical reaction of the water-soluble fiber in an aqueous medium without causing a deterioration of its fiber structure. Fiber obtained by such procedure is usually insoluble in boiling water, but when the water temperature is raised to 60 °C, it becomes rubbery. Thus, the fiber of hot-water resistance during the early days of research was unsatisfactory. Various experiments were carried out to overcome this difficulty, and it was found that heat treatment of the PVA fiber before its formalization is the best way to improve its hot-water resistance [1].

4-1-2 Physical properties of PVA

4-1-2-1 Orientation

Hot drawing is one of the most important processes in the production of PVA fibers with high strength. In the drawing process, the degree of crystallinity was increased, and the orientation of polymer chains took place. The orientation can be detected through

the change in the X-ray diffraction patterns.

4-1-2-2 Elastic moduli of the crystal lattice

It was found by X-ray diffraction that when the fiber was stretched, the spacing of the lattice plane was extended. The following equation expresses the relationship between the stress (σ) in a direction parallel to the molecular axis, and the strain (ε), i.e., the extension of the spacing of the lattice; the elastic modulus of the crystal lattice (E_1) is calculated according to this equation:

$$\sigma = E_1 \varepsilon \qquad (4.1)$$

The lattice extension is measured by the molecular axis that occurs while stress is being applied to the sample is perpendicular to the change in the spacing of a suitable lattice plane. The stress added to the macroscopic sample is assumed to be homogenous throughout the length and the breadth of the sample; thus, the elastic modulus of the sample can be calculated from the measured values of ε and the stress added to the specimen σ.

4-1-2-3 Melting point and heat of fusion

Various melting points T_m's of PVA have been reported and summarized [2-4] where, they ranged between 220 and 267 °C. When PVA is heated gradually without diluent, decomposition takes place, and hence exact determination of the T_m is difficult. The divergence of the T_m described above may be primarily ascribed to the decomposition. Since the T_m of PVA containing an appropriate amount of diluent is hardly disturbed by the decomposition, the values determined by the extrapolation of the measured ones for PVA containing various amounts of diluent to zero content is quite reliable. The T_m values

determined in this way are as follows: 226 - 267 °C for the typical PVA prepared in a laboratory [5,6]; and 267 °C for commercial PVA used in the production of fiber.

When a sample is not under stress, its apparent T_m can be simply determined by a thermal analysis. However, the T_m values thus determined is lower than the previously described values and depends on the measurement conditions, e.g., with or without tension. Whereas, the melting point determined under tension increases from 237 to 245 ℃ [7].

4-1-2-4 Glass transition

The glass transition temperature T_g of PVA is determined by the basis of the measurement of the change in volume, specific heat, dielectric loss, viscoelastic properties, and nuclear magnetic resonance [8]. Though experimental values are widely varied, they are roughly classified into two temperature groups: about 70 °C and about 80 °C. The thermal history of the samples is the origin of the scattering. Trace amounts of water remaining in the sample is another cause of the scattering. A useful experimental equation has been proposed to account for the effect of a diluent on the glass transition temperature of a polymer:

$$\frac{1}{\mathrm{T}_g} = \frac{W_1}{\mathrm{T}_{g1}} + \frac{W_2}{\mathrm{T}_{g2}} \tag{4.2}$$

where Tg, $\mathrm{Tg_1}$, and $\mathrm{Tg_2}$ are the glass transition temperature (Kelvin) of the mixture, polymer, and diluent, respectively; and $\mathrm{W_1}$ and $\mathrm{W_2}$ are the weight fractions of the polymer and the diluent [9]. Equation 4.2 can be applied not only for polymer diluent but also for copolymers empirically confirmed and for polymer/polymer mixtures. In the latter two cases, $\mathrm{Tg_2}$ refers to T_g of the second polymer, and $\mathrm{W_2}$ to the weight fractions of the second

polymer or of the second monomer in copolymers.

T_g of PVA (Tg_1 = 358 K) and that of water (Tg_2 = 139 K) have been obtained empirically [60]. When these values and W_2 are substituted in equation 4.2, 70 °C is obtained as T_g in the presence of 5% water. Unless special care is taken to dry PVA samples perfectly and to prevent water adsorption to the samples during measurement, the samples tend to contain water owing to their hygroscopicity [10].

4-2 Experimental

4-2-1 Materials

A commercially available PVA (Japan Vam & Poval Co., Ltd., Osaka, Japan) was used; its degree of polymerization and its degree of saponification were 1700 and 99.5 mol% respectively. LiBr was purchased from Tokyo Chemical Industry Co., Ltd., Japan, and used without further purification. On the other hand, sodium sulphate (Na_2SO_4) was purchased from Kanto Chemical Co., Ltd., Japan.

4-2-2 Preparation of PVA aqueous solution, film, and fiber

The PVA aqueous solutions were prepared by dissolving PVA in deionized water at 90 °C using a magnetic stirrer operating at 400 rpm. The concentration of PVA was fixed at 15 wt%. LiBr and was subsequently added while stirring continuously at 400 rpm for approximately 3 h until it had completely dissolved.

Some of the solution was transferred to a polytetrafluoroethylene (PTFE)-coated tray to prepare a film, which was preheated at 70 °C. It was then vacuum dried at 90 °C for 5 h. Before the measurements, the 200-μm thick film sample was further dried at 80 °C under vacuum for another 4 h to avoid the moisture effects.

On the other hand, the wet-spinning process was performed using the aqueous solutions with/without LiBr at 90 °C. The molar ratio of LiBr to the hydroxyl groups in the PVA was 0.1. First, the aqueous solution was poured into a dope tank equipped with an orifice with 250 holes (each 0.1 mm in diameter). The solution was extruded through the orifice at 90 °C into a coagulation bath containing a 420 g/L aqueous solution of Na_2SO_4 at 40 °C. The extrudates were then stretched at a draw ratio of 3.44. After coagulation bath removal, the fibers were spun on rollers. They were then washed in water at 30 °C, dried, and hot-stretched at 170 °C at a draw ratio of 2.80.

Other than that, some of the PVA fibers were used to prepare a film in order to investigate the dynamic mechanical properties of the material. The fibers were cut and dissolved in deionized water at 90 °C until completely dissolved. The solution was then casted on a PTFE-coated tray and preheated at 70 °C for 6 h. The obtained film was then dried at 90 °C under vacuum for another 5 h. Finally, the sample was dried again at 80 °C under vacuum for a further 4 h before the measurements were performed.

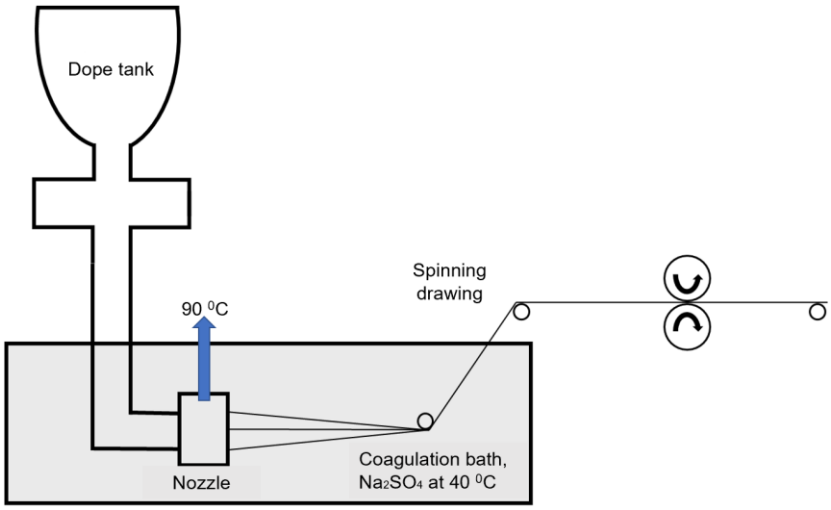

Figure 4.1 Schematic illustration of wet-spinning method.

4-2-3 Measurements

The rheological properties of each solution were evaluated using the parallel-plate rheometer (AR2000ex; TA Instruments, Inc., New Castle, DE, USA), as described in Chapter 2. The frequency sweep tests of the shear storage modulus *G'* and loss modulus *G"* were carried out from 0.05 to 500 rad/s at various temperatures. The gap between the plates was 1 mm.

A dynamic mechanical analyzer (Rheogel-E4000; UBM Co., Ltd., Muko, Japan) was used to measure the temperature dependence of the tensile storage modulus E' and the loss modulus E'' of each sample film between 30 °C and 150 °C. The applied frequency was 10 Hz and the heating rate was 2 °C/min. A sample—which was 5 mm wide and 10 mm long—was cut from the 200-μm thick film. The film was used immediately after the final drying process to exclude moisture, which greatly affects the glass transition temperature T_g.

The thermal properties were measured by differential scanning calorimetry (DSC) using a DSC8500 system (PerkinElmer, Inc., Waltham, MA). Each sample (~10 mg) was encapsulated in an aluminum pan and heated from 25 °C to 250 °C at a heating rate of 10 °C/min under a nitrogen atmosphere. An empty pan was used as the reference cell.

The tensile test was carried out at 25 °C by a small bench tester (LCS-05/300; Tokyo Koki Testing Machine Co., Ltd., Tokyo, Japan) at a stretching speed of 10 cm/min using a fiber with an initial length of 20 cm. The measurements were performed at least 10 times for each sample and the average value was calculated.

Two-dimensional wide-angle X-ray diffraction (WAXD) patterns of the sample fiber were collected using an XRD machine (SmartLab; Rigaku Corp., Akishima, Japan)

with an imaging plate. A graphite-monochromatized CuKα radiation beam, operated at 45 kV and 200 mA, was directed through the sample fiber. The exposure time was 5 min per measurement.

4-3 Results and Discussion

4-3-1 Rheological properties of aqueous solution with salt

Figure 4.2 shows the angular frequency dependence of the oscillatory shear moduli of aqueous PVA solutions with various molar ratios of LiBr at 25 °C. It was clear that the moduli of the solutions containing LiBr with molar ratio of 0.05 and 0.10 were lower than that of solution without LiBr. The difference was found to be pronounced in the shear storage modulus (G') curve in the low frequency region, in which a plateau modulus decreased with the addition of LiBr, except for the sample with 0.15 molar ratio of LiBr. The loss modulus (G'') also decreased with the addition of LiBr, demonstrating that the dynamic viscosity, i.e., G''/ω, was reduced by LiBr. The decrease in modulus/viscosity is most probably due to the reduced inter- and intra-chain hydrogen bonding between the PVA chains [11-14].

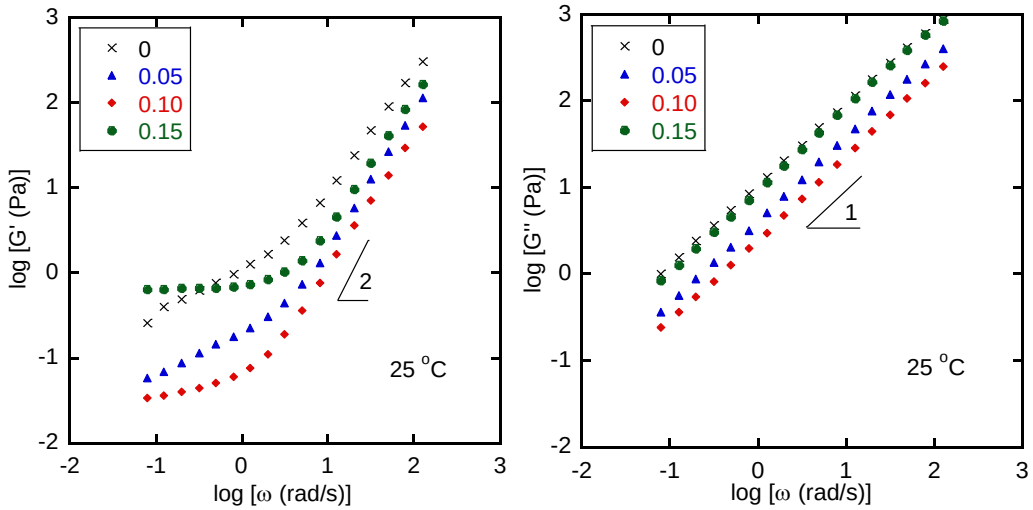

Figure 4.2 Angular frequency dependence of shear storage modulus G' and loss modulus G'' at 25 °C in aqueous PVA solutions with various molar ratios of LiBr

As mentioned in Chapter 3, it was found that the anion is responsible for hydrogen bonding in the PVA chains. Although it is known that Li^+ disrupts hydrogen bonds, the data indicates that the anion species also affects the rheological properties of the PVA solution. For example, Br^-, which is classified as a water-structure-breaker ion in the Hofmeister series, was found to effectively decreased oscillatory shear moduli, and the water molecules subsequently tend to interact with the hydroxyl groups in the PVA. As a result, the inter- and intra- molecular interactions of PVA are reduced. However, in the present study, the plateau modulus for the solution containing a molar ratio of 0.15 is almost equivalent to that of the pure PVA aqueous solution. This indicates that the effect of Br^- was saturated at molar ratio of 0.10. Furthermore, the phenomenon suggests that Li^+ acts as crosslink points via ion–dipole interactions with the hydroxyl groups in the solution with 0.15 molar ratio. As a result, a well-developed network structure is formed in the solution [15-18].

4-3-2 Mechanical properties of film

The temperature dependence of the dynamic tensile modulus at 10 Hz of the films of pure PVA and PVA with LiBr is shown in Figure 4.3. For the pure PVA film, an E' beyond T_g was relatively high, suggesting that the degree of crystallinity is high. Moreover, another broad and weak peak appeared in the E'' curve from 90 °C to 140 °C, which was not apparent in the films with LiBr. This peak must be attributed to the relaxation caused by the crystalline phase. As the LiBr content increased, there was an obvious decrease in E' around at T_g, although the E' values in the glassy region were almost the same as those of pure PVA, demonstrating that LiBr reduces the crystallinity [19]. Because of the reduced crystallinity, the E'' peak ascribed to T_g shifted to a lower temperature and its area increased markedly, i.e., the film acquired relaxation strength.

Above the T_g, the E' values of the films with LiBr were lower than those of the pure PVA film owing to their low crystallinity. The film sample containing 0.15 molar ratio of LiBr had a higher T_g than the other films with LiBr, and its E'' peak became sharp. These results correspond to the viscoelastic properties of the solution. The strong ion–dipole interaction between Li^+ and the hydroxyl groups increased the T_g to some extent, as reported for various polar polymers containing lithium salts [20-24].

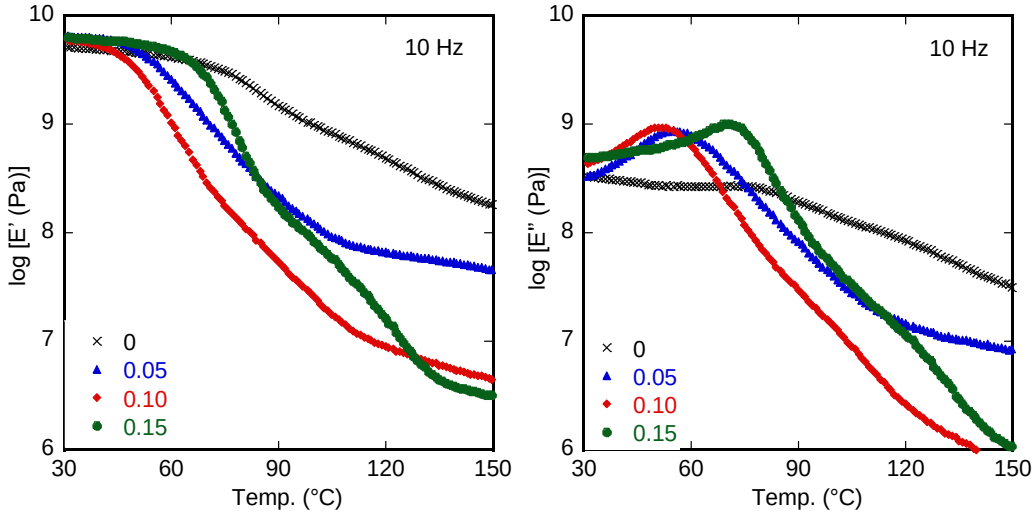

Figure 4.3 Temperature dependence of tensile storage modulus *E′* and loss modulus *E″* at 10 Hz of films with various molar ratios of LiBr

The fibers were prepared by wet-spinning. The fibers dissolved in water was used to prepare a film for the evaluation of its dynamic mechanical properties to estimate the LiBr content in the fibers. The results are shown in Figure 4.4.

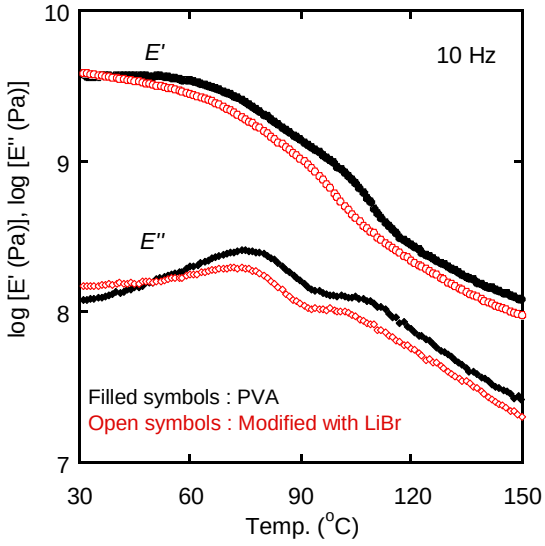

Figure 4.4 Temperature dependence of tensile storage modulus *E′* and loss modulus *E″* at 10 Hz of pure PVA and PVA/LiBr films made from the fibers

As shown in the figure, the dynamic tensile moduli of the film prepared using fibers obtained from the solution with LiBr were almost the same as those without LiBr. The dynamic mechanical properties of the film prepared using the fibers without LiBr were, of course, the same as those of the pure PVA film as shown in Figure 4.4. These results suggested that LiBr was eluted from the fiber during the wet-spinning process, because LiBr was dissolved in the coagulation bath and/or during the post-spinning washing process. As a result, hardly any LiBr remained in the obtained fiber, and the hydrogen bonding between the PVA chains increased.

4-3-3 Thermal properties of film

The DSC heating curves are shown in Figure 4.5. In the case of pure PVA, there was a melting peak at approximately 226 °C and an endothermic peak of 52.1 J/g. The figure clearly shows that LiBr affects the crystallinity. As the amount of LiBr increased (≤ 0.10 molar ratio), the melting point decreased, and the corresponding heat of fusion decreased, i.e., the crystallinity of the film decreased, which must be attributable to the reduction of hydrogen bonds between the PVA chains. As the amount of LiBr increased further to a molar ratio of 0.15, a peak appeared at approximately 140 °C, which is ascribed to the melting point of the LiBr crystals. There was no clear endothermal peak attributable to the PVA crystals.

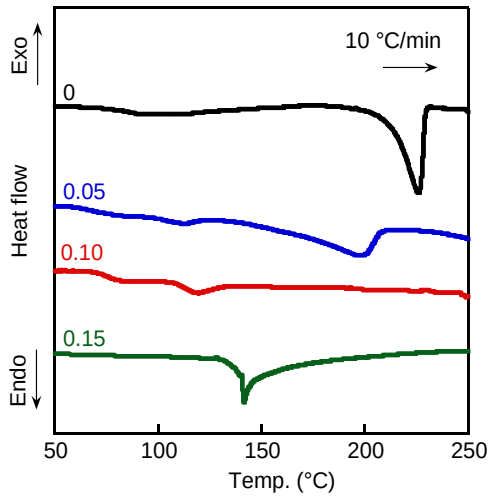

Figure 4.5 DSC heating curves obtained at 10 °C/min for the PVA films with various molar ratios of LiBr

The heat of fusion $\Delta H_{f\text{-}s}$ values, determined from the curves, are provided in Table 4.1 with the degree of crystallization X_c, which was calculated using the following equation:

$$X_c = \frac{\Delta H_f}{\Delta H_f{}^0} \times 100\ (\%) \qquad (4.3),$$

where $\Delta H_f{}^0$ is the heat of fusion for a perfect crystal of pure PVA (152 J/g) [25]. The degree of crystallization was 7.5% for the PVA film with a molar ratio of 0.05, and 1.4% for the film with 0.10 molar ratio; both values were much lower than that of the pure PVA film (33.4 %). Thus, a molar ratio of 0.10 effectively reduced the hydrogen bonds between the PVA chains, resulting in a low level of crystallinity. Therefore, a molar ratio of 0.10 was used to prepare a PVA fiber for further studies.

Table 4.1 Thermal properties of the films containing various contents of LiBr

LiBr content (molar ratio)	T_m (^{0}C)	ΔH_f (J/g)	X_c (%)
0	226	52.1	34.3
0.05	200	11.4	7.5
0.10	118	2.2	1.4
0.15	-	-	-

4-3-3-1 Thermal properties of fiber

Figure 4.6 shows the DSC heating curves of the PVA fibers at a heating rate of 10 °C/min. The initial slope in the low temperature region must be ascribed to the glass-to-rubber transition. The endothermic peak for the PVA fiber appearing at approximately 231 °C was attributable to the T_m of the PVA crystals, and shifted to 240 °C after the hot-stretching process. The heat of fusion $\Delta H_{f\text{-}s}$ determined from the curves was provided in Table 4.2, for which the degree of crystallization of the PVA fibers was calculated using equation (4.3). Although crystallinity seemed to be enhanced by the hot-stretching process, the effect of LiBr in the solution was not obvious.

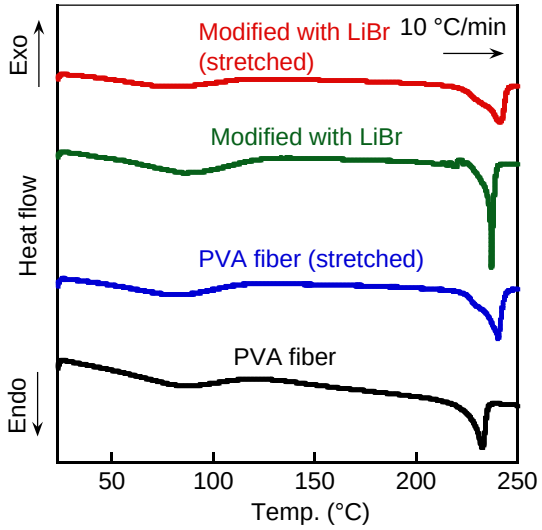

Figure 4.6 DSC heating curves obtained at 10 °C/min for the fiber samples

Table 4.2 Thermal properties of the fibers

Sample	T_m (^{0}C)	ΔH_f (J/g)	X_c (%)
PVA	231	57.2	38
PVA (stretched)	240	61.8	41
Modified with LiBr	234	55.6	36
Modified with LiBr (stretched)	241	59.0	39

4-3-4 Orientation of fibers

It was known that a high level of molecular orientation was barely possible for PVA in general owing to its intermolecular hydrogen bonding, thus, contributed towards a difficulty of PVA fiber stretching [26,27].

Figure 4.7 presents the two-dimensional wide-angle X-ray diffraction (2D-

WAXD) patterns of the PVA fibers. The vertical (i.e., flow) direction is along the fiber axes. The patterns comprised uneven crescent-shaped diffraction rings, indicating that the PVA chains were well-oriented, as will be characterized in detail.

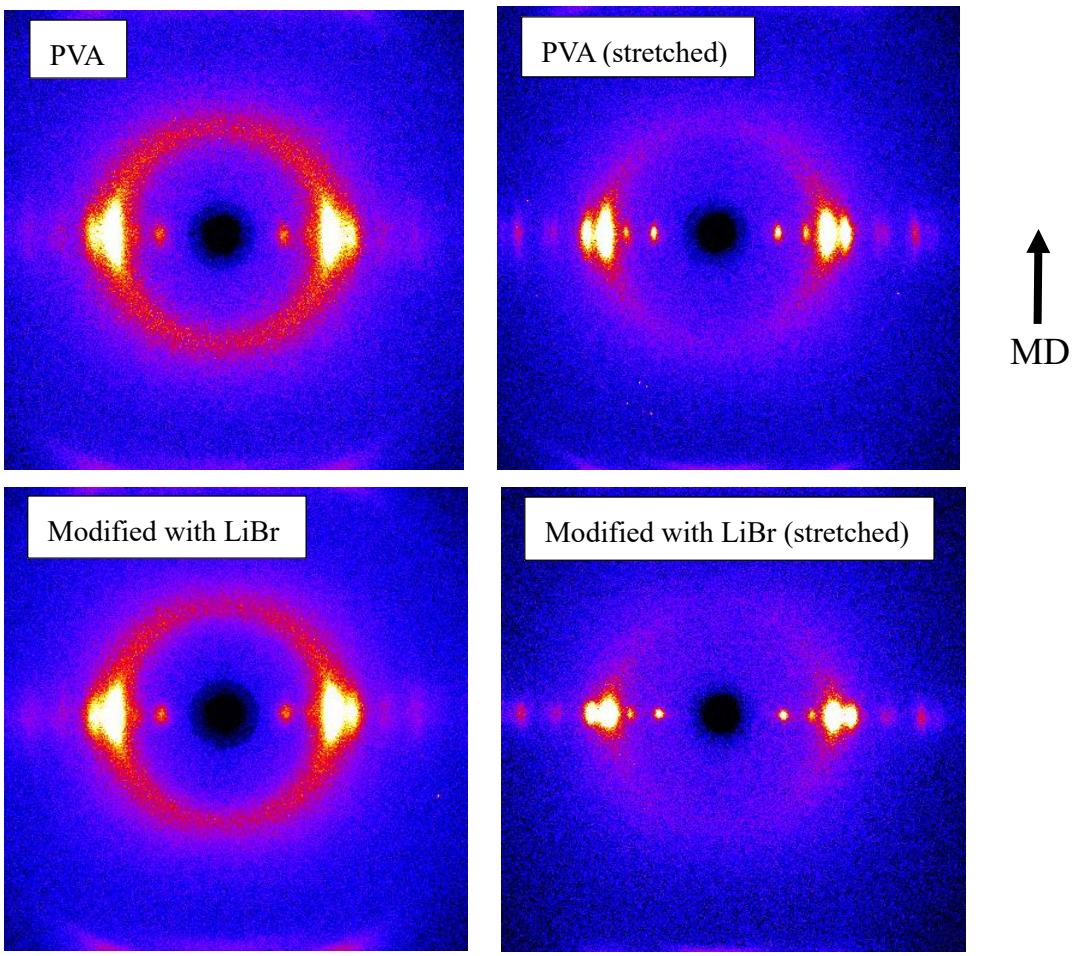

Figure 4.7 2D-WAXD images of the fibers (the machine direction MD was denoted by the arrow)

The 2θ profiles on the equator are shown in Figure 4.8. The profiles included three distinct peaks, which are attributable to the (001), (101), and (200) crystal planes of the α monoclinic crystalline form of PVA, and are easily discernible from the broad amorphous background [28-31]. The crystallinity determined from the crystalline and

amorphous areas after the deconvolution of the peaks was enhanced by hot-stretching. However, the effect of LiBr in the solution was not obvious, in accordance with the DSC results.

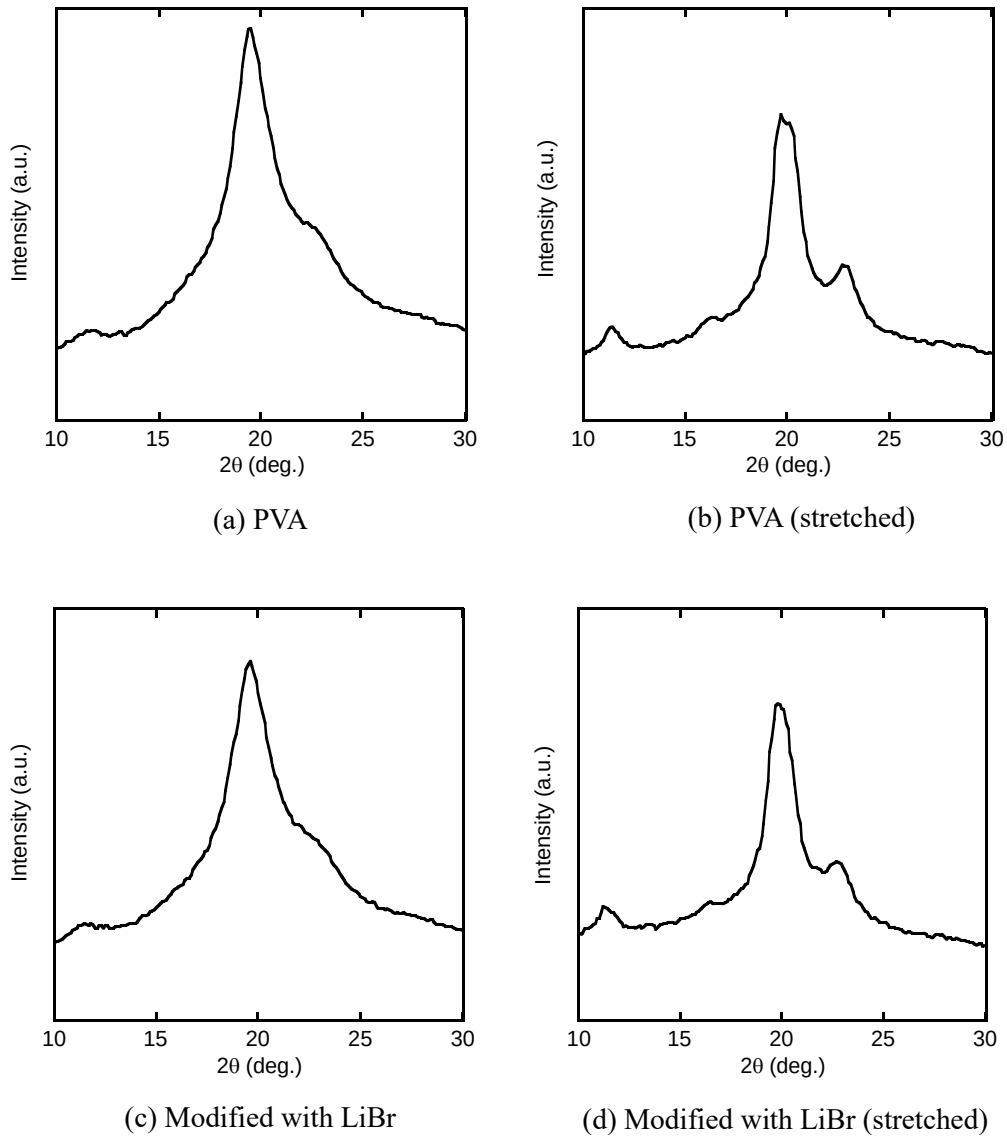

Figure 4.8 2θ profiles of the fibers

As shown in Figure 4.7, the molecular orientation was greatly enhanced after

hot-stretching, for both the PVA fiber with/ without the LiBr modification. Equatorial spots produced by the (001/101) and (200) planes after hot-stretching indicated strong alignment. Furthermore, the equatorial spots of the hot-stretched fiber modified with LiBr were narrower than those of the corresponding PVA fiber, demonstrating that LiBr enhanced the molecular orientation.

The azimuthal distribution of the (101) plane, shown in Figure 4.9, is used to characterize the chain orientation of PVA fibers [28]. The widths of the peaks at azimuthal angle β values of 90° and 270°—i.e., on the equator—were evaluated. The diffraction pattern changed from arc-shaped to spot-shaped during hot-stretching, indicating the enhanced orientation of the crystals [29,30].

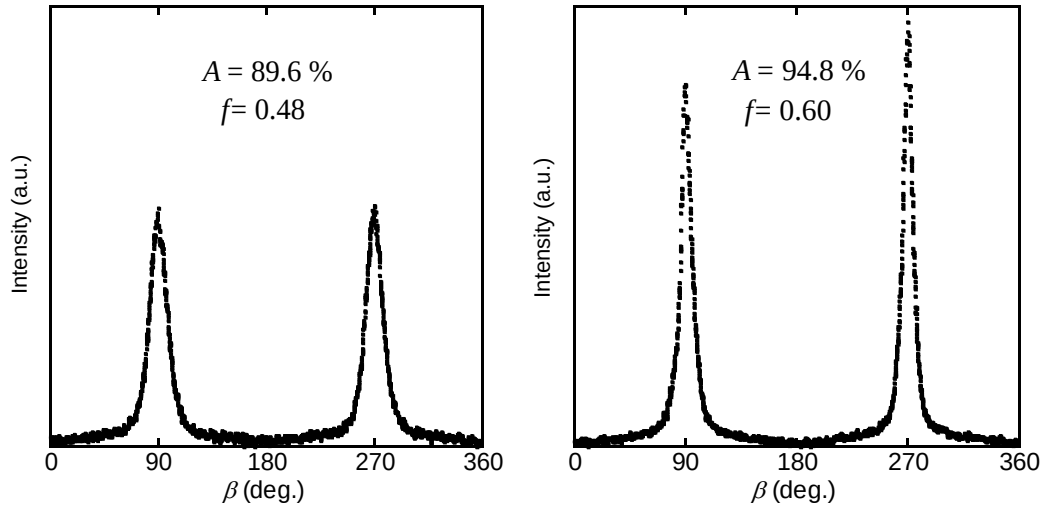

(a) PVA (b) PVA (stretched)

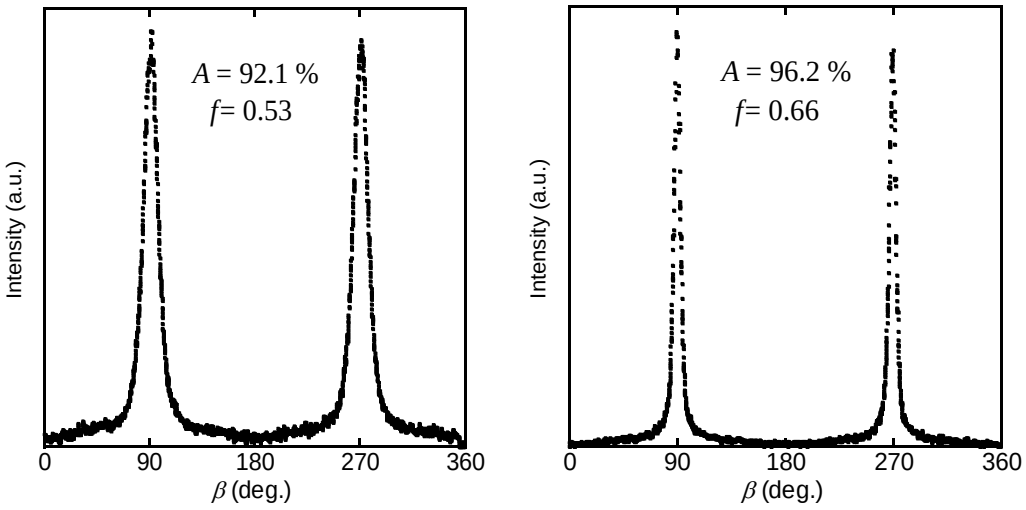

(c) modified with LiBr (d) modified with LiBr (stretched)

Figure 4.9 Azimuthal distribution of the (101) plane

The molecular orientation within the fibers was evaluated quantitatively using the azimuthal distributions in Figure 4.10. The degree of orientation *A* was determined by the half-width method, using the following equation:

$$A\,(\%) = \frac{360\,(deg) - \Sigma W_h}{360\,(deg)} \times 100 \qquad (4.4),$$

where W_h is the width at half the peak maximum. The LiBr in the aqueous solution increased the orientation of the PVA fibers from 89.6% to 92.1%. The difference was still apparent even after hot-stretching, i.e., 94.8% for PVA and 96.2% for PVA fiber modified with LiBr. This was as expected because a high level of orientation is achieved by hot-stretching when using a fiber that originally has a high orientation.

The chain orientation was also characterized by Hermans' orientation function *f*, which is defined in the following equation:

$$f = \frac{3 < cos^2\varphi > - 1}{2} \qquad (4.5),$$

where φ represents the average angle made by a segment with the fiber axis.

Furthermore, $< cos^2\varphi >$ was determined using Wilchinsky's equation [31]:

$$< cos^2\varphi > = 1 - \frac{(1 - 2sin^2\rho_2)(cos^2\phi_1) - (1 - 2sin^2\rho_1)(cos^2\phi_2)}{sin^2\rho_1 - sin^2\rho_2} \quad (4.6),$$

where the subscripts 1 and 2 refer to the (200) and (001) planes, respectively. Thus, the ρ values for (200) and (001)—i.e., ρ_1 and ρ_2—with respect to the α-axis are 0 and 88.3°, respectively [57, 60]. The $<\cos^2\phi_{200}>$ and $<\cos^2\phi_{001}>$ values are calculated using the following equation [57, 61, 62]:

$$< cos^2\phi_{h0l} >= \frac{\int_0^\pi I(\varphi_{hkl}) \cos^2 \varphi_{hkl} \sin \varphi_{hkl} \, d\varphi_{hkl}}{\int_0^\pi I(\varphi_{hkl}) \sin \varphi_{hkl} \, d\varphi_{hkl}} \quad (4.7),$$

where I (ϕ_{h0l}) is the intensity of the ($h0l$) plane at the azimuthal angle β. It is apparent from the A and f values, which are denoted in the figure, that the orientation of the PVA fibers was greatly enhanced by the addition of LiBr to the solution. This phenomenon was confirmed even after hot-stretching.

4-3-4 Tensile properties

The tensile stress–strain curves of the fibers are shown in Figure 4.10, where both stress and strain are engineering values. The results of the tensile tests were summarized in Table 4.3. Figure 4.11(a) shows the results obtained for the fibers without hot-stretching. The tensile modulus of the PVA fiber modified with LiBr (3.56 GPa)—i.e., the fiber produced from the solution with LiBr—was significantly higher than that of the pure PVA fiber (2.92 GPa). The yield stress of the PVA fiber modified with LiBr (59.5 MPa) was also higher than that of the pure PVA fiber (51.6 MPa). In the other words, the stress–strain curves were greatly affected by hot-stretching.

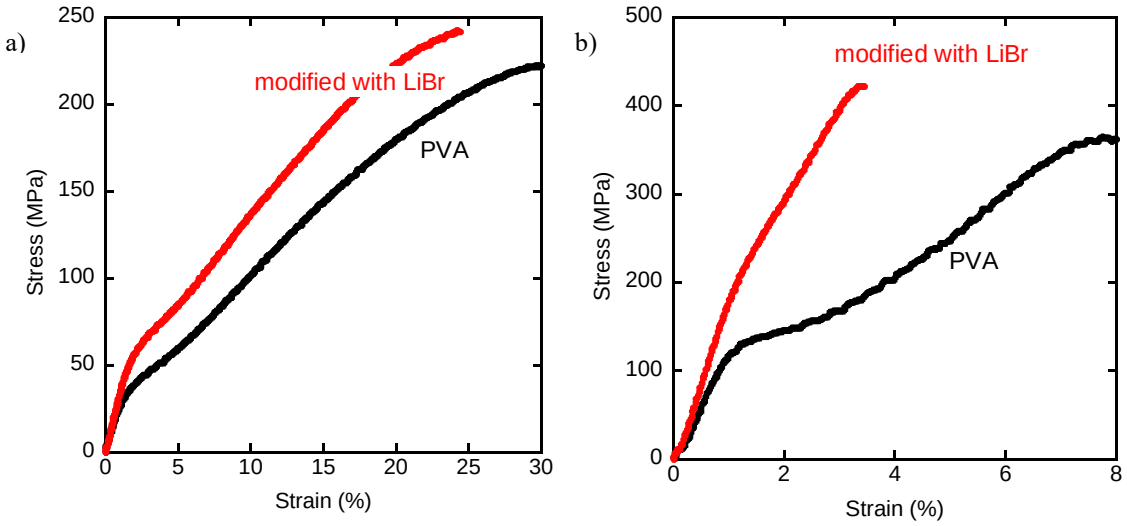

Figure 4.11 Stress–strain curves of (a) fibers without hot-stretching and (b) fibers with hot-stretching process

It should be noted that a yield point was hardly discernable in the fiber modified with LiBr, which had a high tensile modulus. This result must be attributable to the high level of molecular orientation in the fiber.

Table 4.3 Tensile properties of the fibers

Sample name	PVA	Modified with LiBr	PVA (stretched)	Modified with LiBr (stretched)
Tensile modulus (GPa)	2.92 (0.01)	3.56 (0.05)	7.75 (0.01)	17.5 (0.01)
Yield stress (MPa)	51.6 (0.15)	59.5 (0.12)	141 (0.13)	177 (0.20)

Yield strain (%)	1.77	1.67	1.81	1.01
	(0.14)	(0.17)	(0.08)	(0.06)

(standard deviation).

4-4 Conclusion

A novel technique for modifying PVA fibers by the addition of LiBr was proposed in the present study. The appropriate amount of LiBr in terms of the molar ratio of LiBr to the hydroxyl groups in the PVA was determined by the rheological properties of aqueous solutions of LiBr. As a result, 0.10 molar ratio of LiBr was found to effectively reduce the hydrogen bonds between the PVA chains. Even when the fibers were wet-spun, LiBr greatly reduced the inter- and intramolecular hydrogen bondings in the PVA chains, and resulted in a high level of molecular orientation. The LiBr was removed from the fiber during the spinning process in the coagulation bath and during the washing process. As a result, hardly any LiBr remained in the obtained fiber. There was a high level of orientation, even after hot-stretching, which greatly enhanced the modulus and strength. This technique will provide a novel, strong, lightweight super fiber with a high modulus that can be used in advanced fiber-reinforced plastics.

References

1. S. Lee, H. Kawakami, K. Hitomi, Kasen Koenshu, Jpn. Pat. 5, 1940, 115.
2. T. Osugi, Man-made fibers, Interscience, New York, 1968, Vol, 3, pp. 258.
3. R.K. Tubbs, T.K. Wu, Polyvinyl alcohol, John Wiley & Sons, London, 1973, pp.169.
4. J. Brandrup, E.H. Immergut, Polymer Handbook, 2nd ed. John Wiley & Sons, New York, 1975, pp.89.
5. I. Sakurada, A. Nakajima, H. Takida, Kobunshi Kagaku, 12, 1955, 21.
6. F. Hamada, A. Nakajima, Kobunshi Kagaku, 23, 1966, 395.
7. K. Kikukawa, S. Nozakura, S. Murahashi, Kobunshi Kagaku, 25, 1968, 19.
8. R.K. Tubbs, T.I. Wu, Polyvinyl alcohol, John Wiley & Sons, London, 1973, pp.168.
9. C.G. Berry, T.G. Fox, The viscosity of polymers and their concentrated solutions, In Fortschritte der Hochpolymeren-Forschung, Springer, Berlin, Heidelberg, 1968, pp. 261-357.
10. I. Sakurada, Kobunshi Kako, 28, 1979, 316.
11. V. Beachley, X. Wen, Effect of electrospinning parameters on the nanofiber diameter and length, Mater. Sci. Eng. 29 (2009) 663-668.
12. A. Mráček J. Varhaníková M. Lehocký L. Gřundělová A. Pokopcová V. Velebný, The influence of hofmeister series ions on hyaluronan swelling and viscosity, Molecules 13 (2008) 1025-1034.
13. Z. Peng, D. Chen, Study on the nonisothermal crystallization behavior of poly (vinyl alcohol)/attapulgite nanocomposites by DSC analysis, J. Polym. Sci. B: Polym. Phys. 44 (2006) 534-540.
14. E. Thormann, On understanding of the Hofmeister effect: how addition of salt alters the stability of temperature responsive polymers in aqueous solutions, Rsc. Adv. 2

(2012) 8297-8305.

15. J. Wang, M. Satoh, Novel PVA-based polymers showing an anti-hofmeister series property, Polymer 50 (2009) 3680-3685.
16. S. Nihonyanagi, S. Yamaguchi, T. Tahara, Counterion effect on interfacial water at charged interfaces and its relevance to the Hofmeister series, J. Am. Chem. Soc. 136 (2014) 6155-6158.
17. O.N. Tretinnikov, S.A. Zagorskaya, Effect of inorganic salts on the crystallinity of polyvinyl alcohol, J. Appl. Spectros. 78 (2012) 904-908.
18. Y. Ren, D.R. Picout, P.R. Ellis, S.B. Ross-Murphy, Solution properties of the xyloglucan polymer from Afzelia Africana, Biomacromolecules 5 (2004) 2384-2391.
19. A. Miyagawa, V. Ayerdurai, S. Nobukawa, M. Yamaguchi, Viscoelastic properties of poly(methyl methacrylate) with high glass transition temperature by lithium salt addition, J. Polym. Sci. B: Polym. Phys. 54 (2016) 2388-2394.
20. Y. Sato, A. Ito, S. Maeda, M. Yamaguchi, Structure and optical properties of transparent polyamide 6 containing lithium bromide, J. Polym. Sci B: Polym. Phys. 56 (2018) 1513-1520.
21. C.N. Walker, C. Versek, M. Touminen, G.N. Tew, Tunable networks from thiolene chemistry for lithium ion conduction, ACS Macro. Lett. (2012) 737-741.
22. N. Tsugawa, A. Ito, M. Yamaguchi, Effect of lithium salt addition on the structure and optical properties of PMMA/PVB blends, Polymer 146 (2018) 242-248.
23. S. Tomie, N. Tsugawa, M. Yamaguchi, Modifying the thermal and mechanical properties of poly (lactic acid) by adding lithium trifluoromethanesulfonate, J. Polym. Res. 25 (2018) 206.

24. M. Yamaguchi, R. Takatani, Y. Sato, S. Maeda, Moisture-sensitive smart hot-melt adhesive from polyamide 6, SN Appl. Sci. 2 (2020) 1-8.

25. X. Wang, S.Y. Park, K.H. Yoon, W.S. Lyoo, B.G. Min, The effect of multi-walled carbon nanotubes on the molecular orientation of poly(vinyl alcohol) in drawn composite films, Fibers Polym. 7 (2006) 323-327.

26. K. Yamaura, Polymeric Materials Encyclopedia, CRC Press, Boca Raton, 1996, Vol, 9, pp. 6998.

27. D. Lai, Y. Wei, L. Zou, Y. Xu, H. Lu, Wet spinning of PVA composite fibers with a large fraction of multi-walled carbon nanotubes, Prog. Nat. Sci.: Mater. Int. 25 (2015) 445-452.

28. T. Takahashi, K. Suzuki, T. Aoki, K. Sakurai Banded structure of gel-drawn poly (vinyl alcohol) fibers, J. Macromol. Sci. B: Phys. 30 (1991) 101-118.

29. M.L. Minus, H.G. Chae, S. Kumar, Single wall carbon nanotube templated oriented crystallization of poly (vinyl alcohol), Polymer 47 (2006) 3705-3710.

30. L. Kou, C. Gao, Bioinspired design and macroscopic assembly of poly(vinyl alcohol)-coated graphene into kilometers-long fibers, Nanoscale 5 (2013) 4370-4378.

31. R. Ricciardi, F. Auriemma, C. De Rosa, F. Lauprêtre, X-ray diffraction analysis of poly (vinyl alcohol) hydrogels, obtained by freezing and thawing techniques, Macromolecules 37 (2004) 1921-1927.

32. Z.W. Wilchinsky, Measurement of orientation in polypropylene film, J. Appl. Phys. 31 (1960) 1969-1972.

33. J. Peng, T. Ellingham, R. Sabo, L.S. Turng, C.M. Clemons, Short cellulose nanofibrils as reinforcement in polyvinyl alcohol fiber, Cellulose 21 (2014)

4287-4298.

34. J. Peng, T. Ellingham, R. Sabo, C.M. Clemons, L.S. Turng, Oriented polyvinyl alcohol films using short cellulose nanofibrils as a reinforcement, J. Appl. Polym. Sci. 132 (2015) 42283.

Chapter 5 Impact of magnesium salt addition to poly(vinyl alcohol)

5-1 Introduction

5-1-1 Magnesium salts

The effect of lithium salts on PVA structure was revealed in Chapter 1, 2, and 3. However, most of the manufactures prefer the salt that gives least harmful side-effect and good cost-performance for the industrial application [1,2]. In this chapter, magnesium salts were focused to give the interesting and outstanding results. Previously, there were a few studies that used magnesium salts to improve PVA properties. Other researchers have proved that $Mg(NO_3)_2$ and $MgCl_2$ have a high plasticizing efficiency for PVA, and the compatibility between these metal salts and PVA is very good [1,2]. Moreover, it was reported in the literature that a magnesium salt has the smallest cation radius and the largest lattice energy. Therefore, its stability and the strength of ionic bond are the highest, which contributes to form stronger hydrogen bonding between PVA and magnesium salts [3]. In general, the main factor that could influence the lattice energy of ionic crystals is the ionic charge. The lattice energy increases as the charge increases. The second factor is the ionic radius, as the lattice energy increases with the decrease in the ionic radius. Therefore, the selection of a magnesium salt in this study was appropriate as it has high charge, compared to lithium. Furthermore, to the best of my knowledge, there is still no research focused on the effect of magnesium salts with various anion species on the mechanical properties of a PVA film.

Kubo et al. revealed that $Mg(NO_3)_2$ decreases the crystallization rate of PVA, and shifts T_g to a low temperature. Since the salt reduces PVA crystallinity, it enhances the segmental motion [1]. However, the effect of anion species of a salt was not

investigated in these studies. Besides, the effects of magnesium salts with various anion species on the thermal and mechanical properties have not been clarified in detail yet. Therefore, the selection of a magnesium salt to modify the structure and properties of PVA in terms of crystallinity and hydrogen bonding could be considered as an appropriate research.

5-1-2 X-ray reflection in accordance with Bragg's Law

The structures of crystals and molecules are often being identified using x-ray diffraction studies, which are explained by Bragg's Law [4]. The law explains the relationship between an x-ray light shooting into and its reflection off from the crystal surface. Bragg diffraction (also referred to as the Bragg formulation of X-ray diffraction) was first proposed by William Lawrence Bragg and William Henry Bragg in 1913 in response to their discovery that crystalline solids produced surprising patterns of reflected X-rays (in contrast to that of, say, a liquid) [5]. They found that in these crystals, for certain specific wavelengths and incident angles, intense peaks of reflected radiation (known as Bragg peaks) were produced [6]. W. L. Bragg explained this result by modeling the crystals as a set of discrete parallel planes separated by a constant parameter d. It was proposed that the incident X-ray radiation would produce a Bragg peak if their reflections off the various planes interfered constructively[7]. Bragg's law gives a simple condition under which a diffracted beam can be observed. Figure 5.1 shows a beam of parallel X-rays penetrating a set of parallel lattice planes with indices h,k,l of spacing d and at an angle of incidence θ. The lattice planes are represented behaving as a mirror.

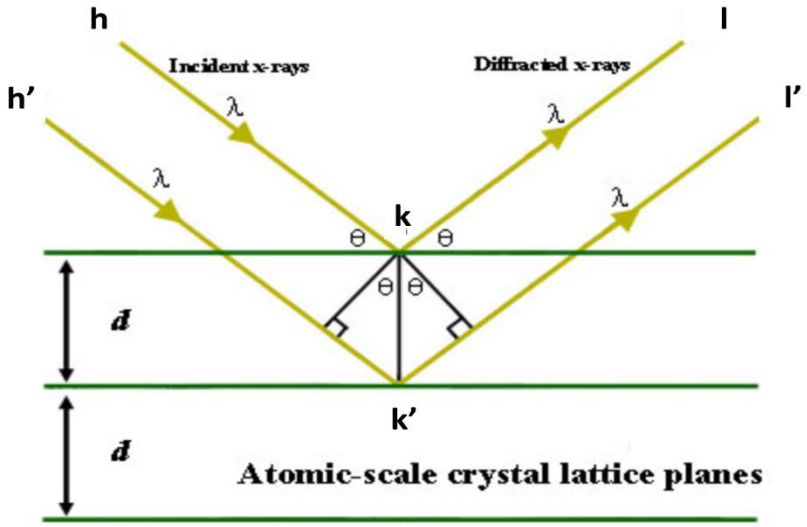

Figure 5.1 Bragg's Law diffraction [8]

When a crystal is bombarded with X-rays of a fixed wavelength (similar to spacing of the atomic-scale crystal lattice planes) and at certain incident angles, intense reflected X-rays are produced when the wavelengths of the scattered X-rays interfere constructively. In order for the waves to interfere constructively, the differences in the travel path must be equal to integer multiples of the wavelength. When this constructive interference occurs, a diffracted beam of X-rays will leave the crystal at an angle equal to that of the incident beam. To illustrate this feature, consider a crystal with crystal lattice planar distances d (right). Where the travel path length difference between the ray paths *hkl* and *h'k'l'* is an integer multiple of the wavelength, constructive interference will occur for a combination of that specific wavelength, crystal lattice planar spacing and angle of incidence (θ). Each rational plane of atoms in a crystal will undergo refraction at a single, unique angle (for X-rays of a fixed wavelength) [8].

The general relationship between the wavelength of the incident X-rays, angle of incidence and spacing between the crystal lattice planes of atoms is known as Bragg's Law, and is expressed as:

$$n\lambda = 2d \sin\theta \tag{5.1}$$

where n (an integer) is the "order" of reflection, λ is the wavelength of the incident X-rays, d is the interplanar spacing of the crystal and θ is the angle of incidence.

5-2 Experimental

5-2-1 Materials

The polymeric material used in this study was a commercially available PVA, kindly provided by Kuraray Co., Ltd. The degree of polymerization was 1700 and the degree of saponification was 99.8 mol%. Magnesium perchlorate $Mg(ClO_4)_2$ was purchased from Kanto Chemical Co., Ltd., Japan. Magnesium bromide $MgBr_2$ and magnesium acetate $Mg(CH_3COO)_2$ were purchased from Wako Pure Chemical Industry Ltd., Japan. Magnesium chloride $MgCl_2$ was purchased from Nacalai Tesque, Inc., Japan and magnesium sulphate $MgSO_4$ was purchased from Tokyo Chemical Industry Co., Ltd., Japan. All salts were used without further purification. Deionized water was used throughout the study.

5-2-2 Preparation of PVA aqueous solution, film, and fiber

Magnesium salts were added into the PVA solutions at molar ratios of 0, 0.012, 0.025 and 0.050 relative to the quantity of PVA hydroxyl groups, and the PVA

concentration was fixed at 15 wt%. Each aqueous solution was prepared by dissolving 7.5 g of PVA in 42.5 mL of deionized water at 90 °C using a magnetic stirrer operating at 400 rpm. The salt was subsequently added with continuous stirring at 400 rpm for approximately 3 h until complete dissolution. For film preparation, the solutions were then cast onto a polytetrafluoroethylene-coated tray and preheated at 70°C for 6 h. The obtained films were further dried at 100°C under vacuum for another 5 h. Finally, the samples were dried again at 80°C under vacuum for 4 h before the measurements to avoid the effects of moisture.

5-2-3 Measurements

The rheological properties of each solution were evaluated using the parallel-plate rheometer (AR2000ex; TA Instruments, Inc., New Castle, DE, USA), as described in Chapter 2. The frequency sweep tests of the shear storage modulus *G'* and loss modulus *G"* were carried out from 0.05 to 500 rad/s at various temperatures. The gap between the plates was 1 mm.

The film morphology was observed using a scanning electron microscope (SEM; TM3030Plus Hitachi, Ltd, Tokyo, Japan). Prior to observation, all films were coated with Pt and Pd by a sputter coating machine. The energy dispersive X-ray analysis (EDX) was performed after the coating process.

The temperature dependence of tensile storage modulus *E′* and loss modulus *E″* was measured from 20°C to 180°C using a dynamic mechanical analyzer (Rheogel-E4000; UBM Co., Ltd., Mukō, Japan). The frequency and heating rate were 10 Hz and 2°C/min, respectively. Samples were cut from the film (which was 200 μm thick); each

sample was 5 mm wide and 10 mm long. The film was used immediately after the final drying process to avoid the moisture effects, which greatly affects T_g.

The water content in the films with 200 μm thickness (10 mm in width × 20 mm in length) was measured using an 899 Coulometer coulometric Karl Fischer titrator (Metrohm AG, Herisau, Switzerland). The measurements were repeated three times for each film to confirm the reproducibility.

The thermal properties of the films were evaluated by using a differential scanning calorimetry (DSC) (DSC8500; PerkinElmer, Inc., Waltham, MA, USA). The samples were heated from 25°C to 270°C at a heating rate of 10°C/min under a nitrogen atmosphere. DSC evaluation for each sample was carried out on approximately ~10 mg sample weight and encapsulated in a hermetically sealed aluminum pan.

Wide-angle X-ray diffraction (WAXD) analyses were performed using an X-ray diffraction machine (SmartLab; Rigaku Corp., Akishima, Japan) in the reflection mode at a scanning speed of 10°/min by a graphite-monochromatized CuKα beam generated at 40 kV and 30 mA.

Infrared spectra were collected using a Fourier-transform infrared spectrum (Spectrum 100; PerkinElmer) at room temperature. The measurements were performed in the attenuated mode using KRS-5 as an ATR crystal and obtained at a resolution of 4.0 cm^{-1} by averaging 16 scans.

5-3 Results and Discussion

5-3-1 Rheological properties of aqueous solution

Figure 5.2 summarizes the angular frequency dependence of the oscillatory shear

moduli at 25 °C of PVA solution with $Mg(ClO_4)_2$. The salt was added at a 0.050 molar ratio relative to the quantity of hydroxyl groups in PVA. It is evident that the addition of the salt increased the plateau modulus in the low frequency region and also increased the *G"* value over a wide range of frequencies. These data suggested that hydrogen bonding between the PVA chains is enhanced by the presence of the salt, as previously demonstrated in Chapter 2. This phenomenon can be explained by the HS. Since K^+ is a water-structure-maker, the shear viscosity was enhanced with an increased plateau modulus due to the network structure produced by strong hydrogen bonding [9,10]. Besides, this phenomenon might be attributed to fully dissociation of the salt in PVA aqueous solution. It was noticeable that the addition of a magnesium salt enhances the modulus because a magnesium salt has a good stability and the highest strength of ionic bond. However, at 60 °C, the effect of salt addition on the rheological properties became insignificant due to the reduced hydrogen bond. Thus, the addition of magnesium salts into PVA films either enhances or reduces the plateau modulus depending on the temperature because of their temperature sensitivity. To the best of my knowledge, this is a new finding.

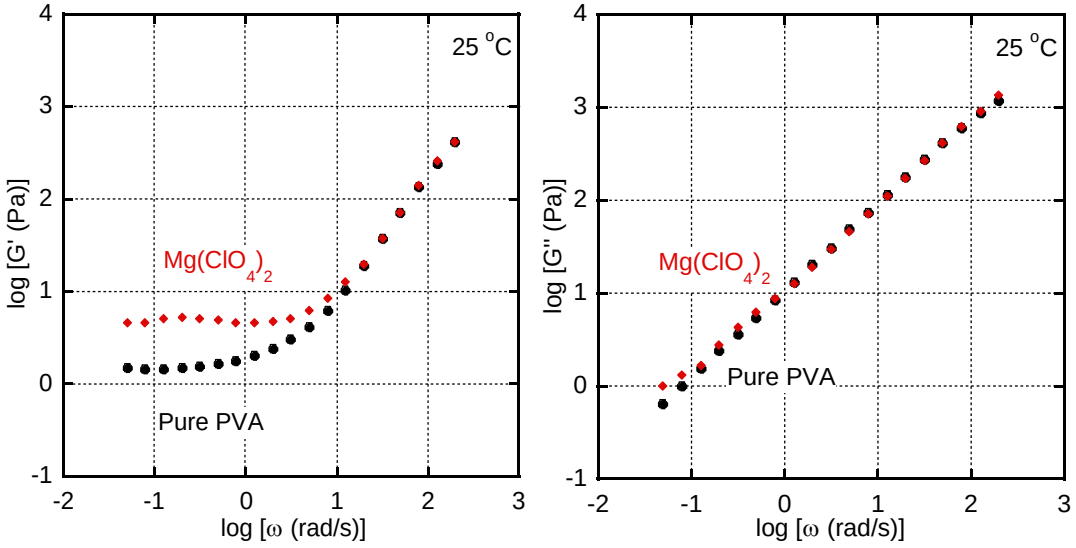

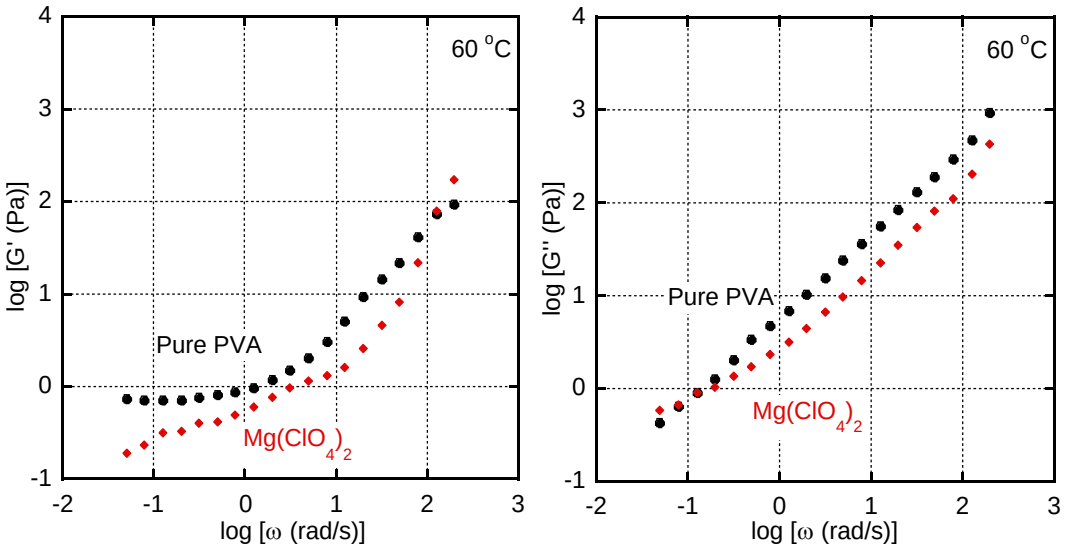

Figure 5.2 Angular frequency dependence of the oscillatory shear moduli at 25 °Cand 60 °C of aqueous PVA solutions with $Mg(ClO_4)_2$ added at a 0.05 molar ratio.

5-3-2 Dispersion of magnesium salts in film

Figure 5.3 exemplifies the film appearance after the salt addition. The PVA film containing $Mg(ClO_4)_2$ was transparent at 0.05 molar ratio. In contrast, the films with $MgSO_4$ were opaque due to light scattering caused by salt segregation, which was pronounced with increasing the salt content. Because all the aqueous solutions used for the film samples were transparent, phase separation, i.e., salt segregation, probably occurred during water evaporation process. The differences in the appearance of the films can be explained by the HS. According to the HS, weakly hydrated anions such as ClO_4^- and Br^- are categorized as a water-structure-breaker, and is highly soluble in aqueous PVA. On the contrary, strongly hydrated anions such as SO_4^{2-} are categorized as a water-structure-maker and shows poor solubility in aqueous PVA. Therefore, the films containing $Mg(ClO_4)_2$, $MgBr_2$, and $MgCl_2$ were transparent. In contrast, the films that

contained sulphate salts were opaque, owing to salt segregation [11,12].

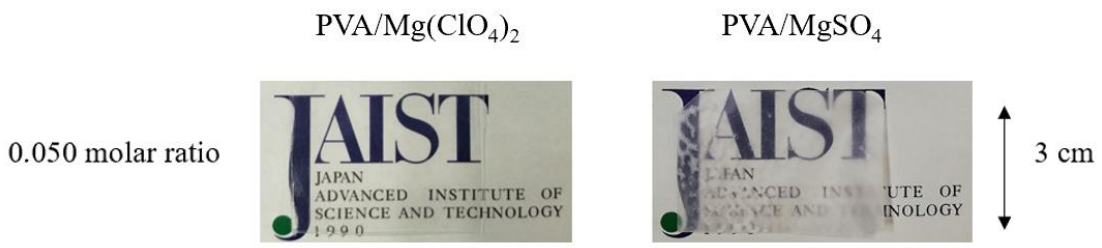

Figure 5.3 Photograph of the films with 200 μm thickness (left) PVA/ $Mg(ClO_4)_2$ and (right) PVA/$MgSO_4$ with 0.050 molar ratio.

The salt distribution in the PVA films containing magnesium salts was investigated using EXD. Figure 5.4 shows the EDX images of PVA films with $Mg(ClO_4)_2$ and $MgSO_4$. Clearly, carbon (green), oxygen (red), chloride (purple), and magnesium (blue) were detected for $Mg(ClO_4)_2$ and carbon (blue), oxygen (green), sulfur (red), and magnesium (purple) were detected for $MgSO_4$. By the addition of $Mg(ClO_4)_2$ the salt was quite homogenous since ClO_4^- is categorized as a water-structure breaker and is highly soluble in PVA aqueous solution. As the additon of $MgSO_4$ was increased, the salt seggregation was obvious. As explained by the HS, SO_4^{2-} is categorized as a water-structure-maker and is poorly soluble in aqueous PVA [13]. Therefore, the films containing SO_4^{2-} anions were opaque which became more obvious with the salt concentration.

0.012 molar ratio $Mg(ClO_4)_2$

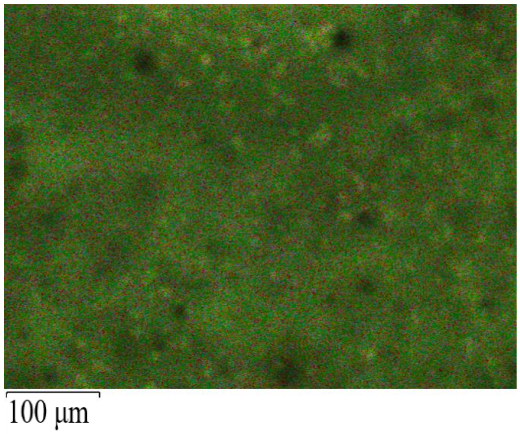

0.025 molar ratio $Mg(ClO_4)_2$

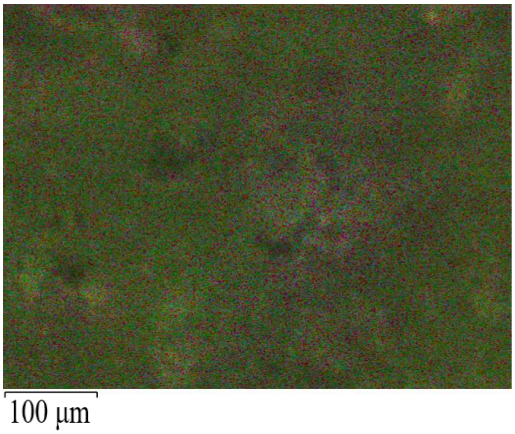

0.050 molar ratio $Mg(ClO_4)_2$

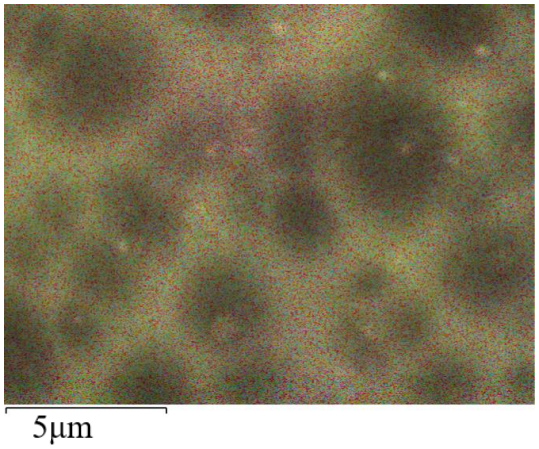

0.012 molar ratio $MgSO_4$

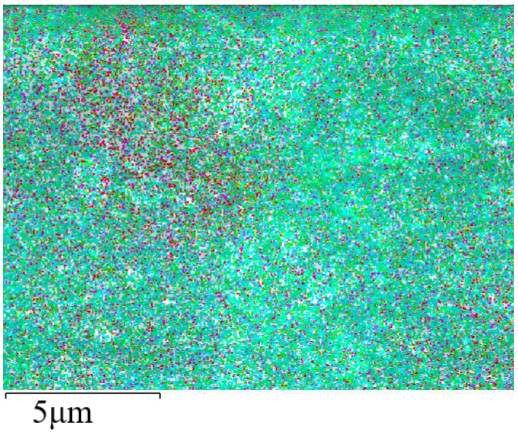

0.025 molar ratio $MgSO_4$

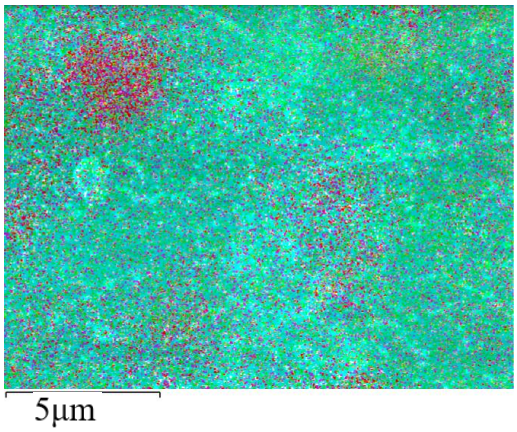

0.050 molar ratio $MgSO_4$

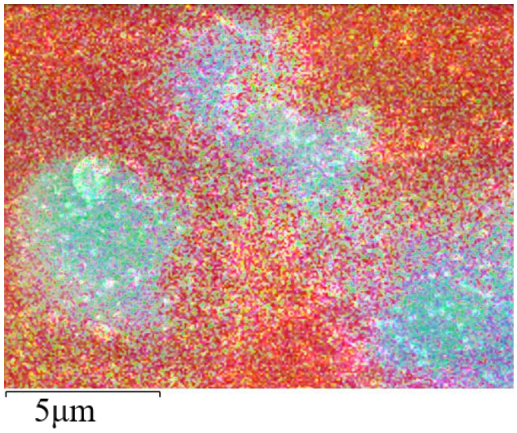

Figure 5.4 Energy-dispersive X-ray spectroscopy images for the PVA films with $Mg(ClO_4)_2$ and $MgSO_4$

5-3-3 Mechanical properties

The dynamical mechanical properties in the solid state of the films containing $Mg(ClO_4)_2$ are shown in Figure 5.5. The peak temperature of E'', i.e., T_g, is found to be affected by the salt addition, which depends on the salt concentration. T_g was greatly enhanced by 0.012 molar ratio. The peak temperature slightly decreased, although the concentration of $Mg(ClO_4)_2$ increased. The T_g was located at 70 °C for pure PVA, 100 °C for PVA with 0.012 molar ratio, 92 °C for 0.025 molar ratio, and 90°C for PVA with 0.050 molar ratio. The width of the E'' peak became slightly broad, and therefore, the E' gradually decreased, especially in the high temperature region. This was attributed to the broadness of ion dipole interaction for PVA containing $Mg(ClO_4)_2$, because there were several kinds of interaction leading to broad relaxation mechanism.

The previous result on the aqueous solution behavior indicated that the hydrogen bonding of PVA chains became enhanced after the dissociation of magnesium salt. It was observed that the plateau modulus enhanced, and the same phenomenon happened even

in a solid state, as the T_g was enhanced. The temperature sensitivity also plays an important role as it affects the ion dipole interaction. As similar to the aqueous solution, the modulus decreased greatly at high temperatures beyond the T_g.

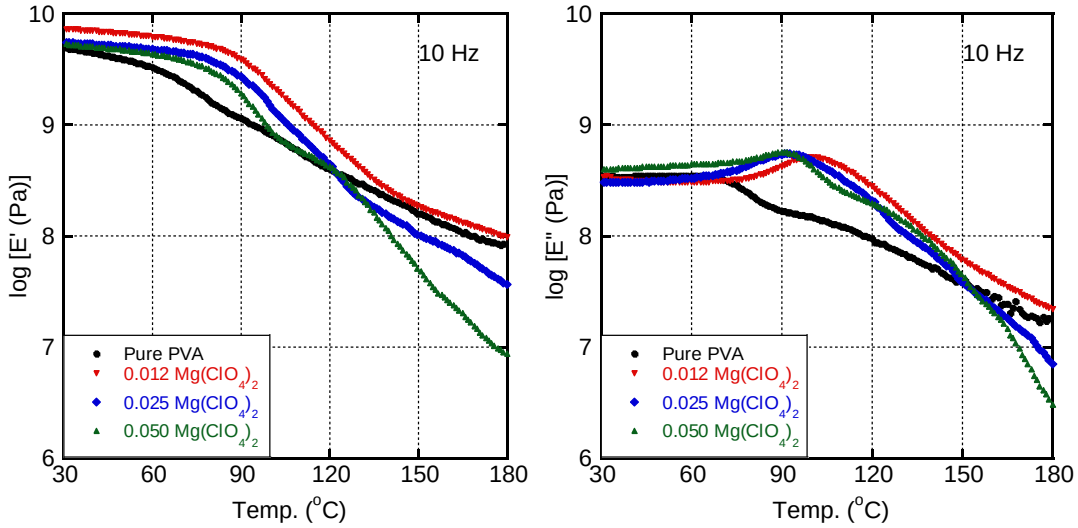

Figure 5.5 Temperature dependence of dynamic tensile moduli such as storage modulus *E'* and loss modulus *E"* at 10 Hz for the films of pure PVA and PVA with $Mg(ClO_4)_2$

5-3-4 Mechanical properties of PVA film with magnesium salt addition

Figure 5.6 illustrates the temperature dependence of the dynamic tensile moduli for PVA films containing various magnesium salts. The PVA films containing $MgBr_2$, $MgCl_2$, $Mg(CH_3COO)_2$, and $MgSO_4$ were prepared with various concentrations, i.e., 0, 0.012, 0.025, and 0.050 molar ratio. It was obvious that adding magnesium salts greatly enhanced T_g. As the concentration of $MgBr_2$ and $MgCl_2$ increased, the peak temperature of *E"*, i.e., the T_g, slightly decreased; T_g 70 °C for pure PVA, 92 °C for PVA with 0.012 molar ratio $MgBr_2$, 81 °C for 0.025 molar ratio $MgBr_2$, and 81°C for PVA with 0.050 molar ratio $MgBr_2$. For $MgCl_2$, the T_g was located at 81 °C, 79 °C, and 76 °C for 0.012,

0.025, and 0.050 molar ratios. Clearly, they have higher E' values than the film comprising of pure PVA, especially near the glass-to-rubber transition. Moreover, these PVA films containing magnesium salts exhibit a sharp peak in E'' at approximately 80-100°C. Therefore, the glass-to-rubber transition of films containing magnesium salts occured in a narrow temperature range, even though they were prepared in the same way as the pure PVA film. There was a clear stepwise decrease in the E' value in the transition region corresponding to the sharp peak in E''.

As the concentrations of $Mg(CH_3COO)_2$ and $MgSO_4$ increased, the moduli were enhanced. Both G' and G'' were found to be increased in a wide temperature region by the salt addition. T_g was located at 70 °C for pure PVA, 77 °C for PVA with 0.012 molar ratio $Mg(CH_3COO)_2$, 86 °C for 0.025 molar ratio $Mg(CH_3COO)_2$, and 91°C for PVA with 0.050 molar ratio $Mg(CH_3COO)_2$. For $MgSO_4$, the T_g was located at 87 °C, 87 °C, and 89 °C for 0.012, 0.025, and 0.050 molar ratio. Both CH_3COO^- and SO_4^{2-} anions are water-structure-makers, and the E' values of the $Mg(CH_3COO)_2$ and $MgSO_4$- containing films were much higher than those of PVA films containing other magnesium salts, i.e., $Mg(ClO_4)_2$, $MgBr_2$, and $MgCl_2$,. This suggests that the other PVA films containing magnesium salts have little or no crystallinity. Correspondingly, the E'' peak was very sharp at low temperatures, implying that the motion of amorphous chains is barely affected by the crystalline phase of the magnesium-containing film.

It can be concluded from the data that small amount of salt concentration, i.e., 0.012 molar ratio, for good water-strucutre-breaker, $MgBr_2$ and $MgCl_2$, was appropriate as it was easily dissociated compared to $Mg(CH_3COO)_2$ that was hardly dissociated. Therefore, for $Mg(CH_3COO)_2$, a high concentration, i.e., 0.05 molar ratio was required to enhance the T_g. In the case of $MgSO_4$ addition, T_g was enhanced but almost constant

irrespective of the concentration. This phenomenon occurs because $MgSO_4$ was a water-structure-maker that had a poor solubility. Therefore, it caused agglomeration and the film became opaque.

Since all films contain Mg^{2+} as cation, anion species must be the important factor to explain the results. Above T_g, the modulus decreases in accordance with the HS: i.e., $SO_4^{2-} < CH_3COO^- < Cl^- < Br^- < ClO_4^-$, indicating that SO_4^{2-} can reduce the solubility of PVA. They are different from Br^- and ClO_4^-, that can increase the solubility of PVA [14-17]. As a result, PVA tends to be agglomerated even if they were dissolved into water. This situation enhances the frequency of polymer-polymer interaction including hydrogen bonding.

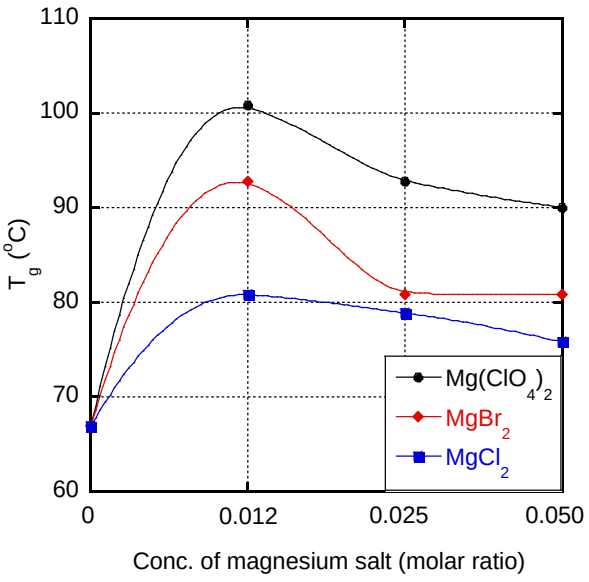

Figure 5.6 Temperature dependence of dynamic tensile moduli such as storage modulus *E'* and loss modulus *E"* at 10 Hz for the films of pure PVA and PVA with magnesium salts

5-3-5 Water content

Generally, water content has a great influence on the mechanical and thermal properties for PVA films. Thus, the effect of the salt addition on the water content in the films was studied using the PVA films containing $Mg(ClO_4)_2$. The Karl Fischer titration was performed after vacuum drying at 80 ℃ for 4 hours. Therefore, the content of water trapped by hydroxyl groups was evaluated by this measurement. As seen in Figure 5.7, the water content of films was only slightly affected by the salt addition. As the salt concentration increased, T_g slightly decreased, and the water content increased. The result indicates that the salt added to an aqueous solution generally affects the structure of water molecules. Besides, it is well known that the addition of magnesium salts which is hygroscopic in nature tends to trap water molecule in the PVA films and results in the increase in water content [18]. However, the amount of water content only gave a small difference for each film, and therefore, it barely affected the film properties. In other words, the modification of structure and properties by the salt addition is not originated from the water content.

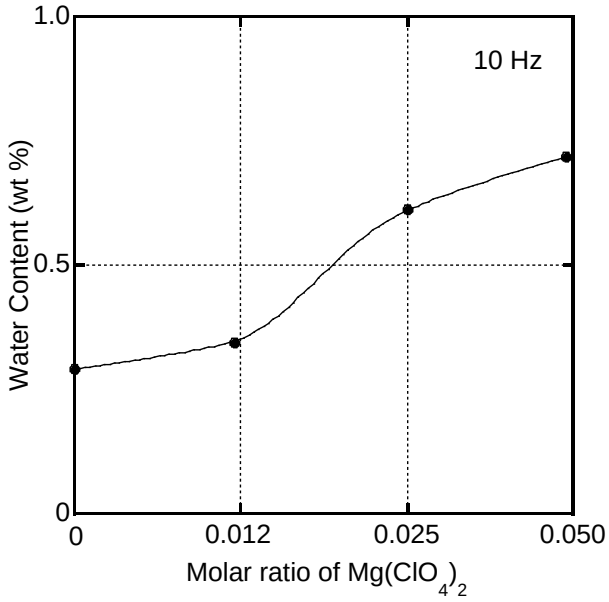

Figure 5.7 Water contents in the films of pure PVA and PVA with $Mg(ClO_4)_2$

5-3-6 Thermal properties of PVA film with magnesium salt addition

Figure 5.8 shows the DSC heating curves at 10 °C/min for the PVA films containing magnesium salts with various concentrations. The thermal properties correspond to the dynamic mechanical properties. As mentioned in Chapter 2, there was a melting peak at approximately 234 °C with a peak area of 74 J/g for pure PVA. The T_m values of the films containing $MgSO_4$ were 232.4 °C (0.012 molar ratio), 233.5 °C (0.025 molar ratio), 231.2 °C (0.050 molar ratio), respectively—i.e., not much different from that of pure PVA.

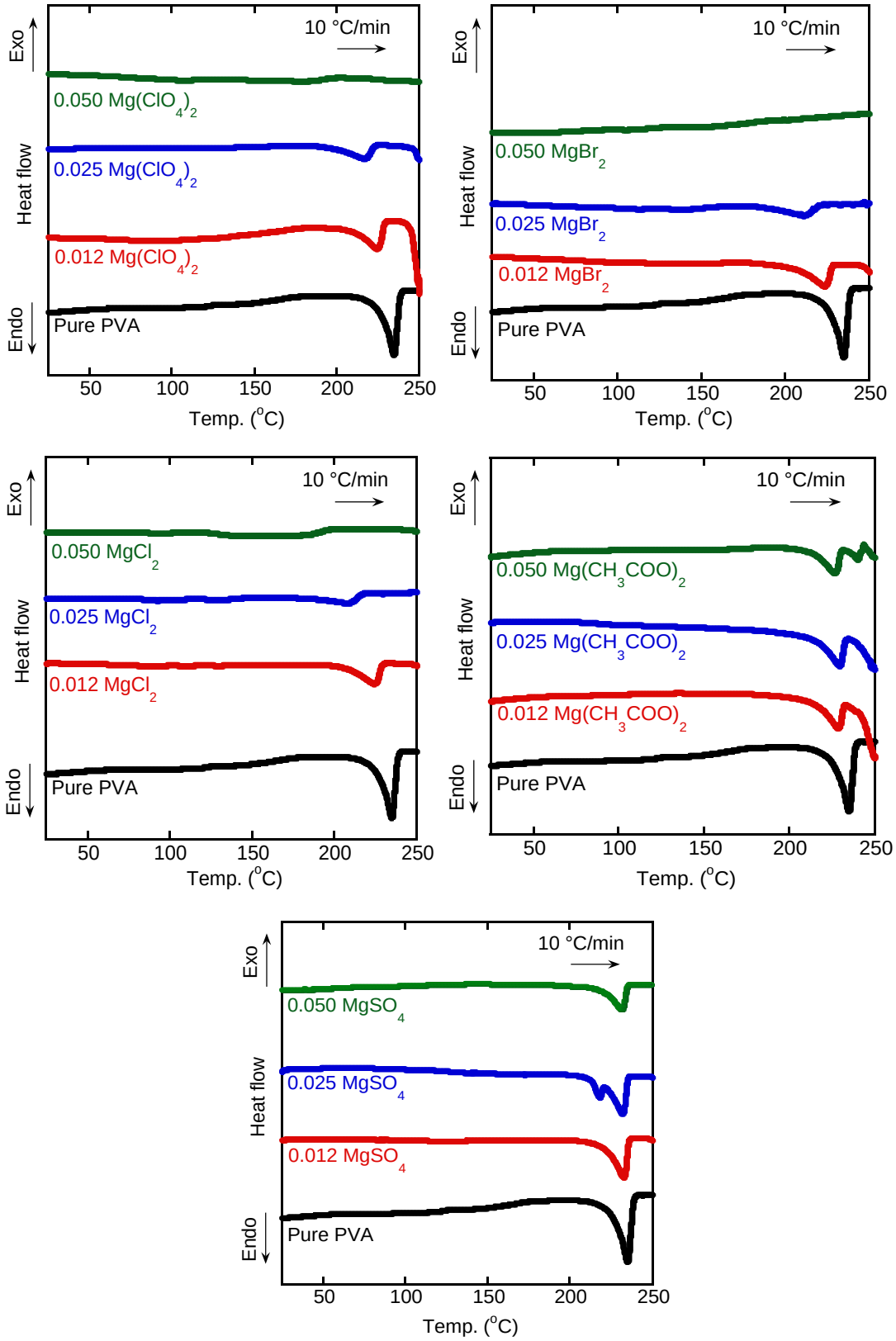

Figure 5.8 DSC heating curves obtained at 10 °C/min for the PVA films with various

molar ratios of magnesium salts

The heat of fusion $\Delta H_{f\text{-}s}$ values, determined from the curves, are provided in Table 5.1 with the degree of crystallization X_c. The degree of crystallization for PVA film containing $Mg(ClO_4)_2$ of 0.012 and 0.025 molar ratio, were 20.2 % and 16.9 % respectively, which were much lower than that of pure PVA film (48 %). For PVA films containing $MgBr_2$ and $MgCl_2$, the degree of crystallization were 24 % (0.012 molar $MgBr_2$), 9 % (0.025 molar), 28.2 % (0.012 molar $MgCl_2$), and 13.6 % (0.025 molar), respectively. Besides, $Mg(ClO_4)_2$, $MgBr_2$, and $MgCl_2$, with a molar ratio of 0.050 were found to effectively reduce the hydrogen bonds between the PVA chains, resulting in a no/low level of crystallinity. Clearly, the addition of a water-structure-breaker magnesium salt reduces the crystallinity.

Table 5.1 Thermal properties of the films containing various contents of magnesium salts

Metal Salt (molar ratio)	Melting point, T_m (°C)	Heat of fusion, ΔH_f (J/g)	Crystallinity, X_c (%)
Pure PVA	234	74	48
0.012 $Mg(ClO_4)_2$	224	30	20
0.025 $Mg(ClO_4)_2$	217	15	16
0.050 $Mg(ClO_4)_2$	-	-	-
0.012 $MgBr_2$	223	36	24
0.025 $MgBr_2$	210	16	9

0.050 $MgBr_2$	-	-	-
0.012 $MgCl_2$	224	42	28
0.025 $MgCl_2$	208	20	13
0.050 $MgCl_2$	-	-	-
0.012 $Mg(CH_3COO)_2$	228	44	29
0.025 $Mg(CH_3COO)_2$	229	49	32
0.050 $Mg(CH_3COO)_2$	226	46	31
0.012 $MgSO_4$	232	52	34
0.025 $MgSO_4$	233	45	30
0.050$MgSO_4$	231	48	31

5-3-7 XRD profiles

Figure 5.9 shows the WAXD profiles, which also indicates the crystallinity. A strong diffraction peak appeared at approximately 20° [19,20], which is attributed to the $(10\bar{1})$ and (101) planes of the orthorhombic form (the numbers in parentheses represent the Miller indices) [20]. The pure PVA film produced another weak diffraction peak at approximately 11°, which is attributed to the (100) plane [21]. This diffraction peak was weak might be due to no formation of chelate structure shown in Figure 5.10 [22].

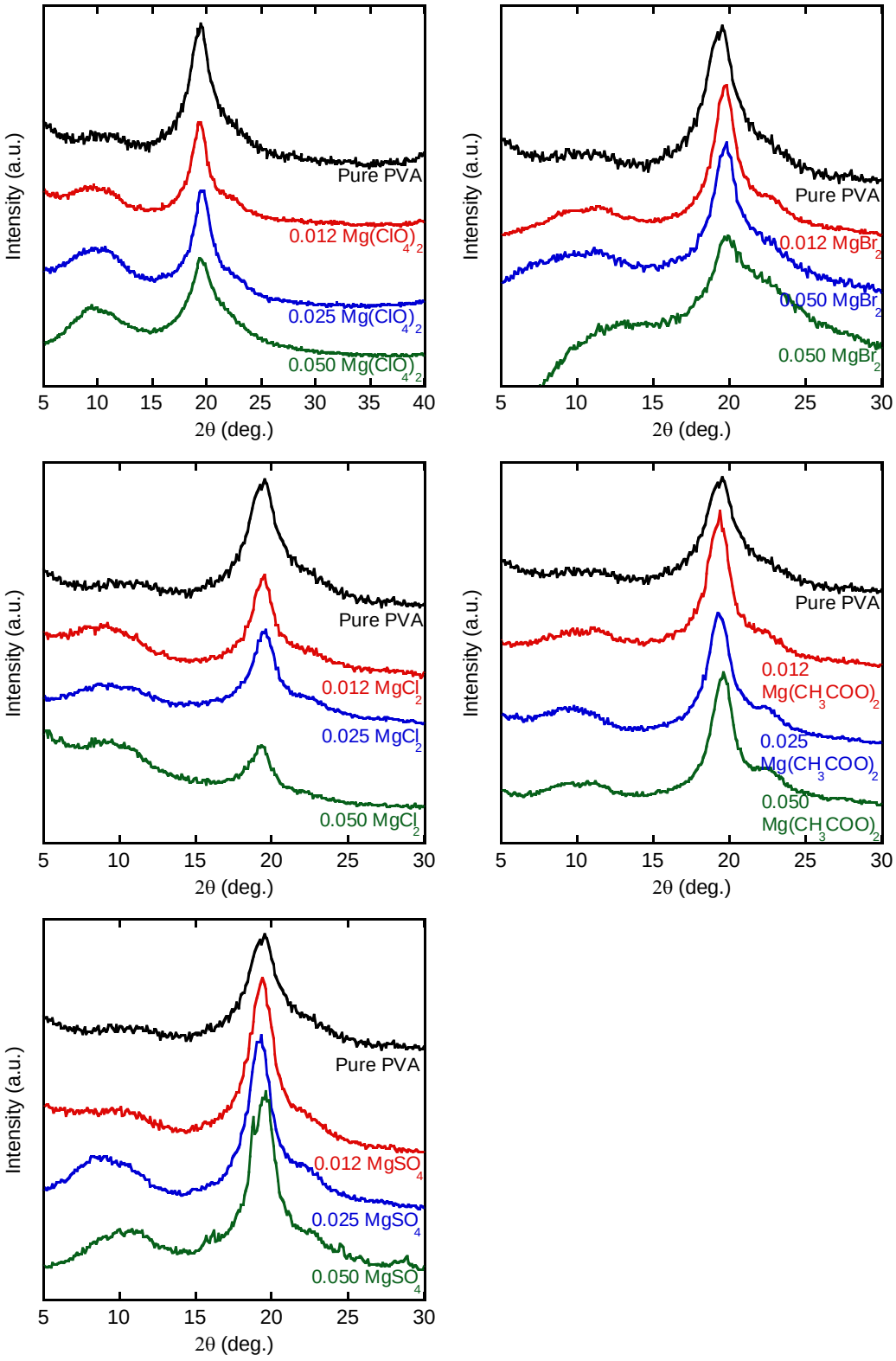

Figure 5.9 WAXD profiles for the films of pure PVA and PVA with magnesium salts

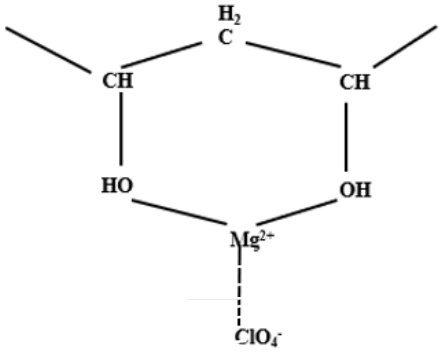

Figure 5.10 Structure for PVA- Mg^{2+} chelate proposed by Zidan [22]

XRD profiles confirmed that the crystallinity is reduced by the addition of $Mg(ClO_4)_2$, $MgBr_2$, and $MgCl_2$. Furthermore, the 2θ position of the strongest peak was slightly shifted to a larger angle for films with low crystallinity. Because this peak comprises a broad overlapping amorphous background, the peak position was affected by the crystallinity of the film. A similar phenomenon has been reported for a PVA film containing lithium salts as shown in Chapter 2. The hydrogen bonding in the PVA chains were greatly affected by the presence of ions because they were able to form strong interactions with PVA molecules and interrupt the intermolecular hydrogen bonding. The addition of $Mg(CH_3COO)_2$ and $MgSO_4$ slightly affect the crystallinity of PVA. The 2θ position of the strongest peak was almost similar to that of the pure PVA film. Besides, it was also noticeable that the diffraction peak at approximately 11° becomes stronger as the magnesium salts were added into PVA films. The small peak observed at 11° is assigned as chelate formation [22], i.e., $Mg(ClO_4)_2$ was fully dissociated and Mg^{2+} reacted with the hydroxyl groups of PVA [23]. The chelate structure proposed by Zidan is shown in Figure 5.10. It seems that most of the magnesium ions introduced in the PVA, i.e., $Mg(ClO_4)_2$, $MgBr_2$, $MgCl_2$, $Mg(CH_3COO)_2$, and $MgSO_4$ are initially linked to hydroxyl

groups.

It can be calculated by the Bragg's law: $\lambda=2d\sin(\theta)$ where λ is the wavelength of the X-ray beam (0.154nm), d is the distance between the adjacent PVA sheets or layers, θ is the diffraction angle. As can be seen in Figure 5.9, the diffraction peak position is at $2\theta= 20°$ and $2\theta= 11°$, representing the (101) planes and (100) planes, the spacing between which is the spacing between the PVA sheets:

$$d = \lambda/2 \sin(\theta) = 0.154nm/2\sin(10°) = 0.443nm.$$

$$d = \lambda/2 \sin(\theta) = 0.154nm/2\sin(5.5°) = 0.803nm.$$

5-3-8 Infrared spectra

The effect of the addition of magnesium salts on the Fourier-transform infrared (FTIR) spectra of the films was shown in Figure 5.11. It is well known that the absorbance band at 3274 cm^{-1}, which is attributable to the stretching vibration of the O-H groups in the PVA, will be shifted to a higher wavenumber following the addition of magnesium salts. This indicates that the hydrogen bonds between the PVA chains were weakened by the salt addition, as demonstrated by the LiCl and LiBr containing films [24-27]. In this study, stretching vibration of the O-H groups at 3274 cm^{-1}, for films containing $Mg(ClO_4)_2$, $MgBr_2$, and $MgCl_2$ salts were almost similar to that of the pure PVA film.

Furthermore, the absorbance of the crystalline band at approximately 1141 cm^{-1} decreased by the addition of $Mg(ClO_4)_2$, $MgBr_2$, and $MgCl_2$. In particular, the band was not detected for the film with 0.05 molar ratio. However, different phenomenon occured for $Mg(CH_3COO)_2$ and $MgSO_4$ -films as the crystalline band stayed strong as pure PVA. The degree of the effect corresponds to the HS, since $Mg(ClO_4)_2$, $MgBr_2$, and $MgCl_2$, known as chaotropes or water-structure-breakers, are responsible for the salting-in effect

and low solubility. while $Mg(CH_3COO)_2$ and $MgSO_4$, known as kosmotropes or water-structure-makers, are responsible for the salting-out effect and low solubility [28,29]. These results corroborate those obtained by DSC and WAXD.

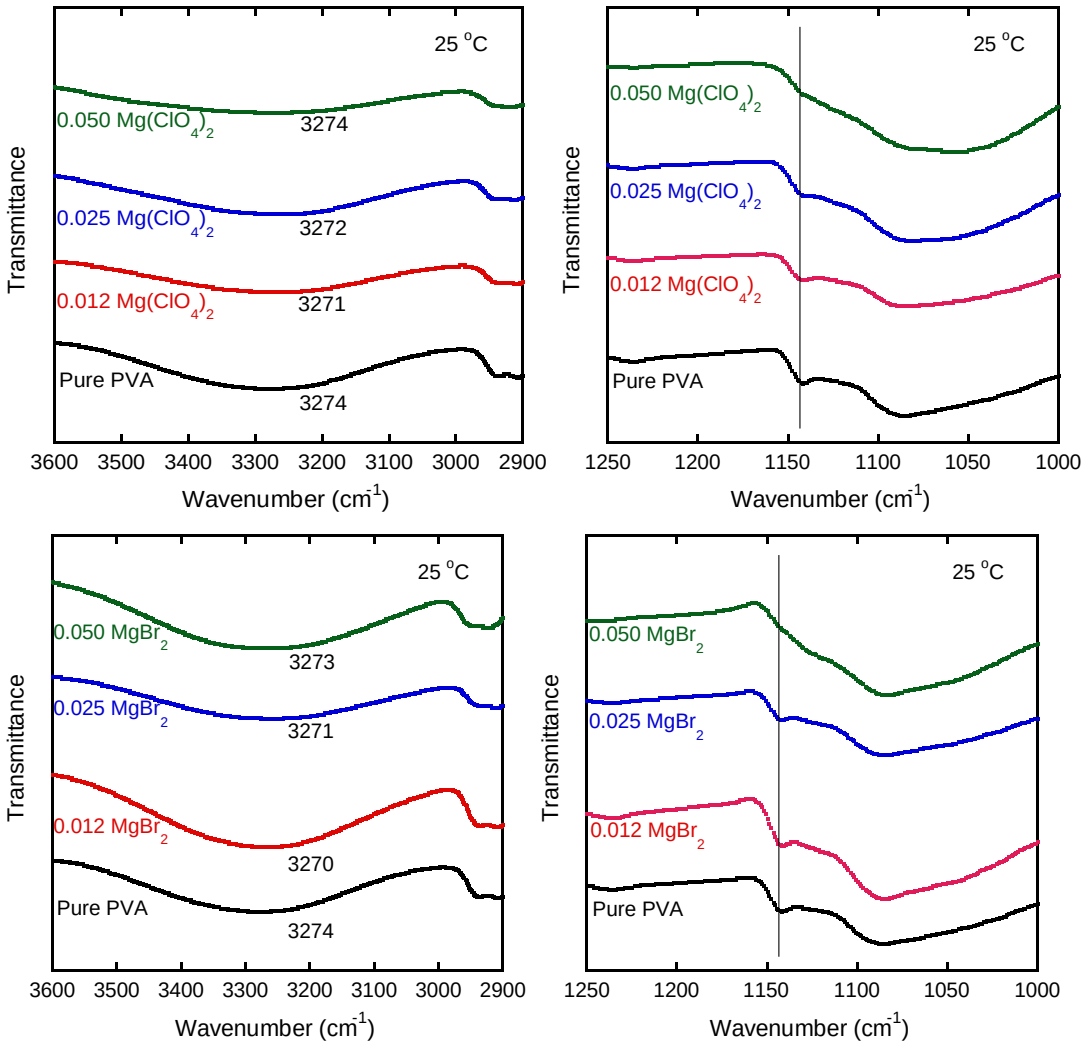

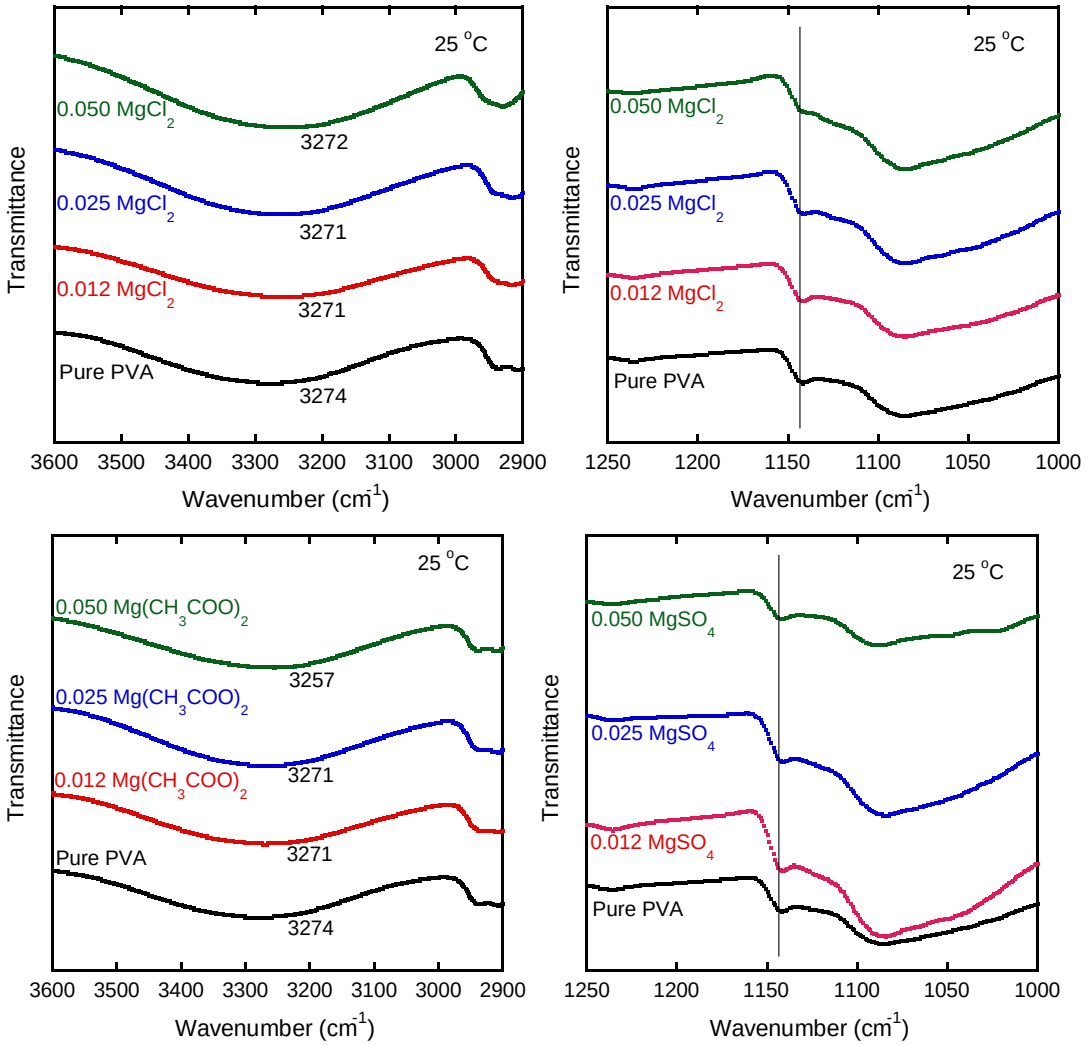

Figure 5.11 IR spectra for the films of pure PVA and PVA with magnesium salts in the wavenumber of 2900-3600 cm^{-1} and 1000-1250 cm^{-1}

5-4 Conclusion

The addition of various magnesium salts was found to modify the rheological properties of aqueous solution and thus give an impact on the hydrogen bonding and crystallinity of a solid film. Consequently, the T_g shifted to high temperatures, and the modulus above T_g was decreased. The study confirmed that water-structure-breaker anion, i.e., ClO_4^-, Br^-, Cl^-, and water-structure-maker anion, i.e., CH_3COO^- and SO_4^{2-}, give an

opposite effect on the mechanical properties of PVA films. This phenomenon can be predicted by the HS. For example, the impact of the addition of $Mg(ClO_4)_2$, $MgBr_2$, and $MgCl_2$ decreased the crystallinity as the concentration increased, but different trend occurred for $Mg(CH_3COO)_2$ and $MgSO_4$. Therefore, the anions were found to have a more significant impact on the structure and mechanical properties of the PVA films. Compared with lithium salts, magnesium salts seem to have a capability to enhance the mechanical properties of PVA.

References

1. J.I. Kubo, N. Rahman, N. Takahashi, T. Kawai, G. Matsuba, K. Nishida, M. Yamamoto, Improvement of poly (vinyl alcohol) properties by the addition of magnesium nitrate, J. Appl. Polym. Sci. 112 (2009) 1647-1652.
2. X. Jiang, T. Jiang, X. Zhang, H. Dai, X. Zhang, Melt processing of poly (vinyl alcohol) through adding magnesium chloride hexahydrate and ethylene glycol as a complex plasticizer, Polym. Eng. Sci. 52 (2012) 2245-2252.
3. B. Wang, C. Lu, J. Hu, W. Lu, Property improvements of EVOH by enhancing the hydrogen bonding, Plast. Rub. Compos. 49 (2020) 18-24.
4. G.N. Eby, Principles of Environmental Geochemistry, Brooks/Cole-Thomson Learning, 2004, 212-214.
5. W.L. Bragg, The Crystalline State: Volume I, The Macmillan Company, New York, 1934.
6. M. Quarrie, A. Donald, Physical Chemistry: A molecular Approach. Sausalito: University Science Books, 1997.
7. W.L. Bragg, The Diffraction of Short Electromagnetic Waves by a Crystal, Proc. Camb. Phil. Soc. 17 (1913) 43–57.
8. D.L.P. Delphine, Encyclopedia of Spectroscopy and Spectrometry, 2nd edn. Academic Press, Oxford, 2010.
9. L.Z. Zhang, Y.Y. Wang, C.L. Wang, H. Xiang, Synthesis and characterization of a PVA/LiCl blend membrane for air dehumidification, J. Membrane Sci. 308 (2008) 198-206.
10. Ahad N, Saion E, Gharibshahi E, et al. Structural, thermal, and electrical properties of PVA-sodium salicylate solid composite polymer electrolyte. J Nanomater. 2012;2012:94.

11. A. Ito A, P. Phulkerd, V. Ayerdurai, M. Soga, A. Courtoux, A. Miyagawa, M. Yamaguchi, Enhancement of the glass transition temperature of poly (methyl methacrylate) by salt, Polym. J. 50 (2018) 857-863.
12. M.A. Saeed, O.G. Abdullah, Effect of Structural Features on Ionic Conductivity and Dielectric Response of PVA Proton Conductor-Based Solid Polymer Electrolytes, J. Electron. Mater. (2020) 1-11.
13. Y. Okazaki, K. Ishizuki, S. Kawauchi, M. Satoh, J. Komiyama, Ion-specific swelling and deswelling behaviors of ampholytic polymer gels, Macromolecules 29 (1996) 8391-8397.
14. T. Nakano, H. Yuasa, Y. Kanaya, Suppression of agglomeration in fluidized bed coating. III. Hofmeister series in suppression of particle agglomeration, Pharm. Res. 16 (1999) 1616-1620.
15. H. Muta, S. Kawauchi, M. Satoh, Ion-specific swelling behavior of uncharged poly (acrylic acid) gel, Colloid Polym. Sci. 282 (2003) 149-155.
16. M. Mori, J. Wang, M. Satoh, Anti-Hofmeister series properties found for a polymer having a π electron system and acidic protons, Colloid Polym. Sci. 287 (2009) 123-127.
17. C. Qiao, X. Wang, J. Zhang, J. Yao, Influence of salts in the Hofmeister series on the physical gelation behavior of gelatin in aqueous solutions, Food Hydrocoll. 110 (2020) 106150.
18. K.E. Lee, I. Khan, N. Morad, T.T. Teng, B.T. Poh, Thermal behavior and morphological properties of novel magnesium salt–polyacrylamide composite polymers, Polym. Compos. 32 (2011) 1515-1522.
19. D. Lai, Y. Wei, L. Zou, Y. Xu, H. Lu, Wet spinning of PVA composite fibers with a

large fraction of multi-walled carbon nanotubes, Prog. Nat. Sci.: Mater. Int. 25 (2015) 445-452.

20. X. Jiang, H. Li, Y. Luo, Y. Zhao, L. Hou, Studies of the plasticizing effect of different hydrophilic inorganic salts on starch/poly (vinyl alcohol) films, Int. J. Biol. Macromol. 82 (2016) 223-230.
21. T. Akahane, T. Mochizuki, Planar orientation of molecular chains in crystalline polymer films, J. Polym. Sci. Pol. Lett. 8 (1970) 487-491.
22. H.M. Zidan, E.M. Abdelrazek, A.M. Abdelghany, A.E. Tarabiah, Characterization and some physical studies of PVA/PVP filled with MWCNTs, J. Mater. Res. Tech. 8 (2019) 904-913.
23. S. Clemenson, L. David, E. Espuche, Structure and morphology of nanocomposite films prepared from polyvinyl alcohol and silver nitrate: Influence of thermal treatment, J. Polym. Sci. A: Polym. Chem. 45 (2007) 2657-2672.
24. H. Muta, S. Kawauchi, M. Satoh, Ion-specific swelling behavior of uncharged poly (acrylic acid) gel, Colloid Polym. Sci. 282 (2003) 149-155.
25. S.I. Song, B.C. Kim, Characteristic rheological features of PVA solutions in water-containing solvents with different hydration states, Polymer 45 (2004) 2381-2386.
26. O.N. Tretinnikov, S.A. Zagorskaya, Effect of inorganic salts on the crystallinity of polyvinyl alcohol, J. Appl. Spectros. 78 (2012) 904-908.
27. D.K. Buslov, N.I. Sushko, O.N. Tretinnikov, IR investigation of hydrogen bonds in weakly hydrated films of poly (vinyl alcohol), Polym. Sci. Ser. A 53 (2011) 1121-1127.
28. X. Jiang, H. Dai, X. Zhang, Effect of magnesium chloride hexahydrate on thermal and mechanical properties of starch/PVA films, Plast. Rub. Compos. 44 (2015) 299-

305.

29. J. Wang, M. Satoh, Novel PVA-based polymers showing an anti-Hofmeister series property, Polymer 50 (2009) 3680-3685.

Chapter 6 General conclusion

PVA is known to show excellent mechanical properties and biodegradability, which are attractive from the viewpoints of sustainable society. Since PVA has numerous hydroxyl groups, it is dissolved in water. Therefore, the salt addition can affect the rheological properties of PVA aqueous solution. Although the effect on a salt on some polar polymers has been studied, the mechanism was not fully understood systematically. In this thesis, a new concept was proposed for the effect of salt addition using the HS. Here are the brief summary of each chapter.

Chapter 2 Rheological properties for aqueous solution of poly(vinyl alcohol) with lithium salts

The effects of the addition of lithium salts such as LiI, LiBr and LiCl on the rheological properties of aqueous solutions containing 15 wt% PVA were evaluated using a parallel-plate rheometer with a specific technique to avoid water vaporization. There was a plateau in the shear storage modulus in the low frequency region, demonstrating that such solutions have a network structure attributed to hydrogen bonding of PVA. The value of the plateau modulus was also found to be decreased with temperature and with the addition of lithium salts. In particular, the effect of the anion species of lithium salts on the rheological properties were firstly investigated in detail. It should be noted that the rheological properties of aqueous PVA solutions with a salt can be summarized by the HS.

Chapter 3 Application of Hofmeister series to structure and properties of poly(vinyl alcohol) films containing metal salt

Structure and properties of the PVA films with a salt which were prepared by the evaporation of water for the aqueous solution, were studied considering the results in Chapter 2. Interestingly, it was found that the concept of the HS also can be applicable even in the solid state, which were confirmed by systematic studies using various metal salts. Although cations play an important role, the structure analyses demonstrated that the strong ion-dipole interactions between anions and PVA chains also have a significant impact on the crystallinity and segmental mobility. Furthermore, the phenomena corresponded with the rheological properties of aqueous solutions; i.e., the HS concept is also applicable to the solid-state structure. Investigations using various bromine salts revealed that Li^+ is more effective to disrupt the water structure than either Na^+ or K^+. Further experiments using lithium salts with various anion species verified that lithium salts play an important role in determining the crystallinity and hydrogen bonding within aqueous PVA, and therefore, affect the dynamic mechanical properties of films. This phenomenon clearly follows the order $LiClO_4$ > LiI > LiBr > $LiNO_3$ > LiCl, which corresponds to the Hofmeister series.

Chapter 4 Modification of poly(vinyl alcohol) fibers with lithium bromide

The effect of salt addition on the structure and properties of PVA fibers obtained by wet-spinning was studied. As a salt, LiBr was employed based on the results obtained in Chapters 2 and 3. The tensile modulus and strength of a PVA fiber were greatly enhanced irrespective of the post-spinning hot-stretching process. The high degree of molecular orientation arose from the reduction in the crystallinity and hydrogen bonding between PVA chains in the solution resulting from the addition of LiBr, which was revealed by the rheological properties of aqueous solutions. The LiBr was removed from the fiber during the spinning process in the coagulation bath, and during the washing process. This ensures strong hydrogen bonding in the fibers, and results in excellent mechanical properties.

Chapter 5 Impact of magnesium salt addition to poly(vinyl alcohol)

In this chapter, magnesium salts were used in regards of industrial purpose, because they show a good cost-performance compared to the lithium salts. Furthermore, magnesium was expected to give interesting and outstanding results because they were known to show a high lattice energy. It was found that the films with magnesium salts show different mechanical and rheological properties compared to those with the other salts. T_g of the films was enhanced, which was attributed to the strong ion-dipole interactions between magnesium salts and PVA chains. In contrast, this interaction was found to be weakened at high temperature, which was confirmed by viscoelastic properties. The effect of the magnesium salt addition strongly depends on anion species whether it is a water-structure-breaker or water-structure-maker, i.e., the HS. The crystallinity and hydrogen bonding were enhanced by the addition of a water-structure-maker salt, although the film appearance was opaque due to the salt agglomeration. Finally, the presence of a water-structure-breaker salt retarded the crystallization of PVA, because the segmental motion of PVA chains was reduced. This phenomenon clearly follows the order $Mg(ClO_4)_2$ > $MgBr_2$ > $MgCl_2$ > $Mg(CH_3COO)_2$ > $MgSO_4$, which corresponds to the Hofmeister series.

Future Scope

Water soluble polymers such as PVA have a significant impact on our lives because of their versatility and a high demand due to SDGs. The findings in the thesis on the modification of PVA rheological properties, mechanical properties, and thermal properties, by the salt addition would be very useful for new material design in the future. Since this systematical study on PVA was firstly summarized in relation to the HS, it will be easier to understand and also applicable to not only PVA but also various polymers. Besides, by the addition of different types of salts, there are a plenty of possibilities to control the characteristics of a single polymer, which provide a new specific function. It is expected that further interesting findings can be obtained, not only in basic research but also for the industrial aspect.

Achievements

Publications

1. **R.A. Saari**, R. Maeno, R. Tsuyuguchi, W. Marujiwat, P. Phulkerd, M. Yamaguchi, Impact of Lithium halides on rheological properties of aqueous solution of poly(vinyl alcohol), J. Polym. Res. 27 (2020) 1-8.

2. **R.A. Saari**, R. Maeno, W. Marujiwat, M.S. Nasri, K. Matsumura, M. Yamaguchi, Modification of poly(vinyl alcohol) fibers with lithium bromide, Polymer 213 (2020) 123193.

3. **R.A. Saari**, M.S. Nasri, W. Marujiwat, R. Maeno, M. Yamaguchi, Application of the Hofmeister series to the structure and properties of poly (vinyl alcohol) films containing metal salts, Polym. J. 53 (2021) 1-8.

4. **R.A. Saari**, M.S. Nasri, M. Yamaguchi, Application of the Hofmeister series to the structure and properties of poly(vinyl alcohol) films containing magneisum salts, In preparation.

Other Publication

1. N. Moonprasith, M.S. Nasri, **R.A. Saari**, P. Phulkerd, M. Yamaguchi, Viscosity decrease by interfacial slippage between immiscible polymers, Polym. Eng. Sci. 61 (2021) 1096-1103.

Presentations

International Conferences

1. **R.A. Saari**, R. Tsuyuguchi, M. Yamaguchi,
   "Effect of metal salt incorporation of poly(vinyl alcohol) on the structure and property",
   Novel Trends in Rheology VIII, Zlin, Czech, July 2019.

2. **R.A. Saari**, M. Yamaguchi, "Rheological properties of poly(vinyl alcohol) containing metal salts",
   JAIST World Conference 2020—International Symposium for Innovative Sustainable Materials and
   The 7th International Symposium for Green-Innovation Polymers (GRIP2020), JAIST, Japan, November 2020.

Domestic Conferences

1. **R.A. Saari**, R. Tsuyuguchi, M. Yamaguchi, "Structure and properties of PVA containing metal salt", 68th Annual Meeting of the Society of Polymer Science (SPSJ), Osaka, Japan, May 2019.

2. **R.A. Saari**, M.S. Nasri, K. Matsumura, M. Yamaguchi, "Modification of poly(vinyl alcohol) fibers incorporated with metal salt", 70th Annual Meeting of the Society of Polymer Science (SPSJ), Osaka, Japan, May 2021.

Award

1. Best Presenter Poster Award, Novel Trends in Rheology VIII, Zlin, Czech, July 2019.
2. Receiver of Japanese Government (Monbukagakusho) MEXT Scholarship.